THE

LONDON, EDINBURGH, AND DUBLIN

PHILOSOPHICAL MAGAZINE

AND

JOURNAL OF SCIENCE.

[SEVENTH SERIES.]

SUPPLEMENT, AUGUST 1933.

XXVII. *The Hall Effect and some other Physical Constants of Alloys.*—Part I. *The Lead-Bismuth Series of Alloys.*

By W. RHEINALLT THOMAS, *M.Sc., and* Prof. E. J. EVANS, *D.Sc., Physics Department of the University College of Swansea* *.

THE present investigation is a continuation of the work † carried out in the Physics Department of the University College of Swansea on the Hall effects and other physical properties of binary alloys. The main object of this research was to study in greater detail the reversal of the Hall coefficient with variation of the magnetic field in the case of the bismuth rich alloys. This phenomenon had been previously investigated for three alloys of the lead-bismuth series by A. W. Smith ‡. In addition, the resistivities temperature coefficients of resistance, thermoelectric powers, and the densities of the alloys have been measured. These measurements were made with the same plates as were employed in the investigation of the Hall coefficients.

Although, at the present time, satisfactory explanations of the electrical and galvanomagnetic properties of alloys

* Communicated by the Authors.

† Stephens and Evans, Phil. Mag. (Jan. 1929); Stephens, Phil. Mag. (September 1929); Richards and Evans, Phil. Mag. (February 1932).

‡ A. W. Smith, Phys. Rev. (2) x. p. 358 (1917).

are not available on existing theories, it is important, in order to furnish data for theoretical discussion, to carry out all measurements of the physical constants on the same material. As the values of the various constants depend on the physical state of the material, it is necessary to pay attention to the problem of annealing. Information on this point can be obtained from the work carried out by metallurgists on the system under investigation. The lead-bismuth system has been the subject of many investigations, but even now the nature of the equilibrium diagram has not been finally settled. Herold * found that a solid solution of bismuth in lead containing up to about 22 per cent. of bismuth exists at the lead end of the system, and also a solid solution of lead in bismuth containing up to 1 per cent. of lead at the bismuth end of the system. These results he deduced from thermal analysis and from measurements of the electrical conductivity. According to the equilibrium diagram in the 'International Critical Tables' †, the solid solution of bismuth in lead at low temperature (the α phase) extends from 0 to about 17 per cent. bismuth, and the solid solution of lead in bismuth (the β phase) extends over a short range of composition containing from 0 to 1 per cent. of lead. The remaining compositions form the $\alpha+\beta$ phase.

An X-ray investigation of the system has been carried out by Solomon and Jones ‡, who examined the alloys containing 90, 80, 75, 67, and 50 per cent. by weight of lead. According to their investigation, if we proceed along the equilibrium diagram from the lead end, addition of bismuth up to 20 per cent. by weight causes a small expansion (4·930 Å.U. to 4·946 Å.U.) of the face-centred cubic lattice of the lead. At this percentage of bismuth a new crystalline structure, which is hexagonal close packed, begins to appear. When the alloy contains 25 per cent. of bismuth the whole structure is hexagonal, and this persists until the alloy contains 33 per cent. of bismuth. The addition of bismuth over this range causes a slight expansion of the hexagonal lattice (3·477 Å.U. to 3·483 Å.U.). From 33 per cent. bismuth to 100 per cent. bismuth the crystal structure of the alloys consists of

* Herold, *Zeit. Anorg. Chem.* cxii. p. 131 (1920).
† 'International Critical Tables,' ii. p. 414.
‡ Solomon and Jones, Phil. Mag. xi. p. 1090 (1931).

a mixture of the hexagonal close-packed lattice (3·483 Å.U. and axial ratio 1·66) and the face-centred rhombohedral lattice of bismuth. Clara di Capua * has shown that bismuth is soluble in lead up to 34 per cent., and lead soluble in bismuth up to 4 per cent.

The resistivities of alloys of the lead-bismuth series have been measured by Mathiessen †, Mathiessen and Vogt ‡, and Schenck §, and the thermoelectric powers by Batelli ||, and Darling and Rinaldi ¶.

Preparation of Plates.

The materials used in the preparation of the plates were of a high degree of purity. The lead and bismuth did not contain more than 0·0043 and 0·1 per cent. by weight of impurities respectively. The chief impurities in the lead were :—

Silver	·0005 per cent.
Copper	·0003 ,,
Bismuth.....	·0015 ,,
Iron	·0012 ,,
Zinc	·0003 ,,

The chief impurities in the bismuth were :—

Silver	·01 per cent.
Lead	·06 ,,
Iron	·01 ,,

As the melting-points of lead and bismuth are 327° C. and 269° C. respectively, the alloys of various compositions could be readily prepared by heating the constituent metals in a crucible over a Bunsen flame. Oxidation was prevented, as far as possible, by covering the melt with a layer of carbon. The melt, after being well stirred to ensure uniformity of composition, was poured into a heated graphite mould and allowed to cool. The mould was heated to prevent the formation of blowholes. The alloys prepared in this way were malleable at the lead end of

* *Rendi della reale Acad. del Lincei, Roma*, 1922, (5) xxxi. (1), pp. 162–164.
† Phil. Trans. cl. p. 161 (1860).
‡ *Ann. der Phys.* ii. p. 19 (1864); and Phil. Trans. cliv. p. 167 (1865).
§ *Phys. Zeits.* viii. p. 239 (1907).
|| *Mem. Accad. Torino*, xxxvi. p. 487 (1885).
¶ Proc. Phys. Soc. of London, xxxvi. p. 281 (1924).

the series and brittle at the bismuth end. It was found that plates 15 cm. long, 2·5 cm. wide, and from 0·25 to 0·35 cm. thick were suitable for these investigations. They possessed the necessary strength, and could be satisfactorily cast. The plates, after being cast, were filed down until the variation in their dimensions was not greater than about 0·3 per cent. Special attention was paid to the accurate determination of the thickness of each plate, as this dimension offered the greatest possibility of error. Several measurements of the thickness at points along the length of the plate were made by means of an accurate micrometer screw gauge, and the mean value calculated. The thickness was also determined by weighing the plate in air and in distilled water and measuring its area. The values of the thickness obtained by the two methods agreed to within 0·2 per cent. Twenty-six plates were prepared and their compositions checked by chemical analysis.

Chemical Analysis.

The composition of each plate was determined by the following method. Normal bismuth oxalate (prepared by the addition of ammonium oxalate to a nitric acid solution of the alloy, and the precipitate boiled with successive portions of water) was converted into the basic oxalate. This was titrated with potassium permanganate in the presence of sulphuric acid. The bismuth content of each plate was determined several times and the results agreed to within 0·1 per cent. The percentage by weight of lead was determined by difference. The composition of the plates is given in Table A.

TABLE A.

0	per cent.	Bi	100	per cent.	Pb	58	per cent.	Bi	42	per cent.	Pb
5	,,	Bi	95	,,	Pb	60	,,	Bi	40	,,	Pb
10	,,	Bi	90	,,	Pb	65	,,	Bi	35	,,	Pb
16	,,	Bi	84	,,	Pb	70	,,	Bi	30	,,	Pb
17	,,	Bi	83	,,	Pb	80	,,	Bi	20	,,	Pb
18	,,	Bi	82	,,	Pb	90	,,	Bi	10	,,	Pb
20	,,	Bi	80	,,	Pb	96	,,	Bi	4	,,	Pb
25	,,	Bi	75	,,	Pb	97	,,	Bi	3	,,	Pb
32	,,	Bi	68	,,	Pb	97·3	,,	Bi	2·7	,,	Pb
37	,,	Bi	63	,,	Pb	98	,,	Bi	2	,,	Pb
42	,,	Bi	58	,,	Pb	99	,,	Bi	1	,,	Pb
50	,,	Bi	50	,,	Pb	99·7	,,	Bi	0·3	,,	Pb
56	,,	Bi	44	,,	Pb	100	,,	Bi	0	,,	Pb

Annealing.

Since the electrical properties of alloys depend on their physical state, special attention was paid to the proper annealing of the plates. The annealing was carried out in an electric furnace which provided a constant temperature over a considerable portion of its length. The plates were placed in the furnace, which was then evacuated to a low pressure. The temperature of the furnace was raised to 80° C., and maintained at that point for several days. The current was then switched off, and the furnace allowed to cool gradually to room temperature. The plates were removed and their resistivities at 0° C. determined. The process was repeated until further annealing produced no change in the resistivities. The annealing temperature was now reduced to 60° C., and the above process was again repeated. Finally, the alloys were annealed at 40° C., and when subsequent annealing at this temperature produced no change in the resistivities the alloys were considered to have attained their final reproducible state.

Determination of the Physical Constants of the Alloys.

Resistivity.

As the alloys had been cast in the form of rectangular plates, whose dimensions were approximately $15 \times 2{\cdot}5 \times {\cdot}3$ cm., the low resistances of known lengths of the plates were measured by means of the Kelvin bridge. A plate was fixed across two knife edges attached to light wooden blocks, and the distance between the knife edges was adjusted to be 7·5 cm. The plate was immersed in a bath of melting ice, and the resistance of the length of plate between the knife edges measured. The presence of serious defects in a plate, such as cracks, blowholes, or lack of uniformity in composition, could be detected by measuring the resistance of different portions of the plate. The resistances of all the alloy plates were carefully measured at the temperature of melting ice, and the resistivities of the alloys of various compositions were calculated from the dimensions of the plates.

The values of the resistivities of the alloys in the annealed state at 0° C. are given in Table I. and plotted in Graph I.

It is estimated that the measurements of the resistivities are, on the average, correct to within 0·4 per cent. As

TABLE I.

Composition by weight.	Resistivity at 0° C. in microhms per cm.³ before annealing.	Resistivity at 0° C. in microhms per cm.³ after annealing.
100 per cent. Pb	19·97	19·90
5 „ Bi	24·82	24·16
10 „ Bi	29·32	29·43
16 „ Bi	35·26	34·17
17 „ Bi	35·50	35·10
18 „ Bi	35·89	35·75
20 „ Bi	39·85	36·89
25 „ Bi	42·11	42·31
32 „ Bi	50·95	49·22
37 „ Bi	58·75	56·13
42 „ Bi	66·37	64·51
50 „ Bi	87·16	81·41
56 „ Bi	96·03	96·82
58 „ Bi	102·0	102·13
60 „ Bi	111·3	110·50
65 „ Bi	137·0	132·02
70 „ Bi	154·9	157·01
80 „ Bi	209·9	211·90
90 „ Bi	281·8	280·05
96 „ Bi	315·2	318·4
97 „ Bi	301·0	306·2
97·3 „ Bi	302·6	300·7
98 „ Bi	264·2	275·4
99 „ Bi	230·1	236·5
99·7 „ Bi	183·1	179·1
100 „ Bi	113·5	108·4

previously described, great attention had been paid to the annealing of the alloys, and it is considered that serious errors in the values of the resistivity and the other physical

constants due to inadequate annealing have been eliminated. The constancy of the values of the various physical constants over long periods of time point to this conclusion.

Temperature Coefficient of Resistance.

The mean temperature coefficients of resistance of the various alloys were measured over the temperature ranges 0° to 30° C. and −20° to 0° C. It was only necessary to measure the resistances at 30° C. and −20° C. as the

Graph I.

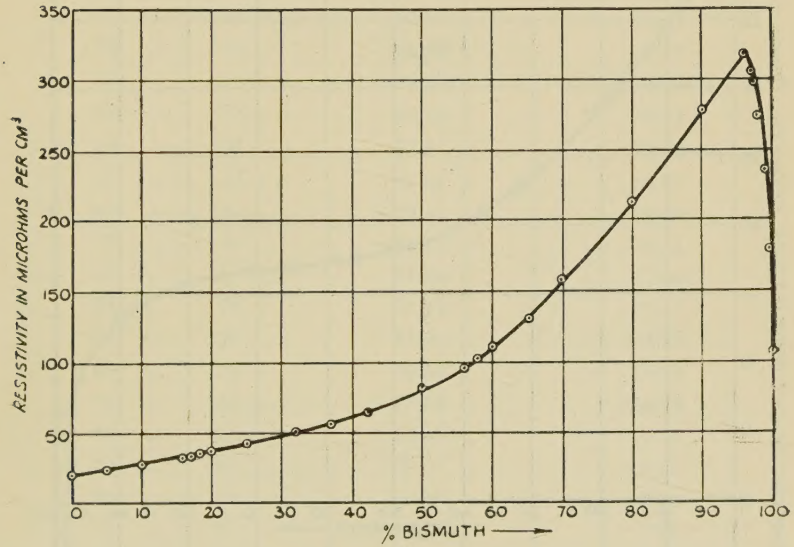

Resistivity-composition curve.

resistances at 0° C. were already known. The ice was removed from the bath, and the plate, fixed between the two knife edges as described above, was raised in temperature to 30° C. by means of a stream of warm water, which passed through the bath at a constant rate. The warm water was supplied by a Davis apparatus, and the variation in the temperature of the bath from one end to the other was not greater than $\frac{1}{5}$° C. Determinations of the resistances were made at other temperatures between 20° and 30° C., and the calculated values of the temperature coefficients agreed within experimental error. The

resistances of the plates were also measured at about $-20°$ C. by immersing them in a freezing mixture of ice and salt, and the temperature coefficients were calculated for the temperature range $-20°$ to $0°$ C. The temperatures in these experiments were measured by means of calibrated thermometers graduated to read $\frac{1}{10}°$ C. The

Graph II.

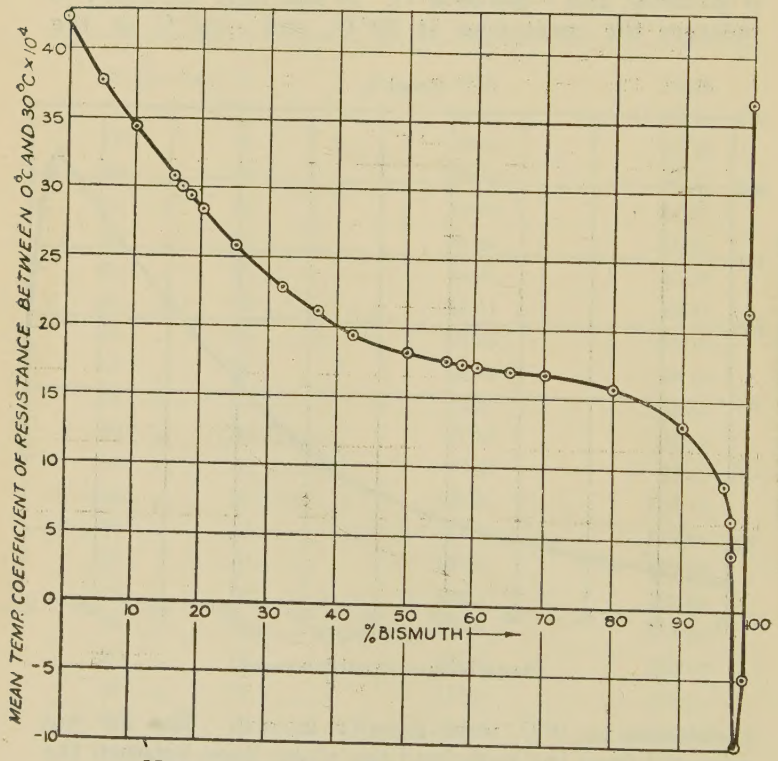

Mean temperature coefficient-composition curve.

accuracy of the determinations of the temperature coefficient depends only on the measurements of temperature and resistance, and is independent of the dimensions of the plate. Taking all factors into account, it is estimated that on the average the values of the temperature coefficient are correct to within 0·5 per cent. The results are given in Table II. and Graph II.

TABLE II.

Composition by weight.			Mean temp. coefficient of resistance $\times 10^4$ between 0° C. and 30° C.	Mean temp. coefficient of resistance $\times 10^4$ between −20° C. and 0° C.
100	per cent.	Pb....	42·25	42·29
5	„	Bi	37·61	37·49
10	„	Bi	34·39	34·41
16	„	Bi	30·62	30·61
17	„	Bi	29·97	30·11
18	„	Bi	29·44	29·37
20	„	Bi	28·30	28·26
25	„	Bi	25·76	25·71
32	„	Bi	22·91	22·86
37	„	Bi	21·07	20·97
42	„	Bi	19·41	19·40
50	„	Bi	18·21	18·23
56	„	Bi	17·55	17·56
58	„	Bi	17·42	17·41
60	„	Bi	17·23	17·19
65	„	Bi	16·93	16·86
70	„	Bi	16·74	16·76
80	„	Bi	15·81	15·79
90	„	Bi	13·15	13·14
96	„	Bi	8·98	8·96
97	„	Bi	6·05	5·98
97·3	„	Bi	3·99	3·98
98	„	Bi	−9·75	−8·40
99	„	Bi	−4·87	−3·12
99·7	„	Bi	21·33	21·32
100	„	Bi	41·35	41·28

Thermoelectric Power.

The thermoelectric powers of the alloys with respect to copper were determined over the range of temperature from 0° to 30° C. Copper leads were clamped to the ends of a plate, and one of the junctions was completely

surrounded with melting ice. The other junction was enclosed in a jacket through which passed a steady stream of warm water from a Davis apparatus. The constant temperature of the junction was measured by means of a calibrated thermometer placed in contact with it. The thermoelectromotive force over the range of temperature was determined by means of a Tinsley Vernier potentiometer and a standard Weston cell. As the copper wire attached to the various alloy plates was not absolutely pure,

Graph III.

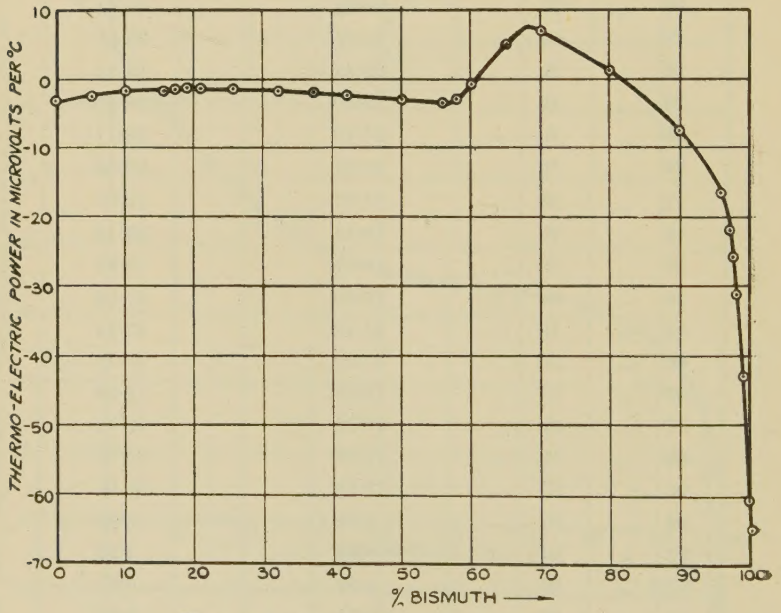

Thermoelectric power-composition curve.

its thermoelectric power with respect to a plate of pure copper was determined, and a correction was applied to the values of the thermoelectric powers of the alloys with respect to the copper wire. The thermoelectric powers of the various alloys were also determined over the temperature range of 0° to 20° C., and the values agreed with those obtained over the wider range of 0° to 30° C. The variation of E.M.F. with temperature difference is therefore linear over the range of these experiments. The values of the thermoelectric powers of the

alloys with respect to pure copper are given in Table III. and plotted in Graph III.

TABLE III.

Composition by weight.	Thermoelectric power with reference to copper in micro-volts per degree Centigrade.
100 per cent. Pb	−3·16
5 „ Bi	−2·43
10 „ Bi	−1·88
16 „ Bi	−1·53
17 „ Bi	−1·51
18 „ Bi	−1·47
20 „ Bi	−1·43
25 „ Bi	−1·50
32 „ Bi	−1·75
37 „ Bi	−2·15
42 „ Bi	−2·32
50 „ Bi	−3·00
56 „ Bi	−3·43
58 „ Bi	−2·94
60 „ Bi	−0·74
65 „ Bi	+4·98
70 „ Bi	+6·80
80 „ Bi	+1·26
90 „ Bi	−7·40
96 „ Bi	−16·42
97 „ Bi	−21·72
97·3 „ Bi	−25·51
98 „ Bi	−30·93
99 „ Bi	−43·01
99·7 „ Bi	−60·87
100 „ Bi	−65·10

The Density of the Alloys.

The densities were found by weighing the plates in air and in distilled water at a known temperature, and the results are given in Table IV. and plotted in Graph IV. (p. 348).

TABLE IV.

Composition by weight.	Density in grm. per c.c. at mean temperature of 16° C.
100 per cent. Pb	11·38
5 „ Bi	11·30
10 „ Bi	11·21
16 „ Bi	11·12
17 „ Bi	11·09
18 „ Bi	11·08
20 „ Bi	11·04
25 „ Bi	10·96
32 „ Bi	10·86
37 „ Bi	10·77
42 „ Bi	10·71
50 „ Bi	10·59
56 „ Bi	10·51
58 „ Bi	10·47
60 „ Bi	10·45
65 „ Bi	10·39
70 „ Bi	10·33
80 „ Bi	10·21
90 „ Bi	10·08
96 „ Bi	9·98
97 „ Bi	9·92
97·3 „ Bi	9·91
98 „ Bi	9·80
99 „ Bi	9·53
99·7 „ Bi	9·56
100 „ Bi	9·79

The Hall Effect of the Alloys.

If a metal plate carrying an electric current is placed between the poles of an electromagnet so that the lines of magnetic force are perpendicular to the plate, and to the direction of the electric current, a difference of potential is set up between two points on the edges of the

plate. These two points before the application of the field were at the same potential, and the difference of potential generated by the magnetic field is known as the Hall potential difference. It has been shown experimentally that the Hall potential difference E is expressed by the formula

$$E = \frac{RHI}{d},$$

where H, I, d, and R represent the magnetic field, electric current, thickness of plate, and a constant depending on the nature of the substance composing the plate respectively. This constant R is known as the Hall coefficient of the substance, and its value for most substances is independent of the intensity of the magnetic field. For the ferromagnetic metals and the highly diamagnetic metals, bismuth and antimony, the value of the Hall coefficient does depend on the strength of the magnetic field.

The Hall effect can be regarded as a rotation of the equipotential lines in the plate by the applied magnetic field. In some substances the rotation is in one direction, whilst in others it is in the opposite direction. The convention used for the sign of the effect is readily understood by reference to fig. 1. The rectangle X represents the plate, and EF the direction of the primary current. The circle Y (with the arrows indicating the direction of the current in the electromagnet) represents the magnetic field ; and AB the position of an equipotential line before the application of the field. If the equipotential line is rotated in the direction of the current in the electromagnet as shown in the figure the effect is positive, and if the equipotential line is rotated in the opposite direction the effect is negative.

Measurement of the Hall Coefficient.

The coefficient has a large negative value for bismuth and a very small positive value for lead. The low value of the Hall potential difference for plates containing a large percentage of lead necessitated the use of a sensitive instrument, and consequently a Paschen galvanometer was used. The instrument was mounted on a stone pillar built into the foundations of the laboratory, and was protected from the effects of stray magnetic fields

by enclosing it in a double shield of soft iron. The large circular electromagnet used in these experiments possessed pole-pieces of circular cross-section having a diameter of 9 cm., and the magnetic field was uniform over the air gap of 1·5 cm. The electromagnet was placed at a distance of $7\frac{1}{2}$ metres from the galvanometer, and was rotated into such a position that its effect on the latter was a minimum.

Fig. 1.

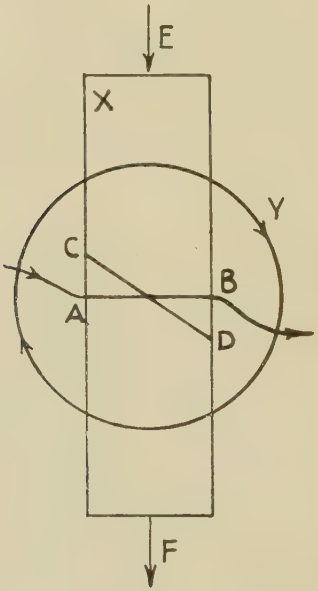

The alloy plate under investigation was rigidly fixed in a vertical position in the centre of the air gap between the pole-pieces by means of two brass clamps, which also served as leads for the primary current. These brass clamps were attached to a specially constructed wooden frame, which also supported the secondary electrodes, consisting of spring contacts carried by bars of ebonite. These two electrodes, which could be moved vertically along the edges of the plate, were connected to the galvanometer by long, well-insulated, flexible leads. These leads were pulled taut to eliminate vibrations, which produced induced currents in the galvanometer.

The current of 4 amperes (primary current) passing through the alloy plate was measured by a sensitive Weston ammeter. It could be read quite easily to within 1 part in 1200, and its indication was periodically compared with that of a large standard Weston ammeter. The error in the measurement of the primary current could not be greater than 0·1 per cent.

The magnetic field in the air gap of the electromagnet was measured for magnetizing currents varying from 1·0 to 8·0 amperes. These currents 1·0, 1·5, 2·0, 2·7, 4·0, 6·0, and 8·0 amperes were measured by means of an ammeter, whose readings were periodically checked by comparison with those of the large standard ammeter. The magnetic fields corresponding to the various magnetizing currents were determined by means of suitable search coils and a fluxmeter. The kicks measured on the fluxmeter were considered to give fairly accurate relative values of the magnetic fields, but the absolute values were calculated from the known absolute value of the magnetic field corresponding to a magnetizing current of 2·0 amperes. This magnetic field was determined by means of a carefully made search coil of known area and a ballistic galvanometer. It is estimated that the magnetic fields have been determined correctly to within 1 in 200.

According to Ettingshausen and Nernst* the magnitude of the Hall coefficient depends to a certain extent on the length of the plates. They found that the Hall effect in bismuth was less when short plates were used, and advocated the use of plates in which the ratio of length to breadth was at least 3 : 2. The plates employed in the present investigation easily satisfied this condition.

The Hall coefficient also shows a slight variation with temperature, and consequently a thermometer with its bulb resting on the plate was used to determine the temperature of the alloy when measurements of the Hall potential difference were in progress.

The arrangement of the apparatus for the measurement of the Hall potential difference is given in fig. 2.

B_1 is the battery which sends a current through the magnetizing coils M of the electromagnet. The current, which can be varied by means of the rheostats R_1 and R_2 and reversed by means of the key K_1, is measured by the

* Ettingshausen and Nernst, *Sitz. Akad. Wiss. Wien*, p. 173 (1886).

ammeter A_1. The primary current I, which is passed through the alloy plate P, is produced by the battery B_2, which forms part of the primary circuit consisting of the two rheostats R_3 and R_4, the Weston ammeter A_2, and the reversing key K_2. By means of this arrangement the current I through the plate can be adjusted to a known value, and can also be reversed when necessary. The secondary circuit consists of the Paschen galvanometer G, whose terminals are connected by flex to electrodes, which touch the plate at two points A and B This circuit is completed by means of the key K_3 In the determination of the Hall coefficient an electric current I is passed through the plate, and the positions of the secondary electrodes are adjusted so that, after closing the secondary circuit, the reversal of the primary current I produces no

Fig. 2.

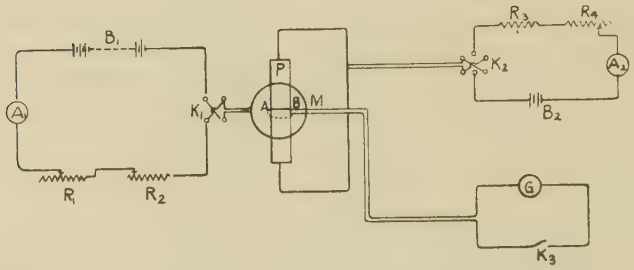

deflexion of the galvanometer. When this condition is satisfied the electrodes are situated on an equipotential line. The magnetic field is then applied, and after allowing a short interval of time for the inductive effects to die away, the secondary circuit is closed and the reading of the spot of light on the galvanometer scale is noted. With the secondary circuit still closed the primary current is quickly reversed and a second reading of the spot of light on the scale is observed. Let the difference between the two readings be $2\theta_1$. Similar experiments are then carried out with the magnetic field reversed, and the value $2\theta_2$ (nearly equal to $2\theta_1$) is obtained for the deflexion due to the reversal of the primary current. The reversal of the magnetic field eliminates any error due to inaccuracy in the adjustment of the equipotential line, and the reversal of the primary current helps to eliminate any

error caused by the potential difference set up at the edges of the plate when there is a flow of heat in a given direction along the plate (Nernst effect). If 2θ be the mean value of the deflexions measured in the above experiments, the potential difference set up between the edges of the plate due to the Hall effect produces a deflexion θ in the Paschen galvanometer. The galvanometer is calibrated by applying known differences of potential to its terminals and observing the resulting deflexions. The deflexion θ will therefore correspond to a known difference of potential applied to the galvanometer, and if the resistances of the galvanometer and the remainder of the secondary circuit have been measured, the potential difference between the two points A and B on the edges of the plate can be readily calculated.

It is, however, important to note that a second effect discovered by Ettingshausen has to be considered in relation to the above experiments. When a plate carrying an electric current is placed in a magnetic field so that the lines of force are normal to the plane of the plate and to the direction of the flow of the current, a transverse temperature difference is set up between the edges of the plate. If the secondary electrodes are made of different material from the plate itself, this temperature difference gives rise to an electromotive force, which is superposed on the Hall potential difference. The Ettingshausen effect is small compared with the Hall effect and can be practically eliminated, as was done in the present experiments, by using electrodes of the same material as the plate itself. The Hall E.M.F. is set up almost instantaneously by the magnetic field, while the Ettingshausen thermoelectromotive force takes time to reach its final value. Therefore in measurements of the Hall P.D. the initial deflexion observed is due to the Hall effect, and this is followed by a gradual creep if the Ettingshausen effect is measurable. In the present experiments no such creep was observed, showing that the use of electrodes of the same material as the plate eliminated the Ettingshausen effect. The Hall coefficients are recorded in Table V. and plotted in Graphs V., VI., and VII. The accuracy of the experimental results depends largely on the composition of the alloy, and also on the intensity of the magnetic field. In some cases the error in the determination of the Hall coefficient is less than

0·6 per cent., but for alloys of high lead content, and for those alloys whose coefficient is near the point of reversal, the error is decidedly larger.

Discussion of Results.

The most interesting variations in the physical properties of the lead-bismuth series of alloys occur in the region of the low lead content. The curves connecting the electrical resistivity, the temperature coefficient of resistance, the thermoelectric power, and the density with the percentage by weight of lead or bismuth in the alloys, have either a well-defined maximum or minimum at a composition which depends on the nature of the particular physical property examined.

If the curve (Graph I.) connecting the resistivities with increasing percentage of bismuth is examined, it will be seen that the resistivity increases slowly at first, and then more rapidly until it attains a maximum at the composition corresponding to 96 per cent. bismuth, 4 per cent. lead. The resistivity then decreases rapidly to its value for pure bismuth. The effect of annealing on the resistivities of the alloys is shown in Table I. The resistivities of the alloys containing from 0 to 50 per cent. bismuth were, in general, diminished by annealing, and the resistivities of the remaining alloys containing a higher percentage of bismuth were in some cases increased and in other cases decreased. The effect in most cases was, however, not large. The distinctive feature of the temperature coefficient of resistance-composition curve (Graph II.) is the well-defined minimum corresponding to the alloy of composition 98 per cent. bismuth, 2 per cent. lead. The curve shows a diminution in the value of the temperature coefficient as the percentage of bismuth is increased from 0 to 90 per cent. Although the rate of diminution is far more rapid between 0 and 40 per cent. bismuth than between 40 and 90 per cent. bismuth, there are no discontinuities over the whole range (0 to 90 per cent.). The curve, therefore, gives no evidence of phase changes in this region. The end of the solid solution of bismuth in lead (α phase) in the neighbourhood of 20 per cent. bismuth according to the equilibrium diagram, is not indicated by any discontinuity in the temperature coefficient of resistance curve. If the resistivity curve is plotted on a larger scale than shown

in Graph I., there is evidence of a slight discontinuity in the neighbourhood of 20 per cent. bismuth. Both the resistivity and the temperature coefficient curves give well-defined singular points (a maximum and minimum respectively) near the bismuth end of the series, but not at the same composition. As pointed out above, the maximum in the resistivity curve occurs at 96 per cent. bismuth, and the minimum in the temperature coefficient curve at 98 per cent. bismuth. If these discontinuities mark the end of the solid solution of lead in bismuth (the β phase), the limit of solubility cannot be fixed with certainty from the results of the present observations.

The results of the X-ray analysis of the structure of the bismuth-lead series by Solomon and Jones * have been discussed in the introduction to this paper. An examination of the resistivity and temperature coefficient curves shows that the beginning of the hexagonal structure, in the neighbourhood of 20 per cent. bismuth, and the end of the face-centred structure, at 25 per cent. bismuth, is not accompanied by well-defined abrupt changes in the curves.

Similarly, at the composition corresponding to about 33 per cent. of bismuth, where the pure hexagonal close-packed structure changes into the mixture of close-packed hexagonal and face-centred rhombohedral structures with increasing bismuth content, there is no evidence of a well-defined singular point on each of the two curves. However, when the resistivity-composition curve (Graph I.) is drawn on a sufficiently large scale slight irregularities are noticed. There are changes of slope in the neighbourhood of 20, 25, and 33 per cent. bismuth. According to Solomon and Jones, the solid solution of bismuth in lead extends up to 33 per cent. bismuth, but the crystal structure changes at about 20 per cent. bismuth. The points giving the resistivities of all alloys containing from 0 to about 32 per cent. bismuth are situated approximately on the straight line joining the points representing the resistivities of lead and bismuth, and the rapid changes in the values of the resistivity occur in the range of composition extending from 70 to 100 per cent. bismuth. In the region of high bismuth content, Solomon and Jones

* Solomon and Jones, *loc. cit.*

found that the crystal structure consists of a mixture of the hexagonal close-packed lattice of constant dimensions ($a_0 = 3{\cdot}483$ Å.U., $C = 1{\cdot}66$), and the face-centred rhombohedral lattice of bismuth. The X-ray experiments could not detect any solid solution of lead in bismuth owing to the small range of solubility, and the approximate equality of the atomic radii of the two metals. The resistivity

Graph IV.

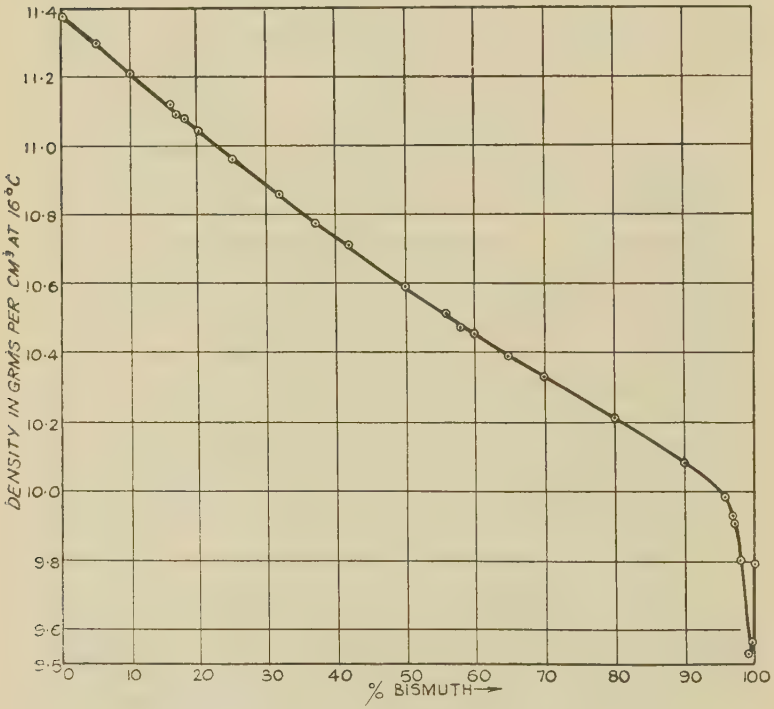

Density-composition curve.

and temperature coefficient curves, however, support the existence of this solid solution (the β phase) at the bismuth end of the series, and the presence of this phase probably accounts for the rapid rise in the resistivity curve between 70 and 96 per cent. bismuth.

The thermoelectric power composition curve (Graph III.) does not show near the bismuth end of the series the well-defined maximum or minimum of the curves pre-

viously discussed. It is, however, noticeable that the curve rises very rapidly in the region between 100 and 97 per cent. bismuth. This rise in the curve represents a decrease in the negative value of the thermoelectric power of the alloys with respect to copper, and persists over the range of composition between pure bismuth and 69 per cent. bismuth. At the latter composition, which does not correspond to a change of phase or crystal

Graph V.

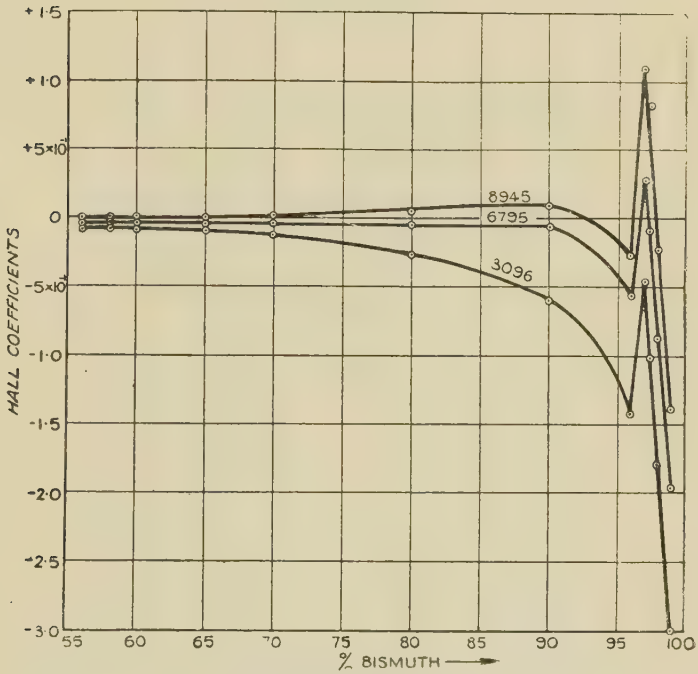

Hall coefficient-composition curve.
For fields 3096, 6795, and 8945 gauss.

structure, the thermoelectric power attains a maximum positive value. It is seen that the solid solution of bismuth in lead has comparatively little effect on the thermoelectric power, but that the solid solution of lead in bismuth produces a rapid decrease in the negative value of the thermoelectric power. The changes in crystal structure over the range from 0 to 34 per cent. bismuth produce comparatively little change in the

thermoelectric power, although the curve shows a maximum at 20 per cent. bismuth, where the hexagonal close-packed lattice makes its first appearance.

The chief characteristic of the density-composition curve (Graph IV.) is the rapid fall in density near the bismuth end of the series. This rapid change occurs within the range of composition from 96 to 100 per cent.

Graph VI.

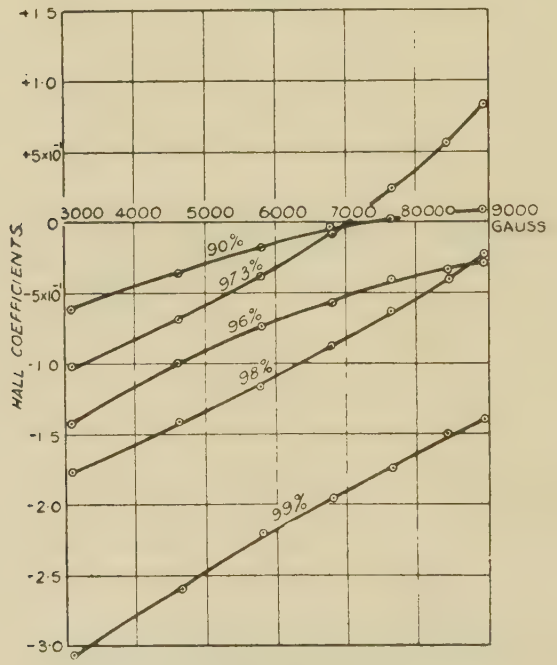

Showing relation between Hall coefficient and field strength for bismuth rich alloys.

bismuth, and an alloy containing 99 per cent. bismuth has the minimum density. The remaining portion of the curve is approximately linear.

The Hall effects of lead-bismuth alloys are of great interest owing to the reversals of sign which occur when the magnetic field is varied. The curves showing the relation between the Hall coefficients and the composition of the alloys for magnetic fields of 3096, 6795, and 8945 gauss are plotted in Graph V. The three curves are very

similar in shape and show discontinuities at the compositions corresponding to 96 and 97 per cent. by weight of bismuth. For the range of composition plotted the curve corresponding to the highest field crosses the line of zero Hall coefficient three times, and the curve corresponding to the field of intermediate intensity crosses the same axis twice. This latter curve, and also the third curve (3096 gauss), which is below the axis of zero Hall

Graph VII.

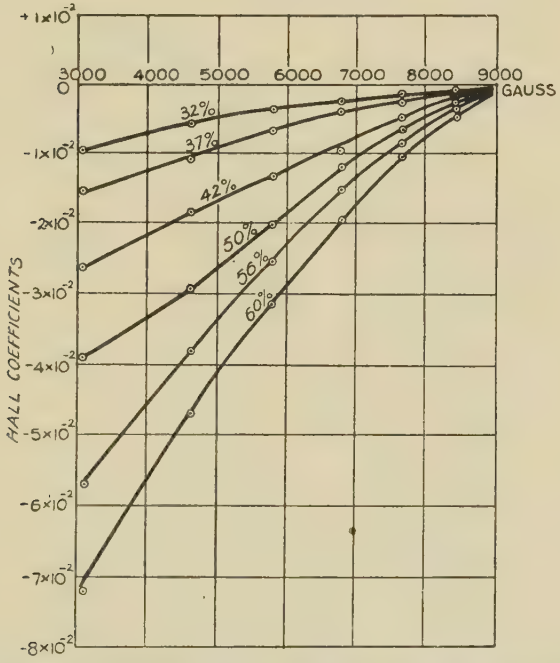

Showing relation between Hall coefficients and field strengths for alloys of low and medium bismuth content.

coefficient for the range of composition considered in Graph V., must cross the axis of zero coefficient at a composition of low bismuth content, as the Hall coefficient of lead is positive.

The curves for other magnetic fields are similar to those plotted in Graph V., and show singular points at compositions corresponding to 3 and 4 per cent. of lead by weight. It is of interest to note that the maximum in

the resistivity-composition curve is given by an alloy containing 4 per cent. of lead.

The variations of the Hall coefficients of alloys of known compositions with increase of magnetic field are shown in Graphs VI. and VII. These graphs indicate that, as the magnetic field increases from its lowest value to that required for reversal, the negative value of the Hall coefficient of an alloy of given composition continually

Graph VIII.

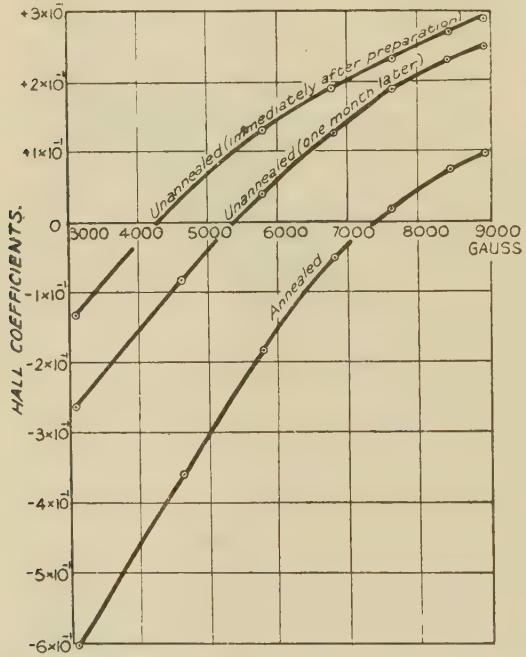

Showing relation between Hall coefficients and field strength for an alloy containing 90 per cent. Bi, 10 per cent. Pb.

diminishes. This result is also true for pure bismuth, whose Hall coefficient does not reverse for the highest magnetic field (8945 gauss) used in the present experiments. An examination of Table V. shows that alloys containing from 0 to about 2 per cent. of lead are not reversed by the strongest magnetic field used in these experiments, and the same is also true of the alloy containing 4 per cent. of lead, and of all alloys containing more than 35 per cent. of lead. The field required to

Composition by weight.	3096	4630	5787
100 per cent. Bi.....	$-7{\cdot}30$	$-6{\cdot}65$	$-6{\cdot}18$
99 „ Bi.....	$-3{\cdot}07$	$-2{\cdot}60$	$-2{\cdot}17$
98 „ Bi.....	$-1{\cdot}78$	$-1{\cdot}43$	$-1{\cdot}16$
97·3 „ Bi.....	$-1{\cdot}02$	$-6{\cdot}75\times10^{-1}$	$-3{\cdot}85\times10^{-1}$
97 „ Bi.....	$-4{\cdot}95\times10^{-1}$	$-2{\cdot}53\times10^{-1}$	$+1{\cdot}03\times10^{-2}$
96 „ Bi.....	$-1{\cdot}43$	$-9{\cdot}98\times10^{-1}$	$-7{\cdot}25\times10^{-1}$
90 „ Bi.....	$-6{\cdot}04\times10^{-1}$	$-3{\cdot}59\times10^{-1}$	$-1{\cdot}84\times10^{-1}$
80 „ Bi.....	$-2{\cdot}67\times10^{-1}$	$-1{\cdot}64\times10^{-1}$	$-9{\cdot}30\times10^{-2}$
70 „ Bi.....	$-1{\cdot}42\times10^{-1}$	$-9{\cdot}63\times10^{-2}$	$-5{\cdot}78\times10^{-2}$
65 „ Bi.....	$-1{\cdot}01\times10^{-1}$	$-7{\cdot}31\times10^{-2}$	$-3{\cdot}39\times10^{-2}$
60 „ Bi.....	$-7{\cdot}20\times10^{-2}$	$-4{\cdot}69\times10^{-2}$	$-3{\cdot}16\times10^{-2}$
58 „ Bi.....	$-6{\cdot}36\times10^{-2}$	$-4{\cdot}31\times10^{-2}$	$-2{\cdot}83\times10^{-2}$
56 „ Bi.....	$-5{\cdot}71\times10^{-2}$	$-3{\cdot}82\times10^{-2}$	$-2{\cdot}54\times10^{-2}$
50 „ Bi.....	$-3{\cdot}90\times10^{-2}$	$-2{\cdot}94\times10^{-2}$	$-2{\cdot}04\times10^{-2}$
42 „ Bi.....	$-2{\cdot}61\times10^{-2}$	$-1{\cdot}83\times10^{-2}$	$-1{\cdot}34\times10^{-2}$
37 „ Bi.....	$-1{\cdot}53\times10^{-2}$	$-1{\cdot}06\times10^{-2}$	$-6{\cdot}58\times10^{-3}$
32 „ Bi.....	$-9{\cdot}41\times10^{-3}$	$-5{\cdot}71\times10^{-3}$	$-3{\cdot}68\times10^{-3}$
25 „ Bi.....	$-5{\cdot}23\times10^{-3}$	$-3{\cdot}34\times10^{-3}$	$-2{\cdot}20\times10^{-3}$
20 „ Bi.....	$-2{\cdot}82\times10^{-3}$	$-1{\cdot}98\times10^{-3}$	$-1{\cdot}32\times10^{-3}$
100 „ Pb	..	*	$+9{\cdot}00\times10^{-5}$

* Campbell, 'Galvanoma

[*To face page* 352.

ents.

gauss.			Temp. in degrees C.
7661	8424	8945	
$-5\cdot81$	$-5\cdot68$	$-5\cdot57$	13
$-1\cdot75$	$-1\cdot50$	$-1\cdot40$	12
$-6\cdot15\times10^{-1}$	$-4\cdot02\times10^{-1}$	$-2\cdot22\times10^{-1}$	12·5
$+2\cdot37\times10^{-1}$	$+5\cdot60\times10^{-1}$	$+8\cdot32\times10^{-1}$	12
$+5\cdot35\times10^{-1}$	$+8\cdot80\times10^{-1}$	$+1\cdot10$	14
$-4\cdot17\times10^{-1}$	$-3\cdot51\times10^{-1}$	$-2\cdot67\times10^{-1}$	13
$+1\cdot48\times10^{-2}$	$+7\cdot15\times10^{-2}$	$+9\cdot32\times10^{-2}$	13·5
$+1\cdot99\times10^{-3}$	$+3\cdot91\times10^{-2}$	$+5\cdot77\times10^{-2}$	12
$+6\cdot09\times10^{-3}$	$+8\cdot98\times10^{-3}$	$+1\cdot80\times10^{-2}$	14
$-1\cdot19\times10^{-2}$	$+\ldots\ldots\ldots$	$+5\cdot07\times10^{-3}$	13
$-1\cdot06\times10^{-2}$	$-4\cdot45\times10^{-3}$	$-1\cdot03\times10^{-3}$	12
$-9\cdot42\times10^{-3}$	$-4\cdot15\times10^{-3}$	$-1\cdot01\times10^{-3}$	12
$-8\cdot60\times10^{-3}$	$-3\cdot10\times10^{-3}$	$-8\cdot20\times10^{-4}$	12·5
$-6\cdot57\times10^{-3}$	$-2\cdot84\times10^{-3}$	$-7\cdot39\times10^{-4}$	12
$-4\cdot86\times10^{-3}$	$-1\cdot70\times10^{-3}$	..	15
$-2\cdot41\times10^{-3}$	$-7\cdot41\times10^{-4}$	..	14
$-1\cdot33\times10^{-3}$	$-3\cdot80\times10^{-4}$	..	14·5
$-7\cdot53\times10^{-4}$	..	..	12
$-4\cdot66\times10^{-4}$	..	..	13·5
..	..	..	..

agnetic Effects,' p. 124.

produce the reversal of the sign of the Hall coefficient thus depends upon the composition of the alloy.

As previously mentioned, the reversal of the Hall coefficient with increasing magnetic field strength has been studied by A. W. Smith *. He investigated alloys containing 3, 5, and 10 per cent. of lead, and found a reversal of sign in each case. The present results for alloys containing 3 and 10 per cent. lead also show reversals with increasing magnetic field, but the values of the field required to produce a reversal are not in agreement with those obtained by Smith. These discrepancies may, however, be due to differences in the heat treatment of the alloys, as is shown by the results of experiments on a second plate containing 90 per cent. bismuth and 10 per cent. lead. The Hall coefficients of this unannealed plate were measured immediately after preparation, and also after an interval of one month. The values of the coefficients are plotted in Graph VIII., which also includes, for the sake of comparison, the results of experiments on the fully annealed plate of the same composition.

The graph shows that, after the unannealed plate had been kept for a month, the field required for reversal had changed from about 4300 to about 5400 gauss. The unannealed curve is gradually shifting towards that obtained for the annealed specimen of the same composition.

XXVIII. *The Relation between Strain and Photo-elastic Effect in Phenolite.* *By* J. Kuno, *Dr.Eng., Assistant Professor of Civil Eng., Kyushu Imperial University, Fukuoka* †.

I. Introduction.

PHENOLITE supplied by the "Riken" in Tokyo is now extensively used in this country as a more suitable material than the others for the purpose of photo-elastic experiments. In this paper the relation between strain and optical effect is examined, with experiments, in order to settle the important question whether the photo-elastic phenomenon in phenolite is caused by the strain or not.

* A. W. Smith, *loc. cit.*

† Communicated by the Author.

As a fundamental relation for the fringe method of the photo-elastic observation, the author described in his previous paper * the law of photo-elastic extinction, *i. e.*,

$$S \cdot d = K \cdot N, \quad . \quad . \quad . \quad . \quad . \quad . \quad (1)$$

where d = the thickness of the specimen tested ;

S = the difference of the two principal stresses at the point extinguished under circularly polarized monochromatic light ;

N = the order of extinction, *i. e.*, a numerical value indicating the order of the black fringe passing through the point under consideration;

K = the coefficient of photo-elastic extinction, which indicates the stress-optical sensibility of the material of the specimen used.

K and N are shown to vary with the time elapsed after loading, in spite of S kept constant. From this fact it may be said that the stress is not the immediate cause of producing the photo-elastic phenomenon. That is the reason why the strain should be investigated.

Before going further the author wishes to acknowledge his indebtedness to Prof. A. Ono for helpful suggestions and criticisms.

II. The Relation between Optical Effect and Time t.

Experiments described in the paper cited above were made with specimens of phenolite under simple stress. The optical effect was measured by Babinet's compensator properly set in the beam of polarized green light (5461 Å.) of the mercury lamp supplied by the "Riken." The data thus obtained are again used for the present purpose.

Regarding the use of the compensator, the notation a stands for the distance through which a wedge is moved in order to replace a dark band with an adjoining one, when no specimen is set in the beam of light. The phase difference increased by the displacement a is equal to 2π. If we insert a specimen properly and apply some load to it, the central band viewed in the field of the compensator is shifted to another position. The wedge

* Phil. Mag. xii. p. 503 (1931).

is then moved by the micrometer screw until the band comes again to the initial position. This distance is referred to as *the band displacement* x. Generally x consists of two parts, one being the optical effect attained at the instant of loading and the other the creep observed at the instant t minutes after loading.

In the case of such measurements the order of extinction may be given by the equation

$$N = x/a, \qquad \ldots\ldots \quad (2)$$

where N is not always integral. A fractional value of N corresponds to the state of stress at the point where the phase difference produced is not equal to 0, 2π, 4π, ... Inserting (2) into (1), we can define the quantity y by the expression

$$y = S/K = x/ad. \qquad \ldots\ldots \quad (3)$$

Then y represents the total optical effect per unit thickness at any instant expressed in multiple of the unit defined by the distance a. As a and d are constants, the quantity y is to be a certain function of stress S and time t, just as the band displacement x is to be.

From the data obtained in the experments mentioned above, the values of y were calculated, and they were plotted to time t on the logarithmic paper. The curve drawn through the points belonging to a definite value of the stress S was found linear. Accordingly it may be represented by the equation of the form

$$y = \beta S t^r.$$

The coefficient β and the index r for $t < 16$ minutes were found as follows :—

$$\beta = 0{\cdot}0939 \pm 0{\cdot}00005,$$

$$r = 0{\cdot}0271 \pm 0{\cdot}0002.$$

Hence we have

$$y = 0{\cdot}0939\, S t^{0{\cdot}0271} \qquad \ldots\ldots \quad (4)$$

This relation holds for any values of t from 1 to 16 minutes. The expression for the values of t greater than 16 minutes was not considered, as the corresponding strain-time relation could not be obtained, the reason being given in the next article.

III. The Relation between Strain and Time t.

The tension specimens and the straining apparatus that were employed in the optical measurements were again used for observing the strain. The elongations on the gauge length of 20 mm. were measured by Huggenberger's tensometers, of which one division of the scale corresponds to 1/1200 mm. A number of tests were carried out under various loads. Each set of observations was performed by keeping the load constant and by taking the reading of the tensometer at intervals of 1 minute for the first 16 minutes. The room temperature during the period of these tests varied from 13° to 18° C. Since the size of the phenolite plates supplied was comparatively small, the tension specimens with relatively long gauge length could not be prepared. This restriction of the gauge length limited the measurements to the first 16 minutes, as the creep for the following 20∼120 minutes was relatively small and it seemed very difficult to measure it with precision.

The tensometer readings for each set of observations were plotted to time on the logarithmic paper. It was then found that the strain-time relation can be represented by the equation of the form

$$\epsilon = \beta' \, S t^z,$$

where ϵ is the strain, S in kg./cm.^{2} and t in minutes.

The coefficient β' and the index z were found as follows:—

$$\beta' = (0{\cdot}2338 \pm 0{\cdot}0002) \, . \, 10^{-4},$$

$$z = 0{\cdot}0288 \pm 0{\cdot}0002.$$

Hence we get for phenolite

$$\epsilon = 0{\cdot}2338 \, . \, 10^{-4} S t^{0{\cdot}0288} \quad . \quad . \quad . \quad . \quad (5)$$

IV. The Relation between Strain and Optical Effect.

In the above two articles it was found that the optical effect and also the strain undergo the time effect ; namely, the equations (4) and (5) are

$$y = 0{\cdot}0939 \, S t^{0{\cdot}0271},$$

$$\epsilon = 0{\cdot}2338 \, . \, 10^{-4} \, S t^{0{\cdot}0288}.$$

The rate of change of y with the time differs slightly from that of ϵ. The difference of the two indices is

$$0{\cdot}0288 - 0{\cdot}0271 = 0{\cdot}0017.$$

The values of $t^{0{\cdot}0288}$, $t^{0{\cdot}0271}$, and $t^{0{\cdot}0017}$ are plotted in fig. 1

If we eliminate the stress S from the above two equations we have

$$y = \mathrm{K}' \epsilon, \qquad \ldots\ldots\ldots \quad (6)$$

where

$$\mathrm{K}' = 4020\, t^{-0{\cdot}0017}.$$

Fig. 1.

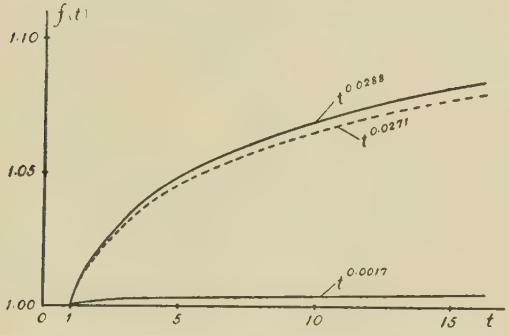

The coefficient K′ calculated for some values of t are shown in the next table, in which the values of $t^{0{\cdot}0017}$ are also given.

t	1	2	5	10	15
K′	4020	4015	4009	4004	4002
$t^{0{\cdot}0017}$	1·000	1·0012	1·0027	1·0039	1·0046

Now it is apparent that, if we neglect some errors less than one per cent., the coefficient K′ may be considered approximately as a constant. Hence it seems that the strain may be the immediate factor in producing the photo-elastic phenomenon, so far as the above experiments are concerned.

V. Consideration of the Lateral Strain.

There is still a question whether the lateral strain takes part in producing the double refraction. In order to investigate this problem, a number of tension tests were made to measure the lateral strain under various

loads. The apparatus employed in the previous experiments was again used. Two specimens of phenolite were prepared for this purpose. The shape of the specimens was nearly the same as those used before (see the figure on p. 506 of the Phil. Mag. xii. (1931)), except that the width was 25 mm. at the centre and 50 mm. at the ends. Each set of observations was carried out by keeping the load constant, and by reading the lateral contraction at intervals of 1 minute for the first 16 minutes. The room temperature during this period varied from 13° to 18° C.

Plotting the observed values of the lateral contraction to time on the logarithmic paper, it was found that the strain-time relation can be represented by the equation of the form

$$\eta = \gamma S t^{w},$$

where η is the lateral strain. It was found that the coefficient γ and the index w are as follows :—

$$\gamma = (0{\cdot}0833 \pm 0{\cdot}0009) \,.\, 10^{-4},$$

$$w = 0{\cdot}0287 \pm 0{\cdot}0002.$$

Hence the lateral strain is given by the expression

$$\eta = 0{\cdot}0833 \,.\, 10^{-4}\, S t^{0{\cdot}0287} \quad . \quad . \quad . \quad . \quad (7)$$

As the longitudinal strain is given by (5), *i. e.*,

$$\epsilon = 0{\cdot}2338 \,.\, 10^{-4} S t^{0{\cdot}0288},$$

the value of Poisson's ratio of phenolite is

$$\begin{aligned} 1/m &= \eta/\epsilon \\ &= 0{\cdot}356\, t^{-0{\cdot}0001}. \end{aligned}$$

The index of t in this expression being smaller than the corresponding probable error in magnitude, it may be said that Poisson's ratio of phenolite undergoes little time effect. We have therefore

$$\left.\begin{aligned} 1/m &= 0{\cdot}356, \\ m &= 2{\cdot}81, \end{aligned}\right\} \quad . \quad . \quad . \quad . \quad . \quad (8)$$

Hence the lateral strain can be represented by the term of the longitudinal strain. We then have

$$\eta = -\epsilon/m.$$

Take for the present the greatest shearing strain e as the immediate cause of the optical effect instead of the

linear strain ϵ taken in the previous article. Then introducing a constant K″, we may put

$$y = \mathrm{K}''e.$$

From the mathematical theory of elasticity it is known that the principal strain difference $(\epsilon - \eta)$ at a point is equal in magnitude to the greatest shearing strain at the point. Hence we may have

$$y = \mathrm{K}''(\epsilon - \eta),$$

and this is the same as

$$y = \frac{1+m}{m}\mathrm{K}''\epsilon \quad . \quad . \quad . \quad . \quad . \quad . \quad . \quad (9)$$

As m is practically independent of the time effect, the coefficient K″ varies with time in a similar way to K′ in the equation (6)

$$y = \mathrm{K}'\epsilon.$$

Thus the consideration of the lateral strain adds nothing new to the interpretation of the creep in the case of phenolite.

VI. Discussion of the Result.

(1) *Photo-elastic Phenomenona in Other Materials than Phenolite.*

As to the relation between strain and optical effect, a number of experiments have been made by various authors with specimens of glass, celluloid, and bakelite.

As for glass, Filon and Jessop* tested a number of blocks of glass with the result that there was neither optical creep during the time the load was left on, nor any trace of residual double refraction on removal of the load. In their tests, the blocks were left under the compressive stress of 149 to 220 kg./cm.^{2} for 17 to 67 hours.

S. R. Savur † showed with specimens of glass that the dark band took its final position simultaneously with the application of the load and that no residual effect could be observed when the load was removed.

The result obtained by K. Okuda ‡ with a tension specimen of glass, which was left under the stress of

* Phil. Trans. A, ccxxiii. p. 91 (1923).
† Phil. Mag. l. p. 459 (1925).
‡ Memoirs, Coll. Eng. Kyush Imp. Univ. iii. p. 171 (1927).

400 kg./cm.^{2} for 17 hours at the room temperature, showed that no residual double refraction was detected in it after the removal of the stress.

As for celluloid, there have been also some investigations *. Experiments carried out by Filon and Jessop with tension specimens indicated that the optical retardation shows an immediate effect on loading, very nearly proportional to the applied load, followed by a progressive creep until an equilibrium value is approached, and that the strain follows the laws closely similar to those of the optical retardation, the initial value being also approximately proportional to the applied load. According to their result, the retardation r and the strain ϵ are connected with the time t by the relations

$$r = r_0 + pt^{1/3} + qt,$$
$$\epsilon = \epsilon_0 + at^{1/3} + bt.$$

In these the constants r_0 and ϵ_0 are proportional to the applied stress T; the constants p and a are very roughly proportional to the square of T; and q and b are small and irregular. On examining the relation between strain and optical effect, the result they obtained does not conform to the hypothesis that stress is the immediate factor in producing the artificial double refraction, and also the hypothesis which makes strain the essential factor. Thus they were led to establish the linear law

$$r = \alpha \mathrm{T} + \beta\epsilon,$$

where the constants α, β are found to vary within fairly narrow limits for any given specimen. They have also shown that Coker and Chakko's result may be expressed by the relation

$$r = a + b\mathrm{T} + c\epsilon,$$

where the first term on the right side shows the initial stress and optical effect existing in the material before loading. Hence it appears that the result of Coker and Chakko is in agreement with that of Filon and Jessop.

As for bakelite, no particular observations seem ever to have been made except the experiments carried out by I. Arakawa†, who measured the optical effect with

* Filon & Jessop, *loc. cit.*; Coker and Chakko, Phil. Trans. A, ccxxi. p. 149 (1921); Ramspeck, *Ann. der Physik*, lxxiv. p. 722 (1924).

† Proc. Phys. Math. Soc. Japan, v. p. 117 (1923).

specimens of bakelite and not the strain. The result of his observations showed that the formula

$$r=r_0+pt^{1/3}+qt$$

also holds good in the case of bakelite, the constants r_0 and p being roughly proportional to the stress T, and the constant q small.

As the experiments show that the constant q is small in celluloid and bakelite, the optical effect r may be expressed approximately by the equation

$$r=r_0+pt^{1/3}. \quad . \quad . \quad . \quad . \quad . \quad . \quad (10)$$

In connexion with this formula, it is worthy of remark that the constant p, the coefficient of t, is roughly proportional to T in bakelite, and to T^2 in celluloid.

In phenolite the optical effect y is proportional to the stress S, as the equation (4) shows. If we compare this fact with the equation (10), it may be said that the stress-optical property of phenolite is very near to that of bakelite. This may be due to the fact that phenolite and bakelite are chiefly made of the same materials, *i. e.*, phenol and formaldehyde.

(2) *Temperature Effect.*

The measurements of strain and optical effect described above were made in a few months, so the room temperature varied from 13° to 21° C. In each series of optical tests, which continued some 20 minutes, the temperature varied within 1°. During each set of the strain measurements the temperature remained nearly constant.

In the temperature range above mentioned the effect of temperature on the optical phenomenon is not clear, but it is likely that this source of effect may exist. In this respect, further investigations are needed by taking a wider range of the temperature, say 30° C. or more.

(3) *The Effect of Heat Treatment.*

It is well known that the elastic properties of steel are changed to a remarkable degree by the heat treatment. A similar fact is recently found in phenolite by M. Nisida *. Phenolite, generally speaking, is finished in an air-bath after being casted by keeping the temperature at 100° to

* Bulletin, Inst. Phys. Chem. Res. xii. p. 1 (1933).

140° C. for several hours. By changing the temperature and time of baking, five kinds of materials are prepared by Nisida. Slightly modifying the results he obtained, we have the next table, where E_0 is the Young's modulus in kg./cm.^{2} at the instant of loading and K_0 the coefficient of extinction in kg./cm. for $t=0$.

Materials.	Treatment.	E_0, 10^4.	K_0.
No. 0	Very soft.	1·2	10·6
No. 1	Not baked.	2·2	13·2
No. 2	100° C.—15 hours.	4·0	14·3
No. 3	120° C.—15 hours.	5·8	14·7
No. 4	120° C.—5 days.	6·6	15·0

The constants for the material used in author's experiments are

$$E_0=4{\cdot}3\times10^4 \text{ kg./cm.}^2 \quad \text{and} \quad K_0=11{\cdot}0 \text{ kg./cm.}$$

Thus the numerical values indicating the properties of phenolite do not remain constant. Nisida's results, which are not written here, however, seem to show that the qualitative nature given in this paper may be consistent with those to be obtained with other kinds of phenolite.

(4) *The Effect of Ageing and Constituents.*

It is likely that the effect of lapse of time after casting on the nature of phenolite appears to be comparatively large. Moreover, phenolite may vary its properties according to a slight change in the proportion of the constituents. In these respects, further investigations are needed.

VII. Summary.

For phenolite, the experiments made by the author show the following :—

(1) The photo-elastic phenomenon is not caused by the stress.

(2) The strain seems to produce the photo-elastic effect.

(3) Poisson's ratio is independent of the time effect.

XXIX. *Some Wave-length Determinations in the very soft X-Ray Region. By* F. C. Chalklin, *Ph.D., Lecturer in Physics, and* L. P. Chalklin, *Ph.D., University College, London* *.

[Plates VI. & VII.]

I. *Introduction.*

UP to the year 1927 the very soft X-rays from solids (X-rays with wave-lengths greater than about 20 Å.) had defied accurate direct measurement. Indirect experiments of the critical potential type, depending in almost every case on photoelectric detection of the radiations, had indeed been carried out, had certainly proved the existence of the soft characteristic radiations, and had given values for the energy levels concerned in the production of the X-rays. The technique involved in these experiments is difficult, and the results are not always easy to interpret. Indeed, in the most recent work the critical potentials are far too numerous for all to be due to ordinary atomic energy levels. There is some evidence that a number of the effects are a feature of the crystalline state of the emitting element †. It was thus very desirable that some method of direct soft X-ray spectroscopy should be developed.

In 1925 Compton and Doan ‡ demonstrated that it was possible to obtain hard X-ray spectra by means of an ordinary plane grating placed so that the X-ray beam struck it at almost grazing incidence. A little later Thibaud § announced the successful application of this method to the spectroscopy of soft X-rays.

II. *Description of Apparatus.*

In 1930 the writers designed a simple form of high vacuum spectrograph, similar to that of Thibaud, for soft X-ray work. In order that adjustments might be made in the open, the optical system was made as a separate unit. A photograph of it is shown in fig. 1

* Communicated by Prof. E. N. da C. Andrade, D.Sc.

† See Richardson and Andrewes, Proc. Roy. Soc. A, cxxviii. p. 63 (1930).

‡ Proc. Nat. Acad. Sci. xi, p. 598 (1925).

§ *Journ. de Phys.* viii. p. 447 (1927).

(Pl. VI.) and a vertical section in fig. 2 *a*. The components are screwed down to a rigid steel bench which can conveniently be slid into the casing of the spectrograph when the adjustments have been performed.

Fig. 2 *a*.

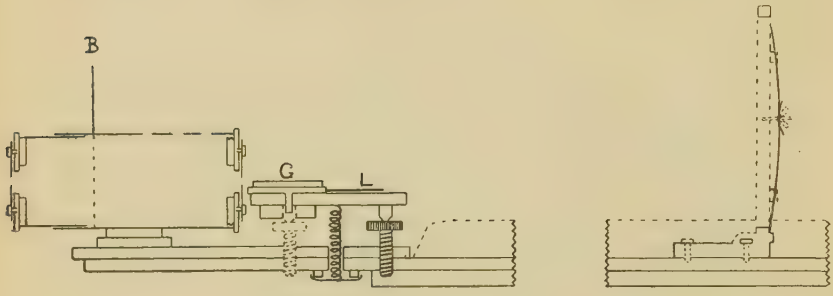

Two horizontal slits, formed by cobalt steel razor-blades, limit the width of the incident X-ray beam. The slit widths have been altered from time to time during the course of the experiments, but were never much greater than 0·1 cm. nor less than ·005 cm. They are 12·5 cm. apart. Each slit can be rotated in a vertical plane,

Fig. 2 *b*.

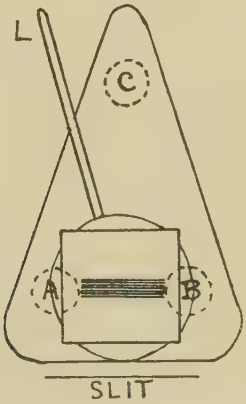

and is adjusted to be parallel to the horizontal base of the optical bench. Immediately beyond the second slit is the grating G, mounted horizontally on a small circular table. This table can be rotated by means of the lever L (fig. 2 *b*) and is mounted on a larger triangular table by

means of the screws A, B, and C. AB is perpendicular to the length of the optical bench, so that, whilst the screws A and B and the rotating table allow the grating to be set parallel to the slits, the screw C controls the angle at which the radiation strikes the grating. The rotating table is mounted directly above AB in order that the height of the grating shall be as little as possible affected by the adjustment of the screw C. The plate-holder, which is vertical, is 50 cm. from the ruled portion of the grating. Our apparatus allows this distance to be increased to 88 cm. if desired, but, in the present series of experiments, the increase in dispersion so obtained was of less importance than the good intensity obtainable at small distances.

The gratings used in these experiments had rulings 2 cm. long, but the width of the ruled surface was in no case greater than 3 mm. Since the incident beam makes an angle of about 1° with the surface of the grating the effective width of the ruled portion is approximately 1/20 mm. The grating itself thus forms a slit from which the diffracted X-rays emanate, this slit being in our experiments usually narrower than the adjacent razor-blade slit. The incident beam is in effect, therefore, limited by the first slit and the grating, the second razor-blade slit merely serving as a screen.

The two horizontal slits having been adjusted, a beam of light is passed through them and the grating adjusted, by screws A, B, and C, to lie centrally in the beam and at the desired angle of incidence. The rotating table is then turned until the midpoints of the spectral lines lie in a vertical plane through the source, centre of the grating, and centre of the plate-holder.

The vacuum chamber can be seen in fig. 3 (Pl. VI.). It consists of a cylinder, constructed of cold drawn steel, to flanges of which gun metal end-plates are bolted. These joins are rendered air-tight by rubber gaskets. The end-plates are readily removed and can be replaced speedily without danger of a leak occurring. The far end-plate in fig. 3 (Pl. VI.) projects into a dark-room in order to facilitate the loading and immediate development of the plates. The whole apparatus is singularly air-tight, and the overnight leak is less than 1/50 mm. of mercury. The pumping line, constructed of 3·5 cm. tubing and including a liquid-air trap, is connected to the

body of the spectrograph. Pumping is effected by means of a Gaede three-stage mercury vapour-pump, backed by a rotary oil-pump. The pressure, recorded by a McLeod gauge, is usually a little greater than 10^{-5} mm. of mercury. It is probably not so good as this, since the McLeod gauge does not record the pressure of condensable vapours.

To afford ease of adjustment and dismantling, and simplicity of construction, the X-ray tube has been made of transparent silica, with stoppers sealed in by means of hard red sealing-wax. It carries a water-cooled anti-cathode. The upper neck, which carries the filament stopper, is made narrow in order that the sealing-wax join should be heated as little as possible by the hot portions of the X-ray tube. It was, nevertheless, necessary to cool this and the filament lead seals by means of water-baths. A side-tube, level with the anti-cathode, slides over a short brass tube which projects from the near end-plate of the spectrograph (see fig. 3 (Pl. VI.)). This side-tube is sealed to the body of the spectrograph, and the constriction A in fig. 2 *c* ensures that the brass tube, cooled by its connexion with the body of the instrument, shall efficiently protect this seal from radiation from the anti-cathode.

Owing to the presence of the hydrocarbon vapours, which emanate from the walls and gaskets of the spectrograph, carbon is deposited on the cold anti-cathode surface during the exposures. This deposit not only tends to prevent the bombarding electrons from reaching the anti-cathode, but also tends to absorb the X-rays emitted from the surface of the latter. If short wave-length X-rays are to be examined and high voltages employed, the difficulty is not serious, but since, in the present research, it was proposed to measure wave-lengths of the order of 50 Å., and since the voltages were comparatively low, it became necessary to avoid the deposit *. The difficulty may be overcome by depositing on the anti-cathode a film of the required element during the actual exposure, thus ensuring that there is always a certain amount of the element at the

* Owing to this it was found that the water-cooled platinum and palladium anti-cathode, very kindly constructed for us by Dr. V. E. Pullin, of the Radiological Research Department, Woolwich Arsenal, did not yield satisfactory spectra for these elements.

surface. This method was employed by Thibaud and Soltan *. They produced the film by using as the cathode of their X-ray tube a hot filament of the element under examination, which then served not only as the source of electrons, but also deposited the required metal with the carbon on the anti-cathode. We have employed

Fig. 2 *c*.

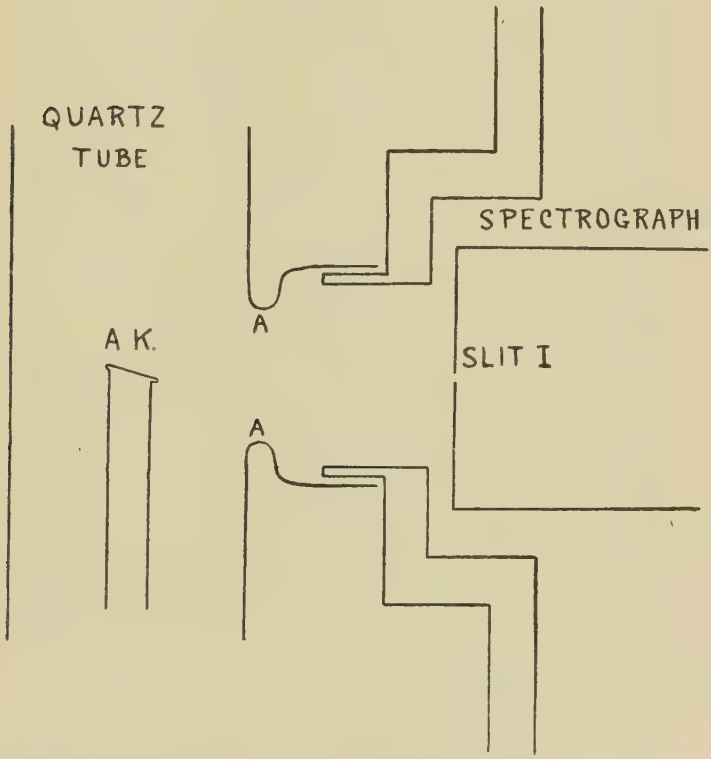

this method for tungsten, tantalum, and molybdenum but there are obviously few elements which can be so used. We have therefore adopted the practice of allowing our anti-cathodes to be so heated by the electronic bombardment as to allow little carbon to remain on the surface. For this reason, sheet metal anti-cathodes were fixed so as to make only poor thermal contact

* *Journ. de Phys.* viii. p. 484 (1927).

with the water-cooled electrode, and the thermionic current was adjusted so as to raise them to the required temperature.

The cylindrically shaped slit system, sliding into the vacuum chamber, comes opposite to the anti-cathode and projects into a recess in the near end-plate (fig. 2 *b*). To permit efficient evacuation of the X-ray tube ample space is left around the slit system. The arrangement ensures, however, that light, entering from the X-ray tube, must undergo at least two scattering processes before entering the body of the spectrograph. Any light which has succeeded in entering the spectrograph is stopped by the screen B in fig. 1 (Pl. VI.) and fig. 2 *a*.

During the course of our experiments three glass gratings have been used. The first of these had 1134 lines per mm., and with it faint spectra were obtained provided the grating was frequently cleaned. Far greater intensity was obtained with the other two gratings. These were ruled by the Siegbahn engine at Uppsala. Of these two gratings one possessed 300 lines per mm. and the other 600 lines per mm. The 300 line per mm. grating was used for nearly all the wave-length determinations, since it gave good intensity in the higher orders, thus allowing the plates to be calibrated easily. We have observed a spurious image * due to the reflexion, at the under side of the grating, of visible light, which, emitted mostly by the filament of the X-ray tube and scattered by the anti-cathode, passes through the slits along with the X-ray beam. To avoid these images we have ground the under sides of the Siegbahn gratings and have then blackened them with Indian ink. The 1134 lines per mm. grating was already ground.

III. *Photographic Plates.*

Söderhann † has published spectrograms taken with both Schumann and Imperial Eclipse plates. They seem to indicate that although the former are superior at wave-lengths greater than 90 Å., the latter are preferable for shorter wave-lengths. We have made tests with a number of plates of different makes and speeds varying from H and D 25 to H and D 1400, using the molybdenum

* See Siegbahn and Magnusson, *Zeits. f. Phys.* lxii. p. 435 (1930).
† *Zeits. f. Phys.* lxvii. p. 790 (1931).

line at 64 Å. Pairs of plates were placed side by side in the spectrograph in order that the conditions of exposure should be approximately the same for each. An exposure with a single wide plate showed that this condition was satisfied.

In addition to the soft X-ray spectrum and possibly some scattered soft X-rays, the plate receives some visible light diffracted by the slits or scattered at the grating surface. A visual examination of our plates shows that the fogging due to visible light varies much more rapidly with the speed of the plate than does the blackening produced by the soft X-rays. This was finally tested by giving a short exposure to a very fast (Imperial Eclipse) plate and a long exposure to a very slow (Ilford Process) plate, so that the fogging on each plate was about the same. The intensity of the 64 Å. was considerably greater for the Process than for the Eclipse plate. It was therefore decided that slow plates were best for our purpose, and Ilford Process plates were chosen as the most satisfactory. The slow plate has the additional merit of possessing a fine grain.

Optical fogging of the plates, strongest in the neighbourhood of the directly reflected beam, was prevented by placing a thin sheet of aluminium foil over the plate-holder in this region. The aluminium foil was sufficiently thin to allow the directly reflected beam of soft X-rays to penetrate and form a trace on our plates. This trace was, unfortunately, never sufficiently definite to allow of reliable measurements being based upon it.

IV. *Determination of Wave-lengths.*

The results obtained in these experiments have been based on the accurately known wave-length of the copper L_α line (13·306 Å.) derived from crystal X-ray spectroscopic experiments. Hence, since we have not concerned ourselves with absolute determinations, the only measurements involved are those of the positions of the lines on the plates. The microscope measurements of the plates were in some cases supplemented by microphotometer records made from our plates. These records were useful for locating absorption edges and weak or diffuse lines. They were very kindly made for us by Prof. F. J. M. Stratton at Cambridge.

To determine the wave-length of a line, an empirical equation connecting wave-length with displacement from the directly reflected beam was employed. In the equation adopted the wave-length was assumed to be given by the sum of ascending power terms of the displacement, the constants of the terms being found by calibration. To make the equation satisfactory for the large displacements obtained in some of the experiments, terms as far as the fourth power were required. The use of higher power terms was found unnecessary, but, owing to the difficulty of assessing the exact position of the directly reflected beam, it was necessary to include a constant term.

In order to obtain the constants of the empirical equation a long copper exposure is made, the usual tungsten filament being employed. In this way it is possible to obtain five measurable orders of the copper L_α line. Since there are five constants in the equation, measurement of this spectrum would yield just sufficient data to determine them. The five copper orders, however, cover only about one-third of the effective length of the plate. On the other hand, molybdenum gives a very intense line ($M_{IV,\,V}$–$N_{II,\,III}$) of about five times the wave-length of the copper L_α line, and this line can often be obtained in six measurable orders covering the whole length of the plate. The measurements of a molybdenum spectrogram have therefore been referred to the copper spectrogram, thus giving a total of eleven measurements with which to determine the constants of the equation. Since the wave-length of the molybdenum line is unknown, it constitutes a sixth constant to be determined. Dr. L. J. Comrie, Director of H.M. Nautical Almanac Office, very kindly planned the computing of the wave-lengths from the formulæ and arranged to have the work carried out under his supervision *.

The directly reflected beam, some of it reflected from unruled portions of the glass grating, being found unsuitable for measurement, and therefore unavailable as a reference line, it was decided to use actual soft-X-ray lines, narrowed by the "focussing" property of the tangential grating, for this purpose. The following

* The expenses of computation were met by Professor Andrade from a grant made to him by Imperial Chemical Industries Ltd.

procedure was adopted. After an adequate exposure with a copper anti-cathode had been made, the tungsten filament of the X-ray tube was replaced by one of molybdenum, the anti-cathode and the photographic plate in the spectrograph remaining untouched. The exposure was then continued, molybdenum from the filament rapidly sputtered on to the anti-cathode and the molybdenum line, in two or more orders, was superposed on the copper spectrum on the photographic plate. A composite spectrogram obtained in this way is shown in fig. 4 (Pl. VII.). With the aid of these superimposed lines a separate molybdenum spectrogram, having as many molybdenum orders as possible, could be referred to the copper plate.

The constants of the equation having been determined, the wave-lengths of the lines of other spectra can be determined by referring them to the copper-molybdenum calibration spectrum. This reference can again be performed by the molybdenum sputtering method. In addition, the K_α line of oxygen appears on most of our plates in one or more orders, the oxygen being present as an anti-cathode impurity, probably in the form of tungsten oxide. This line has been used as an additional and in some cases as an independent reference.

It is necessary to consider the possibility of a reference error arising if the focal spot of the molybdenum filament does not coincide with that of the tungsten filament. Such a shift, within the limits imposed by the slits, would entail a change in the angle of incidence of the X-ray beam on the grating and a small displacement of the molybdenum lines. This displacement is smallest for long wave-lengths and high orders. Thus for a 300 lines per mm. grating in a typical setting, and for a shift of 0·1 mm. in the directly reflected beam, the first order of the molybdenum line (64·08 Å.) would be displaced 0·037 mm. and the second order 0·028 mm., whilst the first order of oxygen (23·57 Å.) would have a displacement of 0·054 mm. The relatively long wave-length of the molybdenum line is thus an advantage in its use for reference purposes. If the focal spot is diffuse and of a width much greater than that required to fill the slit, then a small change in its position should not alter greatly the average angle of incidence of the beam passing through the slits. In the present type of research, the

heavy thermionic currents and the low voltages employed cause the ordinary focussing cylinder to function but poorly, and the focal spots are actually large and indefinite. In fact, with the narrow anti-cathodes, only 1 cm. wide, used in these experiments, the incandescent spot has in some cases extended across the entire width. The oxygen references, despite the fact that they do not involve the use of a separate filament, are not necessarily free from an error of this type. The oxygen may emanate, particularly for hot anti-cathodes, from a ring of oxide around the focal spot. It is therefore possible for the mean angle of incidence of the oxygen radiation not to coincide with that of the radiation under investigation. The measure of agreement between values of lines obtained by referring to separate reference lines, either on the same plate or on different plates, furnishes the best test of the reliability of the reference lines, and we have come to the conclusion that the reference errors are not much greater than the ordinary errors of measurement. At the expense of intensity, the accuracy of the reference method would be increased by employing narrower slits and would also be increased by making use of the increased "focussing" obtainable with more closely ruled gratings. It might then, however, be less easy to calibrate the plates.

During the course of these experiments a number of calibrating plates have been taken. Each yields a value of the molybdenum lines ($M_{IV,\,V}$–$N_{II,\,III}$). The values so obtained are :—64·01, 63·98, 64·26, 63·85, and 64·32 Å., giving a mean value of 64·08 Å., the maximum error being about one in three hundred. It will be observed that the variation between these values is greater than that for the lines mentioned later in this paper. Yet the latter were, on the whole, more difficult to obtain and to measure, and also involved the use of reference lines.

The larger variation in the molybdenum lines is to be ascribed to differences in the calibration equations, since, while the values listed for the molybdenum line were in each case the result of a separate calibration, the results for the other lines were usually obtained for a single grating setting and a single calibration equation. It must be remembered that the calibration, for relatively long wave lines, despite the use of the many orders of molybdenum, does constitute an extrapolation. Again,

in order to avoid the use of subsidiary standards, it was necessary to obtain copper L_α in a large number of orders and thus, whilst the first order was over-exposed, the highest was inevitably weak and difficult to measure. In addition, the first order reading would be slightly affected by the presence of the weak unresolved L_β line.

V. *Results.*

Molybdenum.

An intense molybdenum spectrum is shown in fig. 5 (Pl. VI.). This was obtained with a hot sheet molybdenum anti-cathode. The molybdenum ($M_{IV,\,V}$–$N_{II,\,III}$) line (A in fig. 5 (Pl. VI.)) is strong in seven orders. The figure shows how the grating used tends to suppress the first and fourth orders of the lines. This effect is much less marked for shorter wave-lengths. The mean value for the molybdenum ($M_{IV,\,V}$–$N_{II,\,III}$) line, whose measurement we have already discussed, is 64·08 Å. $\frac{\nu}{R}=14{\cdot}22$. This line was first observed by Thibaud and Soltan *, who, making an absolute determination, obtained for it the value 65·0 Å. Cork † gives the wave-length as 64·52 Å. The line B in fig. 5 (Pl. VI.) has been measured on a number of occasions, the individual values being :—Order I., 54·74, 54·87 Å.; Order II., 54·63, 54·80, 54·71, 54·81, 54·73 Å. ; Order III., 54·62 Å. The mean value is 54·74 Å., $\frac{\nu}{R}=16{\cdot}65$. There is a certain amount of inaccuracy in the determination of this line, owing to the fact that it is not completely resolved from the tungsten line at 55·29 Å. ; the latter line is, however, on the measured plates, very faint compared with the molybdenum line. Thibaud and Soltan give this line as 54·9 Å., and Cork's value is 55·17 Å.

The extremely faint lines C and D in fig. 5 (Pl. VI.) have not been measurable with the microscope, and our values for them, 59·6 Å. and 68·6 Å., $\frac{\nu}{R}=15{\cdot}3$ and 13·3 respectively, were obtained by means of a photometer

* *Journ. de Phys.* viii. p. 484 (1927).
† Phys. Rev. xxxvi. p. 665 (1930).

record. Cork has observed faint lines at 6·9 per cent. less and 7·2 per cent. greater wave-lengths than the strong molybdenum line. The values for our two lines are 6·7 per cent. less and 7·3 per cent. greater respectively.

The stronger line E has been measurable on two plates, the values being 74·27 and 74·36 Å., mean value, 74·31 Å. $\frac{\nu}{R}=12{\cdot}26$. Of these five molybdenum lines, those at 64·08 Å., 54·74 Å., and 74·31 Å. have also been observed for sputtered molybdenum with roughly the same relative intensities. The remaining two lines would have been too faint to appear.

Table I.

Results for Molybdenum.

Wave-length.	Relative intensity.	Voltage.	$\frac{\nu}{R}$.
54·74 Å.	5	225·6	16·65
59·6 Å.	0	207·1	15·3
64·08 Å.	10	192·6	14·22
68·6 Å.	0	180·0	13·3
74·31 Å.	2	166·1	12·26

Molybdenum Line at 64·08 Å.

This is the strongest of the five lines. It is satisfactorily explained by the level values predicted from hard X-ray data. Thus we find that the transitions (M_{IV}–N_{II}), (M_{IV}–N_{III}), and (M_{V}–N_{III}), all permitted by the selection principle, should, according to the tables given by Lindh *, correspond to values of $\frac{\nu}{R}=14{\cdot}0$, 14·3, and 14·1 respectively: Siegbahn's † tables yield the value $\frac{\nu}{R}=$ 14·4, 14·4, and 14·2. We may safely attribute the observed line to one or more of these processes, and we have, therefore, designated it ($M_{IV,\,V}$–$N_{II,\,III}$). No splitting of the line has yet been observed, even in the sixth order, which

* "Röntgenspektroskopie," Wien-Harms, 'Handbuch der Experimental Physik,' Band xxiv. Teil 2, p. 228 (1930).

† 'Spektroskopie der Röntgenstrahlen' (1931).

has been obtained with good intensity. Prins *, calculating the oscillator strengths, f, of the (M–N) lines of silver on the basis of the eigenfunctions given by Slater, finds that ($M_{IV, V}$–$N_{II, III}$) has the greatest value. The calculation of the relative intensities, however, requires that the f should be multiplied by ν^3. If this is done (M_I—$N_{II, III}$) should be about twice as intense as ($M_{IV, V}$–$N_{II, III}$), whilst ($M_{II, III}$–N_I) should have about the same intensity as the latter. Actually, although it would be expected that the relative intensities for molybdenum should be not very different from those of silver, neither (M_I–$N_{II, III}$) nor ($M_{II, III}$–N_I) has been observed.

Pointing out that the remaining four lines are very nearly symmetrically placed about the very intense ($M_{IV, V}$–$N_{II, III}$) line, Cork suggested that they might possibly be spurious. That we, using a different apparatus and a grating from a different engine, obtain the lines in accurately the same relative positions, seems, however, evidence for the genuine nature of the effects. Further, we do not consider that the symmetry of the lines 54·74 and 74·31 Å. about the line at 64·08 Å. is sufficiently good. There is, in fact, a reasonable explanation for three of the four lines.

Molybdenum Line at 54·74 Å.

This fairly strong line, $\frac{\nu}{R}=16{\cdot}65$, is of slightly less energy than the $M_{IV, V}$ levels $\left(\frac{\nu}{R}=17{\cdot}1\right)$ and might, therefore, be produced by an electron falling into one of these levels from a level very near the surface of the atom. An ($M_{IV, V}$–$O_{II, III}$) or ($M_{IV, V}$–$N_{VI, VII}$) transition would give about the right wave-length. The molybdenum atom is, however, supposed to possess no electron in either of these initial states. The objection does not seem to be very serious, since the K_{β_4} line affords a precedent for the suggested processes. The K_{β_3} line, arising from a (K–M_{II}) transition, is first observed for sodium. There is, however, no electron in the M_{II} level of the normal atom until aluminium (13). Hence, although the O_{II} shell is not normally occupied until indium (49) and the N_{VI} until cerium (58), we are invoking no new principle in

* *Zeits. f. Phys.* lxvii. p. 478 (1932).

designating the 54·74 Å. line as $M_{IV,\,V}$–$O_{II,\,III}$ or $M_{IV,\,V}$–$N_{VI,\,VII}$. For the heavy elements, the $M_{IV,\,V}$–$N_{VI,\,VII}$ radiation is stronger than that of $M_{IV,\,V}$–$O_{II,\,III}$, but it is by no means certain that such would be the case for molybdenum, and we are therefore unable to decide which of the transitions is the cause of the line under consideration.

Molybdenum Line at 74·31 Å.

Prins, among his (M–N) intensity calculations for silver, makes an estimate of the f value for an $M_{II,\,III}$–$M_{IV,\,V}$ transition. The result is 2·09, as compared with 3·77 for $M_{IV,\,V}$–$N_{II,\,III}$, so that the intensity should be about one-fifth of that of the latter line, and the radiation might well be observable. The transition would obey the selection principles relating to the azimuthal and inner quantum numbers, but it would involve a zero change in the total quantum number. As Pauling and Goudsmit * point out, however, such transitions are permitted in ordinary spectra, and, in the case of the alkali metals, give some of the strongest lines. There seems, therefore, no reason to suppose that they should be forbidden in the X-ray region. That these lines are not observed is probably due to their low frequency. Thus in most X-ray experiments they fall outside the wave-length zone for which the apparatus is designed, and, where a special attempt has been made to find the lines, the intensity, which is theoretically proportional to the fourth power of the frequency, has probably been so poor as to preclude their observation. Prins † has drawn attention to the fact that such lines might well be found in the very soft X-ray region, where the frequencies would often be of the same order of magnitude as those of transitions of the usual type. The N doublets of tungsten and its neighbouring elements have been cited as possible examples of this type of emission process; but, as will be shown in a later paragraph, it is difficult to be sure that these radiations are not of the ordinary (N–O) type. The predicted value for the wave-length of molybdenum (M_{III}–$M_{IV,\,V}$) is fortunately very different from that

* 'Structure of Line Spectra,' International Series in Physics, p. 178 (1930).

† *Zeits. f. Phys.* lxix. p. 618 (1931).

of any (M–N) transition. Its $\frac{\nu}{R}$ should be 12·0 according to Siegbahn's tables and 12·7 according to those of Lindh. Our weak line $\lambda=74{\cdot}31$ Å., $\frac{\nu}{R}=12{\cdot}26$ is therefore of particular interest. We believe it to be the strongest evidence so far obtained of an X-radiation arising from a transition between different levels of a group possessing the same total quantum number *.

Molybdenum Line at 68·6 Å.

The very weak line 68·6 Å., $\frac{\nu}{R}=13{\cdot}3$, may also be a radiation of this type. If so, it will represent the transition M_{II}–M_{IV}. Whilst the $\frac{\nu}{R}$ value (14·3) given by Lindh for this transition does not agree well with that of this line, the more recent figure, given by Siegbahn (13·2), fits it excellently. Since it is difficult to find any other explanation for the line, it seems to afford further evidence of the possibility of transitions without change of total quantum number †.

Molybdenum Line at 59·6 Å.

We have been unable to identify the very faint line 59·6 Å., $\frac{\nu}{R}=15{\cdot}3$.

Experiments have been made with the elements palladium, rhodium, and silver, which are in the same group of the periodic table as molybdenum. For each of these elements the line ($M_{IV,\,V}$–$N_{II,\,III}$) has been observed, but in no case were we able to obtain lines corresponding to the other molybdenum radiations. Their absence is

* In a recent paper, which did not come to the present writers' knowledge until this paper was completed, Prins and Takens (*Zeits. f. Phys.* lxxv. p. 741, 1932) announce the measurement of lines for ruthenium, rhodium, palladium, and silver corresponding to the 74·31 Å. and 68·6 Å. lines of molybdenum. Interpreting these radiations in the same manner as that described above, they found good agreement with the predictions from Siegbahn's tables. The evidence for the existence of X-rays due to the transitions of electrons between levels of the same total quantum number must therefore be regarded as very strong.

† Prins and Takens, *loc. cit.*

probably due to experimental causes which prevented us from procuring for these elements such intense spectra as were obtainable for molybdenum.

Rhodium (45).

The element rhodium, used in sheet form and allowed to run hot, gave the ($M_{IV,\,V}$–$N_{II,\,III}$) line with ample intensity, and two good plates were obtained. The results are: Order I., 47·35, 47·40; Order II., 47·34, 47·38; mean value, 47·37 Å.*, $\frac{\nu}{R}=19{\cdot}24$. From Siegbahn's tables we deduce the value $\frac{\nu}{R}=19{\cdot}2$, and from those of Lindh 18·7.

Palladium (46).

Sheet metal was used as the source of our palladium radiation. Since the wave-length of the ($M_{IV,\,V}$–$N_{II,\,III}$) line is almost identical with that of carbon K_α, it was particularly desirable that the anti-cathode should be free of carbon deposit. Our method of allowing the anti-cathode to run hot was therefore of especial value for this element. We were successful in obtaining three measurable plates, which, although showing carbon K_α, did not exhibit it in such strength as to seriously affect the measurement of the line. The calibration plate used for the palladium was based on our measurements of the molybdenum and carbon lines, and was therefore probably not quite so good as those obtained directly from the copper line. The results obtained were:— Order I., 43·57, 43·41, 43·52 Å.; Order II., 43·50, 43·34, 43·38 Å.; mean value, 43·46 Å.†, $\frac{\nu}{R}=20{\cdot}97$. This, again, accords excellently with the Siegbahn prediction of 21·0, Lindh's tables yield the value 20·2.

Silver (47).

The ($M_{IV,\,V}$–$N_{II,\,III}$) line has been obtained for hot sheet silver, but it has been difficult to keep the anti-cathode clean during exposures. Up to the present we

* Prins and Takens obtained the value $\lambda=47{\cdot}55$ Å.

† Prins and Takens obtain the value 43·48 Å., in good accord with our result.

have only succeeded in making one measure of this line, and the result must be regarded as approximate. The value obtained is 39·68 Å.*, $\frac{\nu}{R}=22{\cdot}96$. Siegbahn's tables give $\frac{\nu}{R}=23{\cdot}1$, and those of Lindh 22·5.

In a letter to 'Nature' † we announced some results obtained for tungsten and for tantalum. These elements were examined as sputtered water-cooled, and as hot sheet anti-cathodes. The results from the two types of anti-cathode were not the same. The values obtained are given and discussed more completely below, together with some results for hot sheet platinum. These elements, all of which lie in the sixth group of the periodic table, might be expected to give a number of soft X-ray lines, but normally only two lines appear for each element, and even these are weak.

Tungsten (74).

For hot tungsten the following values were obtained :— (*a*) Short wave-length line: Order II., 55·37, 55·27 Å.‡; Order III., 55·34, 55·19 Å.; mean value, 55·29 Å., $\frac{\nu}{R}=16{\cdot}48$. (*b*) Long wave-length line: Order II., 58·05, 58·19, 58·16 Å.§; Order III., 57·90, 58·22 Å.; mean value, 58·09 Å., $\frac{\nu}{R}=15{\cdot}69$. The lines are seen to form a doublet with a separation of 2·8 Å. The figures given above are obtained from two plates; the one has molybdenum reference lines, and on the other the CK edge is used for comparison. It is unfortunate that the molybdenum line 54·74 Å. is almost coincident with the 55·29 line and is not completely resolved from it. For this reason we were unable to measure the shorter wave-length tungsten line on one plate, but we have attempted to estimate its position by means of a photometer record of the plate. The other plate should give the distance between the two lines pretty accurately, and this distance is checked by the record.

* Prins and Takens value, 39·66 Å., again agrees well.
† 'Nature,' cxxix. p. 906 (1932).
‡ Value obtained from photometer record.
§ Values obtained from photometer record.

In the normal running of our X-ray tube with a tungsten filament and an efficiently cooled anti-cathode, tungsten is speedily deposited on the surface of the anti-cathode. We have measured up a number of the radiations emanating from this deposit. The results obtained are :—

Cold Tungsten.

(*a*) Short wave-length line: Order II., 55·78, 55·79, 55·78 Å. ; Order III., 55·52, 55·45, 55·58 Å. ; mean value, 55·65 Å., $\frac{\nu}{R}=16{\cdot}37$. (*b*) Long wave-length line : Order II., 58·59, 58·53, 58·60 Å. ; Order III., 58·28 Å. ; mean value 58·50 Å., $\frac{\nu}{R}=15{\cdot}58$. This is again a doublet, and its separation is 2·85 Å. in agreement with that obtained for the hot metal. The whole doublet has, however, been shifted ·38 Å. in the longer wave-length direction. It is difficult to believe that this is due to experimental error *. Our sputtered tungsten results are in good accord with those of Prins† ; this author used not only sputtered tungsten, but also an apparently water-cooled solid tungsten anti-cathode. His values are 55·7 and 58·4 Å. Thibaud and Soltan's sputtered tungsten values are 56·0 and 59·1 Å.

Tantalum (73).

A number of tantalum plates have been taken, and, as in the case of tungsten, they demonstrate that the behaviour of the hot element is not the same as that of the material sputtered on to a cold surface. In the form of a hot sheet it gives a doublet of approximately the same separation as that of the tungsten doublet ; in the cold sputtered state the short wave member of the doublet is replaced by two close, fairly sharp lines. Fig. 6 (Pl. VII.) shows a spectrum from each type of anti-cathode. The spectrogram A, obtained with hot tantalum, is the result of an exposure of 18×7 milli-ampère-hours ; the spectrum, B, of sputtered tantalum

* Since both hot and cold determinations are based on the same calibration equation, the shift cannot be due to errors of calibration.

† *Zeits. f. Phys.* lxix. p. 618 (1931).

was obtained with an exposure of $24 \times 5{\cdot}5$ milliampere-hours. The voltages employed were 2000 and 3000 respectively. Even with these exposures, the lines are faint and the measurement of the doubled line extremely difficult. Measures were obtained from two sputtered tantalum plates. On the first it was found easier to set the cross-wires of the microscope on the more distinct member of the doubled line, whilst on the second it was more convenient to take an average setting for the two members. Two satisfactory plates taken with a hot tantalum anti-cathode give the results :—

Tantalum (*Hot*).

(*a*) Short wave-length line: Order II., 57·52, 57·87 Å.; mean value, 57·70 Å., $\frac{\nu}{R} = 15{\cdot}79$. (*b*) Long wave-length line: Order II., 60·32, 60·46 Å.; mean value, 60·39 Å., $\frac{\nu}{R} = 15{\cdot}09$.

Tantalum (*Cold*).

(*a*) Doubled short wave-length line. Longer component: Order II., 58·75 Å., peak of unseparated double line on photometer record; Order II., 58·67 Å. Average setting for double line, Order II., 58·21 Å. (*b*) Long wave-length line: Order II., 60·47, 60·66, 60·42 Å.*; mean value, 60·52 Å., $\frac{\nu}{R} = 15{\cdot}06$.

These figures indicate that there is no displacement of the long wave-length line. Further, the suggestion is justified that one of the members of the doubled line cannot be very different in wave-length from the short wave line obtained for the hot element. The other member is displaced about 1 Å. from this line. Of the two members, the displaced one is seen in fig. 6 (Pl. VII.) to be the stronger.

It is to be emphasised that, although we have only two measurable plates for each type of tantalum anti-cathode, we have in each case a number of plates which are too weak to measure, but, nevertheless, demonstrate the two distinct types of spectrum. On one plate, taken with

* Values obtained from photometer record.

a cold anti-cathode, we do, it is true, obtain the doublet which we have associated with the "hot" exposures. We ascribe this result to a peeling of the sputtered film, to the heating of this film by electronic bombardment, and the consequent approximation to the "hot" conditions. We have never observed a doubling of the short wave line for a hot sheet anti-cathode.

Thibaud and Soltan have used a sputtered tantalum anti-cathode. Possibly for the reason given above, they obtained a simple doublet. Their measurements of the lines are 58·3 Å. and 61·4 Å.

Platinum (78).

Platinum, like tungsten and tantalum, yields a doublet when used as a hot anti-cathode. The results obtained from three of our plates are :—(*a*) Short wave line : Order I., 47·91 Å. ; Order II., 47·88, 48·06 Å. ; mean value, 47·95 Å., $\frac{\nu}{R}=19{\cdot}00$. (*b*) Long wave line : Order I., 50·75, 50·83 Å. ; Order II., 50·63, 50·76 Å. ; mean value, 50·74 Å., $\frac{\nu}{R}=17{\cdot}95$.

Thibaud and Soltan give the short wave line as 48·0 Å., and the long wave line as 51·0 Å. These results were obtained with a water-cooled solid platinum anti-cathode.

Before considering the levels from which the observed lines are derived, it is desirable to discuss the reason for the difference between the "hot" spectra and the "cold sputtered" spectra of tungsten and tantalum. Two possibilities suggest themselves : the hot anti-cathode may have a different crystal structure from that of the cold deposited layer ; or the element may, in the two cases, be in different chemical states. That tungsten actually possesses two distinct crystal structures has been shown recently by Hartmann, Ebert, and Bretschneider*. They show, however, that β-tungsten, heated in a vacuum above 700° C., is converted into the usual α-tungsten. Hence there can be no possibility that the "hot" tungsten results are due to the former modification. Again, the tungsten deposited in lamp bulbs has been

* *Zeits. f. An. Chem.* cxcviii. p. 116 (1931).

found to be of the usual structure *. We may therefore conclude that the difference in the two sets of tungsten results is not due to a difference in the crystal structures of the two types of anti-cathode. A chemical difference is a much more likely cause. The deposition of tungsten on the cold anti-cathodes is probably, in the main, due to the oxidation of the incandescent filaments by water vapour, which is certain to be plentiful in an apparatus containing so much unbaked metal. This view is supported by the fact that deposits are observable before the voltage is applied to the X-ray tube, and hence before any positive ion sputtering could take place. The rapid pumping of our system may be sufficient to remove enough of the hydrogen, formed in the reaction, to prevent reduction of all the deposited oxide. Hence it is probable that the deposited oxide is in part oxidised. On the other hand, it is probable that the tungsten anti-cathode run at a high temperature is comparatively free from oxides. An examination of our spectrograms supports this view. Thus the "cold" spectrograms showing tungsten show also a strong OK_α line: on the "hot" spectrograms this line is weak. We therefore believe that the true tungsten values are those expressed by the "hot" spectra. Since the cold anti-cathode is likely to consist of both tungsten and its oxide, the observed lines are in this case unresolved doublets. The measured wave-length will therefore be between that of tungsten and that of the oxide. This explains a curious feature of the cold tungsten results. In these the second order values are very consistent. The third order values are, however, in every case lower and much nearer to the "hot" values. That this is not due to a faulty calibration equation is shown by the fact that the values for carbon K_α in different orders on these plates are consistent. We attribute the difference to the greater dispersion and "focussing" of the components in the third order which might well cause the measurer to set on a different position on the composite line. This would imply that one component is considerably stronger than the other.

For tantalum also it is probable that the "cold" values are due to an, at least partially, oxidised surface, and

* Smithells and Rooksby, Journ. Chem. Soc. p. 1882 (1927).

that the "hot" tantalum values are due to the unoxidised metal. In this case we have the satisfactory result that tantalum, tungsten, and platinum all give similar soft X-ray spectra, namely, a doublet.

With the hard X-ray data, supported by critical potential determinations, it is not difficult to identify the final levels involved in the lines of the doublets.

TABLE II.

Short Wave-length Line.

$\frac{\nu}{R}$.

Element.	Thibaud and Soltan.	Chalklin.	(N_{IV}–N_{VI}) Idei.	(N_{IV}–$O_{II, III}$) Idei.
Ta (73) ...	15·6	15·79	15·9	15·0
W (74) ...	16·3	16·48	16·4	16·0
Pt (78) ...	18·9	19·03	18·8	20·2
Au (79) ...	19·5	—	19·6	21·7

Long Wave-length Line.

			(N_V–$N_{VI, VII}$).	(N_V–$O_{II, III}$).
Ta (73) ...	14·8	15·09	15·0	14·0
W (74) ...	15·4	15·69	15·4	14·9
Pt (78) ...	17·8	17·98	17·8	19·0
Au (79) ...	18·4	—	18·4	20·4

For the shorter wave line there is N_{IV}, and for the other N_V. These levels form a relatively spin doublet. Lines formed by transitions to these levels from a common initial level should have a wave-length separation independent of the atomic number. The observed separations of the doublets are :—Ta, 2·70 Å.; W, 2·80 Å.; Pt, 2·81 Å. If the ordinary X-ray quantum rules are observed, the lines will have had their origin in the following transitions :— (N_{IV}–$O_{II, III}$) for the short line, and (N_V–O_{II}) for the

longer line. The predicted values for such transitions are not very different from the experimental values for our lines. However, the N_{VI} and N_{VII} levels are close to O_{II} and O_{III}, and, if zero change in total quantum number is permitted, (N_{IV}–N_{VI}) and (N_V–$N_{VI, VII}$) are possible transitions. The predicted values for these would agree quite well with our results. The ν^4 term in the theoretical expression for the intensity should here be greater for the (N–N) than for the (N–O) transitions, rendering this case a favourable one for the appearance of radiations involving zero change in the total quantum number.

Investigating this problem, Idei * carried out new hard X-ray experiments to obtain the levels concerned with greater accuracy. His results are listed in Table II., together with the soft X-ray measurements of Thibaud and Soltan and the values obtained by us for hot anti-cathodes.

To the data given in the table we may add the following :

Prins.—Measurement of "cold" Tungsten N doublet. $\frac{\nu}{R}=16{\cdot}36$ for the short wave line, and $\frac{\nu}{R}=15{\cdot}60$ for the long wave line.

Richardson and Chalklin†.—Soft X-ray critical potentials of Tungsten. Resulting values for transitions :—

N_{IV}–N_{VI}, $\frac{\nu}{R}=16{\cdot}7$; N_V–$N_{VI, VII}$, $\frac{\nu}{R}=15{\cdot}4$; N_{IV}–$O_{II, III}$, $\frac{\nu}{R}=16{\cdot}5$; N_V–O_{III}, $\frac{\nu}{R}=15{\cdot}1$.

In their magnitude, and in their variation with atomic number, the (N–N) predictions agree with the measured lines better than do the (N–O) values. Idei does not give an estimate of the accuracy of his determinations, but the difference between the N–O values and our experimental results seems outside the experimental error. This would lead to the conclusion that the short and long wave-length lines are respectively due to (N_{IV}–N_{VI}) and (N_V–$N_{VI, VII}$). In this case the short line is single and the long wave line is an unresolved doublet. This, unfortunately, leads to a difficulty in

* 'Nature,' cxxiii. p. 643 (1929).
† Proc. Roy. Soc. A, cx. p. 247 (1926).

the interpretation of the tantalum cold anti-cathode results. For tungsten either identification of the outer level is satisfactory. Thus, since both lines are displaced by the same amount, it appears that a movement of a level common to both lines is the cause of the shifts. According to the one identification the initial levels of the two lines are N_{VI} and $N_{VI, VII}$, and the shift is thus attributable to a deepening of the $N_{VI, VII}$ level by 1·2 electron volts for oxidised tungsten. With the other identification $O_{II, III}$ would experience the deepening. Both the $N_{VI, VII}$ and the $O_{II, III}$ levels are only about 40 volts beneath the surface of the atom, and it is therefore satisfactory that they, and not the N_{IV} and N_V levels at a depth of about 250 volts, should be affected by chemical combination. For tantalum we have to explain the splitting of the short wave line. With the N_{IV}–V_{VI} interpretation this line is essentially single and, in fact, the N_{VI} level is fixed, since the long wave line, involving $N_{VI, VII}$, does not move. On the other hand, if the short line is N_{IV}–$O_{II, III}$ then, since the long line N_V–O_{III} is stationary, we shall obtain a short line N_{IV}–O_{III} in the same place as for the unoxidised metal, whilst a deepening of the O_{II} level by 3·7 volts will give the observed spectrum of the oxide.

Whilst this paper has been in preparation two new researches on the soft X-rays of the elements of the sixth group have been published. The first of these is by Del Rosario *, and the second by Magnusson †, making use of the new Siegbahn-Magnusson spectrograph. These authors have both used water-cooled anti-cathodes. While the values given by Del Rosario are somewhat higher than ours, those of Magnusson agree, with one exception, reasonably well with the values given in this paper. For tantalum the wave-lengths are :—Del Rosario, 61·3 and 58·3 Å. ; Magnusson, 61·0 and 58·1 ; Chalklin (cold values), 60·5, 58·7, and 57·7. Thus Magnusson's value for the short line falls between the values of our separated components, but the long line, disagreeing by ·5 Å., shows a large discrepancy explicable only by taking the extreme errors allowed by Magnusson and by us. The tungsten values are :—Del Rosario, 59·0 and 56·0 Å. ; Magnusson, 58·5 and 55·8 ; Chalklin (cold values), 58·4

* Phys. Rev. lxi. p. 136 (1932).
† *Zeits. f. Phys.* lxxix. p. 161 (1932).

and 55·6, giving satisfactory agreement between Magnusson and ourselves (and also Prins). For platinum :—Magnusson, 50·9 and 48·0 Å. ; Chalklin (hot values), 50·7 and 48·0. The agreement here is very interesting, since, if, as we have suggested, the difference between hot and cold values is due to oxidation, then for platinum this difference should be absent. This may therefore be regarded as evidence in favour of the oxidation hypothesis. A number of other elements in the group have been examined by these two authors, and, as with results tabulated above, their values accord well with the predictions of the (N–N) transitions rather than the (N–O). Especially interesting is Magnusson's result for thallium. He obtains one line only, whose $\frac{\nu}{R}=19{\cdot}55$ as compared with the predicted value, 19·6, of (N_V–$N_{VI,\,VII}$) and 21·6 of (N_V–$O_{II,\,III}$). The difference between the values is here so large that the agreement between the experimental value and the predicted (N_V–$N_{VI,\,VII}$) must be regarded as very strong evidence in favour of all the lines being of the (N–N) type. If this is the case, it becomes necessary to postulate a new level for tantalum oxide in order to explain the splitting of the short line.

Carbon, Oxygen, and Nitrogen.

Carbon, oxygen and, to a much smaller extent, nitrogen occur in our apparatus as impurities. We have measured the K_α line of each of these elements. For carbon K_α we have the following values :—Order I., 44·37 ; Order II., 44·46, 44·39, 44·46, 44·40 ; Order III., 44·42, 44·39, 44·43, 44·41 ; Order IV., 44·49 ; Order VI., 44·43, 44·53 ; mean, 44·43 Å., $\frac{\nu}{R}=20{\cdot}51$. All the values listed were obtained with a cold anti-cathode. The mean result is a little lower than that usually found by other workers. Söderman * gives the wave-length as 44·54 Å. Prins's value is 44·65 Å. The agreement is satisfactory since the line is extremely diffuse, and has a width dependent on the intensity and always greater than 1 Å. Microscope readings of such a line therefore have little meaning. For oxygen K_α we have the values :—Order I., 23·67, 23·59, 23·52, 23·52, 23·57, 23·63 ; Order II., 23·58, 23·58, 23·52, 23·49, 23·59 ; Order III., 23·54, 23·43, 23·72 ;

* Phil. Mag. x. p. 600 (1930).

TABLE III.

Element.	Wave-length in Å.	$\frac{\nu}{R}$.	Electron-volts.	Probable origin.
Carbon (6)	44·43	20·51	277·9	K_α
Nitrogen (7).....	31·49	28·94	392·0	K_α
Oxygen (8).....	23·57	38·66	523·8	K_α
Molybdenum (42) ..	64·08	14·22	192·6	$M_{IV,\,V}$–$N_{II,\,III}$
	54·7	16·65	225·6	$M_{IV,\,V}$–$N_{VI,\,VII}$ or $M_{IV,\,V}$–$O_{II,\,III}$
	74·3	12·26	166·1	M_{III}–$M_{IV,\,V}$
	68·6	13·29	180·0	M_{II}–M_{IV}
	59·6	15·29	207·2	?
Rhodium (45)	47·4	19·24	260·6	$M_{IV,\,V}$–$N_{II,\,III}$
Palladium (46)	43·5	20·97	284·1	$M_{IV,\,V}$–$N_{II,\,III}$
Silver (47)	39·7	22·96	311·1	$M_{IV,\,V}$–$N_{II,\,III}$
Tantalum (73)	57·7	15·79	214·0	N_{IV}–$O_{II,\,III}$ or N_{IV}–N_{VI}
	60·4	15·09	204·4	N_V–O_{III} or N_V–$N_{VI,\,VII}$
Tungsten (74)	55·3	16·48	223·3	N_{IV}–$O_{II,\,III}$ or N_{IV}–N_{VI}
	58·1	15·69	212·5	N_V–O_{III} or N_V–$N_{VI,\,VII}$
Platinum (78)	48·0	19·00	257·5	N_{IV}–$O_{II,\,III}$ or N_{IV}–N_{VI}
	50·7	17·95	243·3	N_V–O_{III} or N_V–$N_{VI,\,VII}$
Oxidised tungsten ..	55·6	16·39	222·7	N_{IV}–$O_{II,\,III}$ or N_{IV}–N_{VI}
	58·4	15·60	211·3	N_V–O_{III} or N_V–$N_{VI,\,VII}$
	58·7	15·52	210·3	N_{IV}–O_{II} ?
Oxidised tantalum ..	c. 57·7	15·79	214·0	N_{IV}–O_{III} or N_{IV}–N_{VI}
	60·5	15·06	204·0	N_V–O_{III} or N_V–$N_{VI,\,VII}$

mean, 23·57 Å., $\frac{\nu}{R}$ =38·66. The line involved in the 23·43 value was extremely faint. The mean value is in accord with the results of other workers. For example, Söderman gives 23·567 Å., and Prins 23·58 Å. Only on one occasion have we observed a nitrogen K_γ line of measurable strength. Its value, 31·49 Å., $\nu/R=28·94$, is in agreement with that of Prins's determination, 31·53 Å., and also with that of Söderman, 31·557 Å.

Table III. summarises all the wave-length measurements recorded in this paper, and gives the probable levels from which the lines arise. Since in our final values it is necessary to consider the possible error introduced in the calibration, our results will be subject to a possible error somewhat greater than one in three hundred. Hence, in the longer wave-length lines, the figure in the second decimal place of Ångstroms will have little meaning, and has therefore been omitted in the table.

It is evident from the discussion of the results that the interpretation of the lines is not always easy. The difficulty is due to several causes. Firstly, many of the expected lines do not appear. This is partly due to the weakness of the radiations, and partly to the fact that, with the method employed, only a small portion of the radiation can be allowed to strike the grating. Secondly, the resolving power of this type of spectrograph is small, and identification of the lines is hampered by the inability of the instrument to resolve close multiplets. On the other hand, despite these drawbacks, it is probable that, when data are obtained with these instruments for the whole range of elements, most of the difficulties of interpretation will be overcome.

We wish to take this opportunity to acknowledge our indebtedness to Prof. E. N. da C. Andrade for his very kind interest and for the considerable assistance and encouragement which he has afforded us during this work. Prof. Andrade has also lent us on various occasions a calculating machine, purchased by him from a grant made by the Government Grants Committee of the Royal Society, which has greatly facilitated our calculations.

Our apparatus has been very largely constructed with the aid of a grant made to us by this Committee, to whom we wish to express our thanks.

XXX. *The Convection of Heat from Isolated Plates and Cylinders in an Inviscid Stream. By* N. A. V. Piercy, *D.Sc., M.I.Mech.E., and* H. F. Winny, *Ph.D.**

1. *Introduction.*

VARIOUS developments have given new prominence to the study of convection from short heated bodies in a stream of fluid. The analytical problem is complex, and complete treatment, even of simple cases, is scarcely yet begun. If the viscosity of the fluid be neglected and its thermometric conductivity be assumed constant, progress has long been seen to be possible with certain cases of cylinders by virtue of Boussinesq's † well-known transformation. This reduces the problem to that of the convection from a short flat plate caused by uniform streaming. But treatment of the simplified problem has presented unexpected difficulties. Familiar approximate solutions have been given by Boussinesq ‡ and King §, but both depend upon the introduction of further assumptions which limit their utility.

A more general investigation, forming the subject of the present paper, was undertaken in the first place as a necessary step towards a theory of anemometry which would meet modern requirements. Fair agreement with measured heat-transfers in real small motions was assured beforehand by the considerable volume of relevant experimental work that now exists. Examination has been pressed further than was required in this connexion, however, because there soon appeared a qualitative relationship of the results in detail to cases of convection at larger Reynolds numbers. There is thus a hope that, in view of the difficulties in the way of complete treatment, a study of heat-transfer with inviscid flow may prove of interim use in some practical problems when economically compared with experiment.

The present investigation begins with King's integral equation for the distribution of heat-sources along a tangential plate, but natural thermal boundary conditions are introduced which complicate the analysis.

* Communicated by the Authors.
† *Jour. de Mathématiques*, i. (1905).
‡ *Comptes Rendus*, v. p. 133 (1901).
§ Phil. Trans. Roy. Soc. A, ccxiv. (1914).

An approximate method of solution is employed which the authors have found effective in a somewhat similar problem *. Except for small motions the boundary conditions are generalized, for the transformation of the results to cylinders will depend upon selection of a flat plate solution with an appropriate temperature distribution. Applications are subsequently made to cylinders of circular and of another section to permit of brief comparison, in an Appendix, with experiment.

2.

If θ is the temperature at any point in an incompressible moving fluid of thermal conductivity k and heat capacity per unit volume c, the classical equation for the conduction of heat becomes for a steady two-dimensional motion

$$c\left(u\frac{\partial\theta}{\partial x}+v\frac{\partial\theta}{\partial y}\right)=\frac{\partial}{\partial x}\left(k\frac{\partial\theta}{\partial x}\right)+\frac{\partial}{\partial y}\left(k\frac{\partial\theta}{\partial y}\right). \quad . \quad (1)$$

The conductivity and capacity will vary from point to point of the fluid on account of unequal heating, but it is assumed sufficient to choose certain mean values and to regard these as constant. For steady streaming at velocity U parallel to the x-axis, (1) then becomes

$$2n\frac{\partial\theta}{\partial x}=\nabla^2\theta, \quad . \quad . \quad . \quad . \quad . \quad . \quad (2)$$

where $2n$ is written for Uc/k.

Imagine introduced along the x-axis a thin stationary plate of length l. If suitable thermal boundary conditions can be specified, a solution of (2) subject to these determines the temperature distribution in an inviscid fluid flowing past the plate.

3. *King's Solution.*

King observed that since (2) is linear, a solution may be built up by the integration of a distribution of line sources along the plate and, briefly, he proceeded as follows. With the substitution $\theta_1=\theta e^{-nx}$, (2) takes the more symmetrical form

$$n^2\theta_1=\nabla^2\theta_1, \quad . \quad . \quad . \quad . \quad . \quad . \quad (3)$$

* "The Skin Friction of Flat Plates to Oseen's Approximation," Proc. Roy. Soc. A, v. p. 140 (1933).

and a particular solution appropriate to a line source at the origin is

$$\theta_1 = \frac{Q}{2\pi k} K_0(nr), \quad . \quad . \quad . \quad . \quad . \quad . \quad (4)$$

where Q is the rate at which heat issues from the line source per unit length, $K_0(z)$ is the Bessel function of the second kind, defined by

$$K_0(z) = \int_0^\infty e^{-z \cosh w} dw,$$

and $r^2 = (x^2 + y^2)$. Let the origin be taken at the front edge of the plate, and let $u(\xi)\, d\xi$ be the total heat flux from an element $d\xi$ of the boundary. Integration of a distribution of line sources along the plate, *i. e.*, along the x-axis from $x=0$ to $x=l$, gives, at the point x, y,

$$2\pi k\theta = \int_0^l u(\xi) e^{n(x-\xi)} K_0 \mid n\{y^2 + (x-\xi)^2\}^{\frac{1}{2}} \mid d\xi, \quad . \quad (5)$$

and on the boundary

$$2\pi k\theta_b = \int_0^l u(\xi) e^{n(x-\xi)} K_0 \mid n(x-\xi) \mid d\xi. \quad . \quad . \quad . \quad (6)$$

The bars indicate that the absolute value is to be taken.

Equation (6) represents King's solution prior to inserting the boundary conditions. θ_b denotes the temperature of the fluid in contact with the plate and, if this be prescribed, $u(\xi)$ may be determined; if, on the other hand, $u(\xi)$ be given, θ_b will follow. In the original work the second alternative was chosen. The heat-transfer $u(\xi)$ was assumed constant over the boundary and such as to make the temperature of the fluid just leaving the plate equal to that of the plate itself, θ_0, which was also assumed constant.

The particular boundary specification led to simplification of (6) and a solution for the total heat-loss H per unit depth of the stream readily followed, viz.,

$$H = \int_0^l u(\xi)\, d\xi = \frac{2 . \pi k \theta_0 nl}{\int_0^{nl} e^w K_0(w)\, dw}. \quad . \quad . \quad . \quad (7)$$

4. *The Boundary Conditions adopted in the present Paper.*

The thermal assumptions at the boundary leading to (7) involve a discontinuity of temperature across the interface between plate and fluid, given by

$$\frac{\theta_b}{\theta_0} = \left[\int_0^{nl} e^{nx-w}\mathrm{K}_0\,|\,nx-w\,|\,dw\right] \Big/ \left[\int_0^{nl} e^{w}\mathrm{K}_0(w)\,dw\right]. \quad (8)$$

The maximum difference of temperature occurs at the front edge of the plate where the fluid is much the cooler. On the other hand, over a portion of the back part of the plate the fluid is hotter than the plate. This physical anomaly tends to disappear as nl becomes large, but at small values it is marked both in magnitude and extent. Thus at $nl=4$, which may correspond with air as fluid to a value of Ul/ν of about 10, the temperature of the fluid exceeds that of the plate over more than the last one-third part of its length, and the maximum excess amounts to some 10 per cent. of the temperature elevation of the plate. The boundary condition of constant heat-flow must therefore be regarded as artificial, and a change to natural boundary conditions is advisable on two considerations: (*a*) the form of the assumption of constant heat-flow prevents extensions of the theory, (*b*) in some applications of the theory primary importance attaches to estimates of the distribution of heat-transfer.

The first assumption made in the present paper is that the temperature of the fluid in contact with the heated surface is the same as that of the surface at any position along it. There remains to be specified the variation of temperature over the surface. Since the present investigation is not restricted to thin flat plates, but will be applied to cylinders, generality in the specification is desirable. In some cases of practical interest, however, the variation of surface temperature is unimportant; *e. g.*, solid cylinders composed of highly conducting material at small and moderate Reynolds numbers, thin-walled cylinders of larger size filled with steam or other well-mixed fluid to be cooled. It is convenient to assume this special, but usual, boundary condition in the first place and to express the results more generally later.

Referring to equation (6), we assume in the first place, therefore, $\theta_b=\theta_0$, a constant, the temperature elevation of

the plate above the distant fluid. $u(\xi)$ remains to be determined, and the equation for this becomes

$$2\pi k\theta_0 = \int u(\xi)e^{n(x-\xi)}K_0(n\,|\,x-\xi\,|)\,d\xi, \quad . \quad . \quad (9)$$

in which the integration is to extend the length of the plate.

5.

We have not found a general solution of (9) to satisfy the new boundary conditions, but approximate solutions can be obtained (*a*) when nl is small so that first terms only in the expansion of the kernel need be retained, and (*b*) when nl is large so that all terms except the first in the asymptotic expansion of $K_0(z)$ may be neglected.

(a) *Approximate Solution for nl small.*—It is convenient in this paragraph to change the origin to midway along the plate, and it is then appropriate to assume for the distribution $u(\xi)$ of the heat-sources the form

$$\zeta = \frac{A+Bn\xi+Cn^2\xi^2}{\sqrt{\{(nl/2)^2-(n\xi)^2\}}}, \quad . \quad . \quad . \quad . \quad (10)$$

where A, B, C are constants. Expanding the kernel of (9) as far as the squares of small quantities, we obtain, writing χ for $n(x-\xi)$,

$$2\pi kn\theta_0 = \int_{-nl/2}^{nl/2} \zeta\left(1+\chi+\frac{\chi^2}{2}\right) \times\left\{-\left(1+\frac{\chi^2}{4}\right)\left(\log\frac{|\chi|}{2}+\gamma\right)+\frac{\chi^2}{4}\right\}d(n\xi), \quad (11)$$

where γ is Euler's constant $=0{\cdot}5772$. The integrations present no difficulties and (11) reduces to

$$\begin{aligned} 2kn\theta_0 = {}& A\left\{-nx-\frac{7}{8}(nx)^2-\frac{1}{16}\left(\frac{nl}{2}\right)^2\right. \\ & \left.+\left(\log\frac{nl}{8}+\gamma\right)\left[-1-nx-\frac{3}{4}(nx)^2-\frac{3}{8}\left(\frac{nl}{2}\right)^2\right]\right\} \\ & +B\left\{nx+\frac{1}{2}\left[(nx)^2+\left(\frac{nl}{2}\right)^2\left(\log\frac{nl}{8}+\frac{1}{2}+\gamma\right)\right]\right\} \\ & +C\left\{\frac{(nx)^2}{2}-\frac{1}{2}\left(\frac{nl}{2}\right)^2\left(\log\frac{nl}{8}+\frac{1}{2}+\gamma\right)\right\}. \quad . \quad (12) \end{aligned}$$

Equation (11) requires to be satisfied for all values of x between $l/2$ and $-l/2$, and equating coefficients gives

$$\left.\begin{aligned}\frac{2kn\theta_0}{A} &= \left(\log\frac{nl}{8}+\gamma\right)\left[-1+\frac{1}{4}\left(\frac{nl}{2}\right)^2\left(\log\frac{nl}{8}+\gamma-\frac{1}{2}\right)\right],\\ B &= A\left(\log\frac{nl}{8}+\gamma+1\right),\\ C &= \frac{A}{2}\left(\log\frac{nl}{8}+\gamma+\frac{3}{2}\right).\end{aligned}\right\} \quad . \quad . \quad . \quad (13)$$

The total heat-loss per sec. per unit depth of the stream is now found to be

$$H = \int_{-l/2}^{l/2} u(\xi)\,d\xi = \frac{\pi}{n}\left[A+\frac{1}{2}\left(\frac{nl}{2}\right)^2 C\right] . \quad . \quad . \quad (14)$$

On substituting from (13) and rejecting powers of nl greater than its square, we obtain finally,

$$\begin{aligned}H/k\theta_0 &= -2\pi\left[1+\frac{1}{2}\left(\frac{nl}{2}\right)^2\left(\log\frac{nl}{8}+\gamma+\frac{1}{2}\right)\right]\Big/\left[\log\frac{nl}{8}+\gamma\right]\\ &= -2\pi\left[1+\frac{1}{32}\left(\frac{Ulc}{k}\right)^2\left(\log\frac{Ulc}{16k}+\gamma+\frac{1}{2}\right)\right]\Big/\left[\log\frac{Ulc}{16k}+\gamma\right].\end{aligned}$$

$$. \quad . \quad . \quad (15)$$

(b) *Approximate Solution for nl large.*—In all that follows the origin is again located at the front edge of the plate. From the asymptotic expansion of $K_0(z)$, viz.,

$$K_0(z) = \left(\frac{\pi}{2z}\right)^{\frac{1}{2}} e^{-z}\left[1-\frac{1^2}{1.8z}+\frac{1^2.3^2}{2.(8z)^2}-\ldots\right], \quad (16)$$

the kernel of (9) is seen to be negligible when $n(x-\xi)$ is large and negative. The contribution to the integral through the interval of ξ near x, where (16) ceases to apply, tends to become negligible as nl increases. Thus for large values of nl it is nearly true that

$$2\pi k\theta_0 = \int_0^x u(\xi)\left[\frac{\pi}{2n(x-\xi)}\right]^{\frac{1}{2}} d\xi . \quad . \quad . \quad . \quad (17)$$

The solution of (17) is found from Abel's work to be

$$u(\xi)/k\theta_0 = 2(2n/\pi\xi)^{\frac{1}{2}} \quad . \quad . \quad . \quad . \quad . \quad (18)$$

Hence the heat-loss is now given by

$$\mathrm{H}/k\theta_0 = 2\left(\frac{2n}{\pi}\right)^{\frac{1}{2}} \int_0^l \frac{d\xi}{\sqrt{\xi}}$$

$$= 4(2nl/\pi)^{\frac{1}{2}} = 2{\cdot}257\,(\mathrm{U}lc/k)^{\frac{1}{2}}. \quad . \quad . \quad (19)$$

Fig. 1.

① Small motion solution.
② Asymptotic solution.
③ Transitional curve.

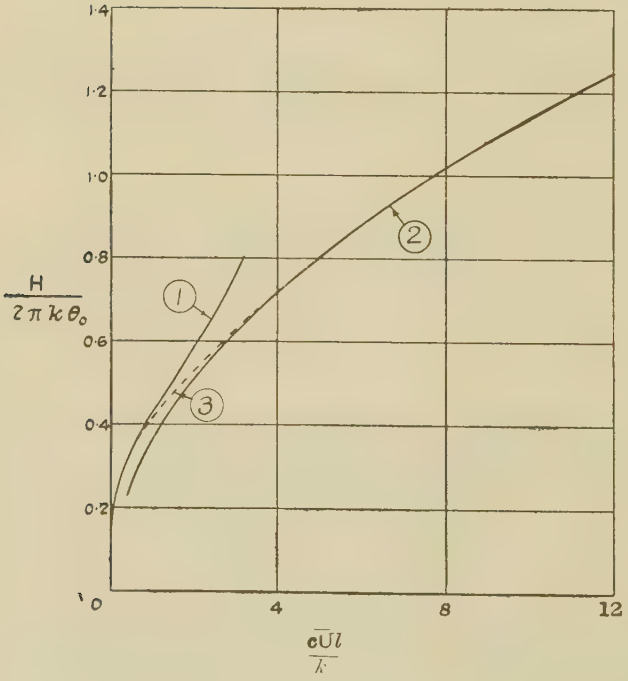

The two solutions (15) and (19) of the equation (9) are plotted as the full lines (1) and (2) respectively in fig. 1. From the measure of agreement of the two expressions at $\mathrm{U}lc/k=2$ it is inferred that no great uncertainty as to the heat-loss exists at any part of the range.

6. *Generalization for prescribed Temperature Distribution.*

With nl large a convenient expression for the heat-loss is readily obtained for those cases where the temperature θ_b of the fluid along the boundary cannot with sufficient accuracy be regarded as uniform. On substitution of $\theta_b(x)$ for θ_0, the equation (17) will give the heat-flow at any position ξ. Making use of Abel's solution but keeping now θ_b variable, we have

$$u(\xi) = 2k\left(\frac{2n}{\pi}\right)^{\frac{1}{2}} \frac{d}{d\xi} \int_0^{\xi} \frac{\theta_b(x)\, dx}{\sqrt{(\xi - x)}}, \quad . \quad . \quad (20)$$

which gives for the total heat-loss, with certain restrictions,

$$\mathrm{H}/k = 2\left(\frac{2n}{\pi}\right)^{\frac{1}{2}} \int_0^{l} \frac{\theta_b(x)\, dx}{\sqrt{(l - x)}}. \quad . \quad . \quad . \quad (21)$$

In applications of this expression $\theta_b(x)$ will be specified from physical considerations concerned with the form and material of particular cylinders and the method of heating.

The asymptotic result (19) is identical with the solution obtained by Boussinesq of the approximation to (2):

$$2n \,.\, \partial\theta/\partial x = \partial^2\theta/\partial x^2,$$

the simple Fourier form, on inserting the boundary conditions: $\theta = \theta_0$ along the plate and $\theta = 0$ from $-\infty$ to the front edge of the plate and from its back edge to ∞. It may be remarked that to obtain (19) the "scale" has been assumed sufficiently great for the heat issuing from a point on the plate to fail to affect the temperature of the fluid directly upstream. Behind the plate the present solution indicates a fluid temperature falling to zero at infinity approximately as $r^{-\frac{1}{2}}$. To simulate Boussinesq's hypothesis we may imagine a cooling surface of zero temperature to extend downstream from the back edge of the plate; the temperature on the plate, and hence its heat-transfer, would remain unchanged at this "scale." The distribution of the temperature in the wake would, however, be different. (19) disagrees with King's solution, but an additional step is necessary before the question can conveniently be discussed.

7.

Particular cases of practical or experimental interest arise in which the temperature variation may be expressed sufficiently closely in the form

$$\theta_b = \mathrm{B}x^p, \quad . \quad . \quad . \quad . \quad . \quad . \quad . \quad (22)$$

where B is a constant. Substituting in (20) and changing the variable x to ξz gives

$$u(\xi)/k = 2\mathrm{B}\left(\frac{2n}{\pi}\right)^{\frac{1}{2}} \frac{d}{d\xi} \int_0^1 \xi^{p+\frac{1}{2}} z^p (1-z)^{-\frac{1}{2}}\, dz. \quad . \quad (23)$$

Hence, making use of well-known formulæ for the Beta and Gamma functions, we find

$$u(\xi)/k = 2\mathrm{B}\sqrt{2n}\,\xi^{p-\frac{1}{2}} \frac{p\Gamma(p)}{\Gamma(p+\frac{1}{2})}, \quad . \quad . \quad . \quad (24)$$

where $\Gamma(p)$ is defined by

$$\Gamma(p) = \int_0^\infty e^{-t} t^{p-1}\, dt.$$

The heat-loss then follows from (21) to be

$$\mathrm{H}/k = 2\mathrm{B}\sqrt{2n}\, l^{p+\frac{1}{2}} \frac{\Gamma(p+1)}{\Gamma(p+\frac{3}{2})}. \quad . \quad . \quad . \quad (25)$$

For purposes of comparison with experiment it is convenient to introduce a mean temperature of the boundary θ_{M}. If this be defined by

$$\theta_{\mathrm{M}} = \frac{1}{l} \int_0^l \theta_b\, dx, \quad . \quad . \quad . \quad . \quad . \quad . \quad (26)$$

(25) reduces to

$$\mathrm{H}/k\theta_{\mathrm{M}} = 2\sqrt{2nl}.\Gamma(p+2)/\Gamma(p+\tfrac{3}{2}), \quad . \quad . \quad (27)$$

agreeing with (19) when $p=0$ and $\theta_{\mathrm{M}}=\theta_0$.

8.

Uniformly distributed heat-flow is a special case of (27), viz., when $p=\frac{1}{2}$, the interpretation being evident from (24), and the expression for the heat-loss then becomes

$$\mathrm{H}/k\theta_{\mathrm{M}} = 3\sqrt{\pi}/2.\sqrt{2nl} = 2{\cdot}659\,(\mathrm{U}lc/k)^{\frac{1}{2}}. \quad . \quad (28)$$

$u(\xi)$=a constant is one of the boundary assumptions of King's theory, but his result does not agree with (28), being for large speeds,

$$\mathrm{H}/k\theta_0' = 1+(\pi \mathrm{U}lc/k)^{\frac{1}{2}}. \quad . \quad . \quad . \quad . \quad (29)$$

It will be remembered in the first place, however, that King defines his temperature elevation θ_0', as that of the fluid just leaving the plate. If this definition were adopted, (29) would result from (25) but without the constant term, yet, although this constant term becomes negligible at very large speeds, it is known to be important in King's solution at moderate speeds when the approximation (28) must be regarded as close. The explanation of the disagreement lies in the fact that in King's theory for large speeds the temperature of the fluid adjacent to the plate rapidly decreases a total amount $\theta_0'/\sqrt{2\pi nl}$ as the trailing edge is finally approached. Thus it is only at very large speeds that the excess temperature of the fluid towards the back of the plate, already noted as a feature of King's boundary assumptions, ceases to be of mathematical impo.tance. Hence King's solution is a special case of the present theory because, with no temperature discontinuity across the boundary, it is conceivable that the particular temperature distribution might be arranged, when the addition of a constant term $\theta_0 k/l$ would be required in (24), but King's interpretation of (29) is arbitrary.

Apart from the above detailed argument, it may be shown that (25) satisfies (6) to the same order as (29) satisfies the integral equation without including in (25) a constant term, as might be expected from fig. 1.

9. *Thickness of Heat Boundary Layer at Large Speeds.*

It is of interest to examine the depth to which the fluid is heated by the plate, and in the case of constant temperature over the plate an estimate is readily obtainable at speeds sufficient to ensure not only that the asymptotic solution applies, but also that the heated layer is thin.

From (5) and (18) there results for the temperature at any point x, y in the fluid:

$$\theta/\theta_0 = \frac{1}{\pi}\left(\frac{2n}{\pi}\right)^{\frac{1}{2}} \int_0^l e^{n(x-\xi)} \mathrm{K}_0 \left| n\sqrt{[y^2+(x-\xi)^2]} \right| \frac{d\xi}{\sqrt{\xi}}. \quad (30)$$

Appropriate assumptions to make to simplify the working * are that $n(x-\xi)$ is large and $y/(x-\xi)$ is small through the effective part of the integration, and the expression then becomes

$$\theta/\theta_0 = \frac{1}{\pi}\int_0^{\delta} e^{-\frac{y^2 n}{2(x-\xi)}} \frac{d\xi}{\sqrt{[\xi(x-\xi)]}}, \quad . \quad . \quad . \quad (31)$$

where δ is a new limit of integration nearly equal to x for large values of nl, but such that (16) remains valid. The substitution $z^2 = y^2 n/2(x-\xi)$ effects a change to a more convenient variable, and the integral may be written

$$\theta/\theta_0 = \frac{2}{\pi}\int \left(\frac{y^2 n}{2x}\right)^{\frac{1}{2}} \frac{e^{-z^2} dz}{z\sqrt{(z^2 - y^2 n/2x)}}, \quad . \quad . \quad . \quad (32)$$

where the limits are from $\sqrt{(y^2 n/2x)}$ to $\sqrt{[y^2 n/2(x-\delta)]}$, which is large. A reduction may now be effected to

$$\theta/\theta_0 = (2/\sqrt{\pi}) \int_a^{\infty} e^{-w^2} dw, \quad . \quad . \quad . \quad . \quad (33)$$

where the integration is to extend from $a = \sqrt{(y^2 n/2x)}$ to ∞ and is rapidly evaluated from tables of the probability integral. When a is large (>2) an approximation is

$$\theta/\theta_0 = e^{-a^2}/(a\sqrt{\pi}). \quad . \quad . \quad . \quad . \quad . \quad (34)$$

In the parallel case of viscous boundary layers it is usual to agree upon some small percentage drop of velocity or some proportionate increment of vorticity as a gauge to measure the depth of fluid affected. The fact that a must then be moderately large permits the following approximate expressions in which Δ denotes the thickness required:

$$\Delta\sqrt{(n/x)} = 2{\cdot}58,\ 2{\cdot}33,\ 1{\cdot}96. \quad . \quad . \quad . \quad (35)$$

for temperature rises of 1, 2, 5 per cent. respectively, of the temperature of the plate. The formula (35) is of the same form as regards variation with Ux as corresponding formulæ deduced from Prandtl's or Oseen's approximations to the equations of viscous motion for the steady viscous boundary layers of flat plates at large speeds, but the comparative thicknesses of the thermal and viscous

* The calculation is the same as that of the viscous boundary layer in the friction paper to which reference has been made. An outline only is given here.

boundary layers vary greatly with the fluid. Thus under normal conditions and with a small temperature elevation the two thicknesses are about the same for air; for water the viscous layer would be four times as thick as the thermal one; while for mercury, on the other hand, temperature changes would occur at four times the depth affected by viscosity.

10. *Extension to Cylindrical Surfaces.*

If ψ, ϕ=constants represent the streamlines and equipotentials of the irrotational flow of an inviscid fluid with unit velocity at infinity past a cylinder without circulation of any form of cross-section, Boussinesq showed that equation (1) could be transformed to

$$2n\frac{\partial\theta}{\partial\phi} = \frac{\partial^2\theta}{\partial\phi^2} + \frac{\partial^2\theta}{\partial\psi^2}. \quad . \quad . \quad . \quad . \quad (36)$$

Comparison with (2) shows that the convection from any cylinder of such section that the equation of transformation is known is directly obtainable, according to the present theory, from a flat plate solution. The particular flat plate solution to be transformed will be specified by the thermal boundary conditions of the cylinder. In the transformed plane, where the coordinates are ψ and ϕ, the plate will lie along the axis $\psi=0$, and its length will be given by the interval of ϕ between the front and back stagnation points in the xy-plane.

11. *Circular Cylinder.*

The case of the circular cylinder of uniform temperature is readily solved. If $z=x+iy$ and $\zeta=\phi+i\psi$, the transformation formula is

$$\zeta = z + \frac{a^2}{z}, \quad . \quad . \quad . \quad . \quad . \quad . \quad . \quad (37)$$

where a denotes the radius of the cylinder. On the $\phi\psi$-plane the cylindrical surface is represented by the two sides of a plate of length $4a$.

For the total heat-loss it follows from equations (15) and (19) that for small motions

$$\mathrm{H}/(2\pi k\theta_0)$$
$$=-\left[1+\frac{1}{2}\left(\frac{c\mathrm{U}a}{k}\right)^2\left(\log\frac{c\mathrm{U}a}{4k}+\gamma+\frac{1}{2}\right)\right]\Big/\left[\log\frac{c\mathrm{U}a}{4k}+\gamma\right], \quad . \quad . \quad . \quad (38)$$

while for large motions

$$\mathrm{H}/k\theta_0=4{\cdot}51\sqrt{\frac{c\mathrm{U}a}{k}}. \quad . \quad . \quad . \quad . \quad (39)$$

In the latter case reference to (18) shows the distribution of heat transfer to be given on the transformed plane by

$$u(\phi)/k\theta_0=2\sqrt{2n/\pi}(2a-\phi), \quad . \quad . \quad . \quad (40)$$

remembering that the origin of ϕ for (37) is midway along the plate. To transform this back we take account of the variable scale by use of the formula

$$h=\tfrac{1}{2}u(\phi)\left|\frac{d\zeta}{dz}\right|, \quad . \quad . \quad . \quad . \quad . \quad (41)$$

where h represents the intensity of heat-flux per sec. at any point. On the boundary in the xy-plane

$$\phi=2x=2a\cos\epsilon,$$

if ϵ gives the angular position round the contour measured from the front stagnation point. Hence

$$h=\pm 4k\theta_0\sqrt{\frac{n}{2\pi a}}\cos\frac{\epsilon}{2}\,^{*}. \quad . \quad . \quad . \quad (42)$$

12. *Streamline Cylinder.*

The methods of Joukowski and others permit of low resistance shapes being transformed from the circle so that the inviscid flow past the "streamline" sections so obtained is fully known. For example, the formula

$$z_1=x_1+iy_1=z+\frac{(0{\cdot}2692)^2}{z} \quad . \quad . \quad . \quad (43)$$

transforms the circle of radius $a=0{\cdot}315$, with centre at $y=0$, $x=0{\cdot}0458$ in the z-plane, to a contour of the form shown in fig. 2 in the z_1-plane; the particular shape has

* The minus sign is unnecessary if ϵ is taken to lie between $-\pi$ and π.

been chosen as permitting a rough comparison to be made with experiment in the Appendix. The ratio of the length of the section to the radius of the circle is 3·492, while

Fig. 2.

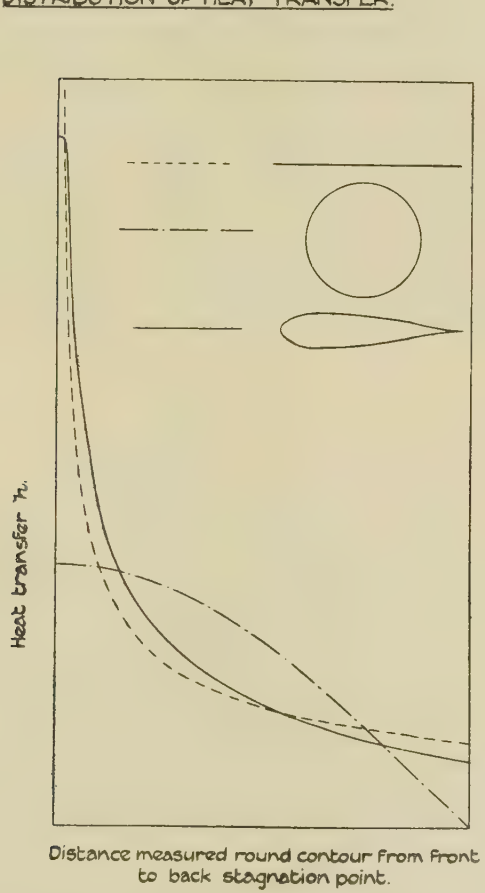

the interval of ϕ between the front and back stagnation points is $4a$, as for the circle.

It follows that at speeds for which (19) may be taken to hold with sufficient accuracy the ratio of the heat-loss from a cylinder of this section to that from one of circular section, the length of the streamline section being equal

to the diameter of the circular cylinder, is 0·756. Compared with a flat plate of equal downstream length, the heat-loss from the streamline cylinder is greater by 7 per cent.

From (43) may be derived the variable change of scale from the streamline to the circular boundary, and hence the distribution of heat transfer round the former contour. Fig. 2 has been prepared to compare, on a basis of equal total heat-loss, the distributions of heat transfer for the flat plate, circular cylinder, and the particular streamline cylinder chosen, the boundary condition of constant temperature being assumed. Infinite intensity of heat transfer, h, occurs at the front edge of an infinitely thin plate, but round the nose of the streamline cylinder h still notably increases. High values of h have been observed by Bryant and others * round the nose of an aerofoil in the wind with the boundary condition of uniform temperature. The feature is absent from the circular cylinder.

Appendix.

Comparison with Experiment.

Little experimental information exists, so far as we know, on the convection of heat from flat plates and cylinders that is suitable for comparison with the foregoing theory. Three sets of measurements of total heat-loss only will be considered, with air as fluid. It is first required to secure agreement on the physical constants employed. To calculate the heat capacity, King chose the specific heat at constant volume; but that at constant pressure is the more suitable, since in experiment variations of pressure are inconsiderable. The following formulæ for various coefficients have been adopted from a recent paper by Fage and Falkner †, t denoting temperature in °C.:—

μ (viscosity) $= (173+0{\cdot}433\,t)\,10^{-6}$;

ρ (density) $= \dfrac{273\times 0{\cdot}001293}{273+t}$ at standard pressure;

σ_p (specific heat at constant pressure) $= 0{\cdot}24$;

k (thermal conductivity) $= 1{\cdot}3\,\mu\sigma_p$ (mean experimental).

* Aero. Res. Com., R. and M., no. 1163 (1928).
† Aero. Res. Com., R. & M., no. 1408 (1931).

It has been necessary to assume constancy of the coefficients in the theory, and those values will be chosen which correspond to the arithmetic mean of the temperatures of the hot boundary and the distant fluid.

Fage and Falkner (*loc. cit.*) have recently carefully observed the total heat-loss from platinum foils, of thickness 0·00127 cm. and of lengths ranging from 0·333 to 1·27 cm., in air-streams increased progressively from 20 to 70 ft. per sec. The average temperature of the air was 22° C., and the mean temperature elevation of the foils 150° C. It is assumed, therefore, that the physical constants may be taken as for 97° C. In the original paper it was assessed that the temperature distribution along the surface of the foils could be expressed as $\theta_b = Bx^{0\cdot4}$.

As regards the present theory it is clear that the asymptotic solution is suitable, and (27) gives

$$H/k\theta_E = 2\cdot583\,(Ulc/k)^{\frac{1}{2}}.$$

The expression becomes

$$H/k\theta_M = 4\cdot77\,(Ul)^{\frac{1}{2}}.$$

The measurements gave

$$H/k\theta_E = 3\cdot15\,(Ul)^{\frac{1}{2}},$$

where θ_E is the mean temperature elevation estimated from electrical resistance. Thus in the present case the inviscid flow theory indicates a total heat-loss 50 per cent. in excess of experiment.

A well-known series of careful observations has been made by King of the heat-loss from wires of circular section moving through air. The diameters of the platinum wires varied from 0·0028 to 0·0153 cm.; their temperatures ranged from 200° C. to nearly 1200° C.; and they were tested at velocities from 0·55 to 28 ft. per sec. The results were given in the form of values of the constants B and C in the formula

$$H = C + B\sqrt{U},$$

radiation loss being allowed for. From these values we have calculated H for each wire and temperature of test at the four velocities: 25, 100, 400, and 900 cm. per sec. Choosing the mean experimental thermal conductivity

and adjusting its value to the mean of the temperatures of the wires and the distant fluid, we obtain the band of points shown in fig. 3. In the figure the curves (1) and (2) represent the solutions (39) and (38) respectively, and the present theory is seen to be capable of giving the heat-loss approximately for small cylinders moving at small velocities, but it considerably overestimates the heat-loss for large motions. The curve (3), viz.,

$$H/k\theta_0 = 1{\cdot}4 + 3{\cdot}1\sqrt{Uac/k},$$

Fig. 3.

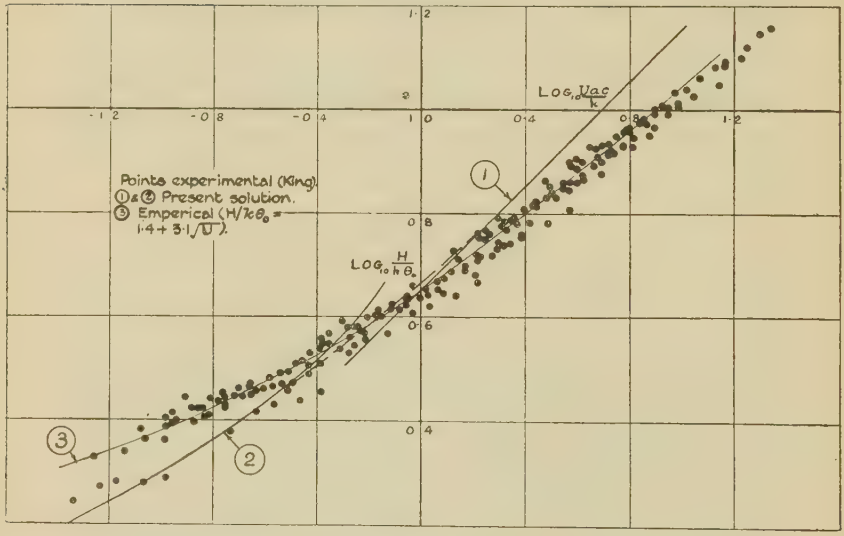

is empirical and is fitted to the experimental results on the assumption that these suggest a modification in the law of variation of $H/k\theta_0$ with Uac/k to occur when the latter quantity approaches 10, which corresponds with air as fluid to the lowest Reynolds number (about 30) at which unsteady flow has been observed to set in with circular cylinders. King's expression (29) becomes for circular cylinders

$$H/k\theta_0' = 1 + 3{\cdot}54\sqrt{Uac/k},$$

and does not fit the observations so well on the present

basis; the question of its rationality has already been discussed.

The experiments finally to be considered are those carried out by Hughes* on a cylinder roughly of the section given in fig. 2. It was formed of copper sheet, 0·2 cm. in thickness, while its contour measured 23·1 cm. Supplied with steam, it was tested for heat-loss in an air-stream of various velocities up to 1200 cm. per sec. The method of heating and the thinness and material of the

Fig. 4.

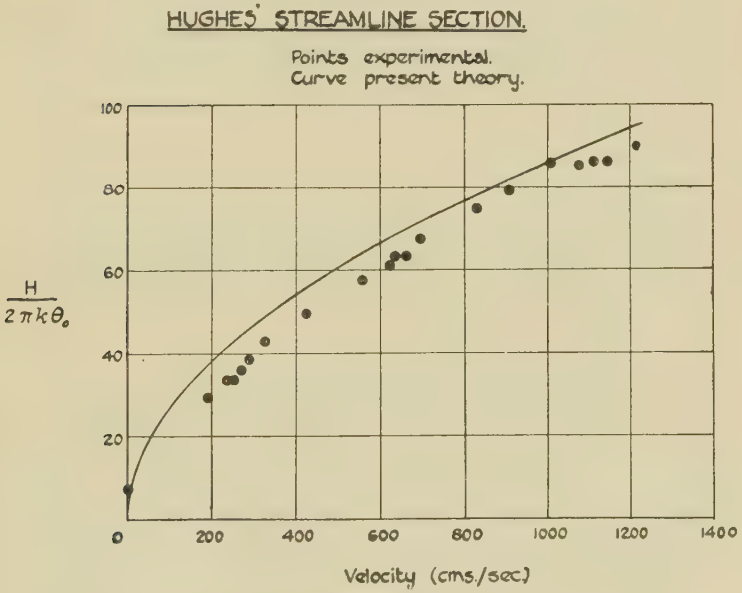

wall permit variation of temperature over the external surface to be neglected. Thus the theoretical heat-loss is appropriately calculated in § 12, according to the present methods. This theoretical result is given as the curve in fig. 4, in obtaining which the broken-line transition curve (3) of fig. 1 between the small and large motion solutions for the flat plate has been assumed, but on the scale of the figure is situated too close to the origin to have significance. The observations are shown as points.

* Hughes, Phil. Mag. xxxi. p. 118.

Discrepancies between the inviscid flow theory and Hughes' experiments with a cylinder of streamline section are seen to be surprisingly less marked than were found in the case of the flat plate with variable temperature over the surface or with wires of uniform temperature distribution, unless small. The heat-loss in the experiments may have been increased by turbulence. It would be of interest to investigate, by means of more comprehensive experiments, whether the present theory is generally capable of giving the heat-loss approximately from cylinders of narrow sections. Even if discrepancies were established to be considerably greater than those of fig. 4, it might be of value to determine empirical corrections to enable advantage to be taken of the simplicity of the theory in some practical applications.

XXXI. *Use of Cathode Ray Oscillograph for obtaining Frequency-response Curves.* *By* A. H. Davis, *D.Sc.*, *Physics Department, National Physical Laboratory, Teddington, Middlesex.**

[Plate VIII.]

OSCILLOGRAPHS are normally used for recording the variation, as time changes, of the response of some electrical system which is under observation. Since, however, cathode ray oscillographs are now part of the normal equipment of laboratories dealing with audio- and radio-frequency electrical currents, it is advantageous to adapt them to various uses for which special equipment would otherwise be required.

The present note shows how a frequency scale can be attained on a cathode ray oscillograph, and used for recording the relation between the response of a loudspeaker and the frequency of the exciting current. The essential features of the arrangement are indicated in fig. 1. An oscillator supplies the loudspeaker with an electrical e.m.f. of constant magnitude but variable frequency, and the acoustical output of the loudspeaker is measured by a microphone circuit which is uniformly responsive at all frequencies. The rectified output from

* Communicated by the Author.

the microphone circuit is applied to two plates of a cathode ray oscillograph and gives a proportionate vertical deflexion to the "spot" of the oscillograph. The same oscillator supplies current to a weighting network so adjusted that the output, when rectified and smoothed,

Fig. 1.

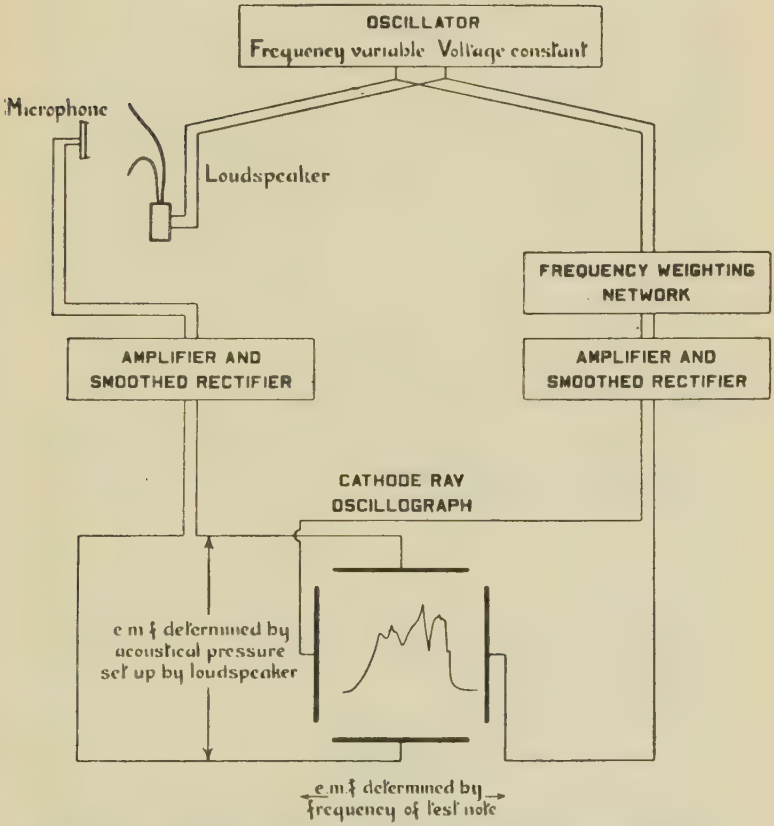
OSCILLATOR
Frequency variable Voltage constant
Microphone
Loudspeaker
FREQUENCY WEIGHTING NETWORK
AMPLIFIER AND SMOOTHED RECTIFIER
AMPLIFIER AND SMOOTHED RECTIFIER
CATHODE RAY OSCILLOGRAPH
e m f determined by acoustical pressure set up by loudspeaker
e m f determined by frequency of test note

Circuit for obtaining frequency response characteristics of loudspeakers by means of a cathode ray oscillograph.

is closely related to the logarithm of the frequency of the exciting current. This output, applied to the other plates of the oscillograph, deflects the "spot" horizontally to an extent determined by the frequency of the note concerned.

As the frequency of the oscillator is varied the oscillograph spot thus traces out a curve showing the relation between the pitch of the note and the output of the loudspeaker as observed at the position of the microphone. Two such curves, each of which was obtained in a few seconds, are shown in fig. 2 (Pl. VIII.). The frequency scale was calibrated by causing the spot to re-traverse the screen horizontally (the loudspeaker having been switched off) with pauses at standard positions known from the scale of the oscillator. The vertical response scale was obtained by a somewhat similar procedure when the frequency network was switched off and the microphone amplification varied in a known manner.

The arrangement is not limited to the study of electro-acoustical systems. Clearly the loudspeaker-microphone combination can be replaced by any system which can be adapted so that an electrical output results from an electrical input. As an illustration, fig. 3 (Pl. VIII.) shows the frequency response curve of an electrical amplifier. and also the response of the same amplifier after it had been fitted with a low-pass electrical filter.

I am indebted to Mr. E. G. Butcher, Junior Observer in the Physics Department, for assistance with the experimental arrangements.

XXXII. *The Perfection of Crystal Laminæ. By* W. N. Bond, *M.A., D.Sc., F.Inst.P., Lecturer in Physics in the University of Reading.**

[Plate IX.]

Summary.

Reference is made to experiments of the third Baron Rayleigh and others on the perfection of the surfaces and uniformity of the effective thickness of cleavage laminæ of actual crystals. Laminæ of muscovite of about 1/100 mm. in thickness are tested by examining the banded spectrum of white light that has been reflected at the mica. (By using plane polarized light it is possible to make a biaxal crystal act as if it were isotropic.)

* Communicated by the Author.

Formulæ are derived for the resolution obtained at nearly grazing incidence, and the formulæ agree with experiment. The measurements of the thickness of the mica have an absolute error of about $\pm 2\times 10^{-8}$ cm., together with an uncertainty common to them all of about 1/40 per cent. It is shown that the mica lamina consists of several portions of different thickness, each of which is certainly uniform in effective thickness to 8×10^{-8} cm., and probably to 2×10^{-8} cm. or less. The stringency of the test is from 50 to 100 times that of the third Baron Rayleigh's experiments. If the different thicknesses are all integral multiples of the length of the unit cell of muscovite, it is shown that the length of the unit cell must be less than $(23{\cdot}4\pm 3{\cdot}1)\times 10^{-8}$ cm.: a length of unit cell of $(19{\cdot}84\pm 0{\cdot}06)\times 10^{-8}$ cm. is indicated, but not uniquely determined.

Introduction.

THOUGH many actual crystals are far from regular in their structure, it is interesting to enquire to what extent the more perfect specimens conform to the ordered arrangement of unit cells that is revealed by X-ray analysis. We may confine our attention to the case of a lamina bounded by a pair of parallel cleavage planes, and may assume the crystal to be non-volatile. Apart from elastic deformation, such a lamina may have internal and surface defects. The surfaces may have been cleaved in an irregular step formation, may have become contaminated, and may have an abnormal density owing to the action of surface-tension forces.

Contamination of the surfaces would probably make the transition from crystal to air less abrupt, and this abruptness has been tested by the polarization produced in light incident at the polarizing angle. Reference may be made to the work of the third Baron Rayleigh *. The general conclusion is that a fresh cleavage surface of a crystal is nearly perfect, in contrast to a polished glass surface or a contaminated liquid surface.

The degree of abnormality of the density of a crystal near its free surfaces has been estimated theoretically by

* Phil. Mag. xxxiii. pp. 1–19 (1892); xvi.. pp. 444–449 (1908); xxiii. pp. 431–439 (1912).

Lennard-Jones *. The effect, for all but the smallest crystals, seems to be practically confined to the outermost layer of unit cells, and is small even for that layer.

The cleavage of the surfaces in an irregular step formation may be detected in the case of mica. A cleavage lamina of mica, viewed by monochromatic light, appears to consist of a number of contiguous patches, each of uniform thickness. A similar conclusion is reached by placing the lamina in one of the beams of a Michelson Interferometer, or by viewing it between crossed nicols. For very thin laminæ a simple examination by reflected white light reveals a number of contiguous patches of colour, each of which seems uniform in hue.

A simple experiment shows that these patches are really of different thicknesses and are not due to the refractive index being different in different parts of the crystal. If a thin lamina of mica be illuminated by a point source of light, the mica is generally found to be crossed by a number of fine dark lines, some of which intersect. These lines mark the boundaries of the patches mentioned above. Let the mica be split into two pieces. If the pieces be replaced, but not exactly in their original relative position, the two pieces will cling together, and certain of the dark lines will be found to be duplicated. These mark irregularities common to the two surfaces in contact. The two pieces of mica are found to be in close contact, except near the double lines. That is to say, the irregularities on the pair of adjacent faces prevent the two pieces of mica from getting into intimate contact, but the mica bends and gets more nearly in contact at places remote from the double lines. To show that the irregularities indicated by the lines do not extend through the thickness of the lamina, it is only necessary to split one of the pair of laminæ again and inspect the outer portion. Some of the lines on this piece correspond to some on the adjacent pair, but in no case do they correspond to the double lines on the pair.

The third Baron Rayleigh found a few pieces of mica that seemed almost uniform in thickness †. Examining

* Proc. Roy. Soc. cxxi. pp. 247–259 (1928); *Zeit. f. Krist.* lxxv. (3–4) pp. 215–216 (1930).

† Phil. Mag. xix. pp. 96–99 (1910).

a piece by reflected monochromatic light, he concluded that the mica nowhere had an abrupt change in thickness of more than 2×10^{-6} cm., nor had it any gradual change of as much as 4×10^{-6} cm. By cutting two pieces of equal area from the same lamina, and weighing them, he decided that the mean thicknesses of the two parts did not differ by more than 3×10^{-6} cm. (though they appeared to show a definite difference of about that amount). He saw no reason for doubting that the thickness over finite areas may be as uniform as is consistent with a molecular structure. He also remarked that "the stringency of the optical test might probably be increased a few times by silvering the surfaces after the manner of Fabry and Perot."

Considerably increased reflecting power, and consequent increase in the stringency of the test, has been achieved in the present experiments without recourse to the process of silvering. It may be remarked that a silvered surface would not be the original crystal surface.

General Theory of the Experiments.

If a beam of white light be incident on a parallel-sided transparent isotropic lamina of thickness t and refractive index μ, at an angle i to the normal, the spectrum of the reflected light is crossed by dark bands whose centres are at wave-lengths, λ, given by

$$n\lambda=2t\sqrt{\mu^2-\sin^2 i}, \quad . \quad . \quad . \quad . \quad . \quad (1)$$

where n is an integer aud μ is an unknown function of λ. With the help of equation (1) it is possible to measure the thickness of the lamina and to test its uniformity.

By keeping t and λ (and consequently μ) constant, and finding how many bands pass the chosen value of λ in the spectrum as i is changed, it is theoretically possible to deduce t from the equation

$$t=\frac{-\lambda\dfrac{\partial n}{\partial i}}{2\sqrt{\sin i.\cos i.\dfrac{\partial^2 n}{\partial i^2}\dfrac{\partial n}{\partial i}+\sin^2 i-\cos^2 i}}.$$

A more convenient method would be to measure the total number of bands that passed as i changed from 0°

to 45° and from 45° to 90°. Again, a previous knowledge of μ would considerably simplify matters. In the present experiments, where n was small, a simpler procedure was adopted, which is described later in the paper.

Application to Biaxal Crystals.

Fig. 1 represents an eighth of the wave-surface of a biaxal crystal (it is drawn as if for an optically negative crystal, such as muscovite). Circular sections of the wave-front are indicated by continuous lines, and the arrows show the direction of the electric vector in the wave.

If the plane of cleavage is parallel to one of the three principal optical directions in the crystal (as seems to be the

Fig. 1.

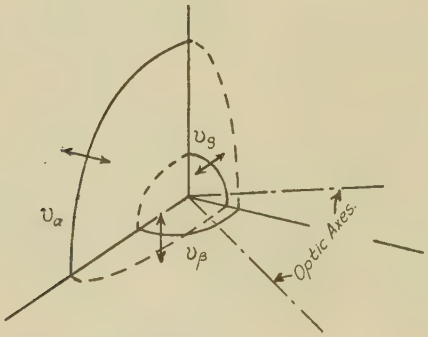

case in the majority of crystals), then plane polarized light incident in a plane at right angles to the principal optical direction concerned, and having the plane of incidence the plane of polarization, will have the same refractive index (one of the principal values) for all angles of incidence. As the planes of incidence and polarization coincide, some light is reflected for all angles of incidence.

In the case of muscovite mica, which is monoclinic and pseudo-hexagonal, the cleavage is parallel to the basal pinacoid (001). The ortho-axis coincides with one of the three principal optical directions (the α and β); and the clino-axis is almost, but not quite, parallel to a second of the principal optical directions (the α and γ). The plane containing the optic axes is parallel to the ortho-axis and

almost at right angles to the cleavage plane. The conditions for constant refractive index will thus be satisfied by having the common plane of incidence and polarization either the plane containing the optic axes or the plane at right angles to this.

Arrangement of Apparatus.

A piece of muscovite was chosen, and the plane containing the optic axes determined. A thin lamina ($0{\cdot}5 \times 0{\cdot}5 \times 0{\cdot}001$ cm.) was split from the mica, careful note being taken of the position of the axes relative to the lamina. The lamina was then mounted on a theodolite stand, so that it could be adjusted into the required position. The mica was only fixed near two edges, so that there was air on both sides of the lamina, and care was taken in designing the mount so that it would not reflect stray light into the spectroscope.

Light from part of one filament of an incandescent electric lamp was brought to a focus on the mica by means of a small-aperture long focal length lens. A nicol prism was inserted betwen the lens and the mica. Light reflected from the mica passed to the spectroscope. In front of the slit a plate of glass was inserted, at 45° to the beam, enabling light from a helium or neon lamp to pass into the spectroscope and be superposed on the light from the mica.

The spectroscope was fitted with a pair of 60° flint glass prisms. The telescope was moved by a micrometer screw, a hundredth of a turn of the screw corresponding to about 1 Å.U. Single readings of a fine spectrum line could be taken to an accuracy of about 0·15 Å.U. Almost all the experiments were made by direct visual observation.

Experiments.

In order to measure the refractive index for different wave-lengths, experiments were carried out at nearly normal and nearly grazing incidence. For these positions $\sin^2 i$ varies very slowly with i, and the value of i can be found accurately by measuring the perpendicular distance between the slit and the incident beam (or the

part of the beam that has passed just above or below the mica).

To a first approximation n may be obtained by assuming in equation (1) that μ is independent of λ and plotting the values of $1/\lambda$ for the dark bands against successive integers. When light enters the spectroscope simultaneously from two parts of the mica that have different thickness, two sets of dark bands are observed. The ratio of $\partial n/\partial\lambda$ for the two sets can be measured and is equal to the ratio of the thicknesses of the two parts of the mica: it is also equal to the *ratio* of the pair of values of n corresponding to any particular value of λ. The *difference* between the corresponding values of n is small, and consists of a small integer, together with a fractional part of an order which can be measured. These data were accurate enough to deduce the small integer, and hence the orders of all the lines in the two series. The results can be checked subsequently by the mutual agreement of values of t deduced from lines in different parts of the spectrum, and by an independent measurement of μ by a critical angle method.

In the present experiments it was found (for instance) that $\mu_\beta = 1{\cdot}5930 \pm 0{\cdot}0003$ for sodium light from air to muscovite. A determination by a critical angle refractometer gave 1·5932. The thicknesses of the laminæ were thus uncertain by a *common multiplying factor* of about $(1{\cdot}000{,}0 \pm 0{\cdot}000{,}25)$ owing to inaccuracy in the determination of μ.

Apart from all the determinations of thickness being subject to this small error in common, very accurate determinations may be made of the *relative* thickness. When two sets of dark lines can be obtained in the field of view at the same time, and the orders of all the lines are known, then by careful interpolation the ratio of the two values of n for the same wave-length can be estimated, (several determinations being made in different parts of the spectrum). In the present experiments the piece of mica chiefly used had six or more portions of different thickness. The values of n ranged from about 20 to 30. All the measurements of relative thickness were carried out at *nearly grazing incidence*, for the dark lines are finest under these conditions (as will be explained later in the paper.) The fineness of the lines is illustrated in fig. 2 (Pl. IX.) which shows a comparison

spectrum and a single series of lines obtained with an angle of incidence $i = 88{\cdot}2°$.

A typical set of measurements is as follows :—

$$\frac{\text{Thickness A}}{\text{Thickness B}} = \begin{cases} 1{\cdot}044{,}53 \\ 1{\cdot}044{,}73 \\ 1{\cdot}044{,}50 \\ 1{\cdot}044{,}63 \\ 1{\cdot}044{,}61 \end{cases}$$

The final results were as follows :—

TABLE I.

Thicknesses expressed in 10^{-8} cm., or Å.U., and all subject to a common multiplying factor of amount $1{\cdot}000{,}0 \pm 0{\cdot}000{,}25$

A–B = 3123·1 ± 1·9	A–E = 19258·0 ± 1·7
B–C = 790·3 ± 2·4	E = 53898·3 ± 1·2
C–D = 7260·7 ± 1·9	E–F = 793·2 ± 2·4
D–E = 8074·7 ± 4·0	E′–E = 195·3 ± 2·1
(Deduced from the above :— A–E = 19248·8 ± 5·4.)	E″–E = 218·7 ± 2·3

The difference between the direct and indirect estimates of (A–E) is 9·2 Å.U., and a difference of the order 5·6 Å.U. would be expected on account of the probable errors. Now, the portion of the B thickness that was used in the A–B determination was almost certainly not the portion that was used in the B–C determination (and so on), but was probably at a part of the mica lamina about 1 mm. away. We must conclude that each of the parts of the lamina is uniform in thickness to 3 Å.U. or less in 1 mm. or so. There is often not a step of as much as one unit cell in passing along the lamina a distance of 1,000,000 unit cells. In other words, the two faces of each part of the lamina are inclined at an angle of less than 1/20″ of arc.

The close agreement of (B–C) and (E–F) is probably not fortuitous. The step-like cleavage affects both faces, and hence a small step on one face may cross a large step on the other face. The difference (E–F) – (B–C) is 2·9 Å.U., where the measurements would be expected to differ by

an amount of the order 3·4 Å.U. Again we can conclude that the mica is uniform to about 1 Å.U. in 1 mm.

The small steps (E′–E) and (E″–E) were only found after a considerable search had been made for such small steps. Probably only quite small parts had thicknesses E′ and E″, near the junction of thicknesses D and E.

Search for Periodicity.

An attempt was made to test the measurements given in Table I. for periodicity. The results obtained are not conclusive, but are worth a brief discussion Firstly, the difference (E″–E)—(E′–E) is (23·4±3·1) Å.U. The difference is definitely real; and if it be due to a whole number of unit cells, the unit cell must have a length of *not more than* (23·4±3·1) Å.U. in a direction perpendicular to the cleavage.

According to an X-ray analysis made by C. Mauguin *, the unit cell of muscovite has a length of 20·0 Å.U. and contains two molecules. In the specimen he used, the angle between the principal and clino axis was 96°. Hence the length of the cell perpendicular to the cleavage was 19·9 Å.U. The two molecules are end-to-end, and Manguin gave 9·95 Å.U. as the distance between the cleavage planes. (An earlier measurement by de Broglie † gave 10·1 Å.U.) In some of my previous work ‡ I found evidence of such a periodicity. In the present experiments it would not be possible to establish evidence for so small a periodicity. There is, however, a certain amount of internal evidence indicating that the periodicity is in the present case double that value. This appears to me not unlikely, as muscovite has the full monoclinic symmetry, and its top and bottom faces would therefore be expected to have the same properties, implying that the spacing must have the double value of about 20 Å.U.

In fig. 3 I give the relative probabilities of the measurements in Table I. having periodicities of any value between 18·5 and 21·5 Å.U. A periodicity of value 19·84±0·06 Å.U. is indicated. But I would again point out that though there is definite evidence for such a

* *Comptes Rendus*, July 25th, 1927, p. 288.
† *Journ. de Physique*, iv. p. 265 (1914).
‡ Phil. Mag. vii. p. 1163 (June 1929).

periodicity being possible or likely, yet there is *not enough evidence to determine it uniquely.*

The Degree of Resolution.

The degree of resolution of the banded spectrum depends on the perfection of the mica, on the angle of incidence, and on the slit width and resolving power of the spectroscope. Let us consider the second of these.

The energy at any part of the banded spectrum is that of the continuous spectrum multiplied by the expression

$$\frac{1}{1+\dfrac{(1-R^2)^2}{4R^2\sin^2\dfrac{d}{2}}}, \quad \ldots\ldots (2)$$

Fig. 3.

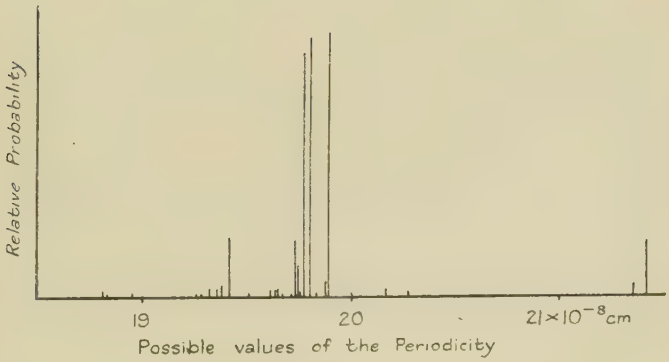

where

$$R = \frac{\text{amplitude of the light reflected at the front of the mica}}{\text{amplitude of the incident beam of light}}$$

and d is the phase difference between successive beams reflected at the back surface of the mica.

From the electromagnetic theory we have, when the planes of polarization and incidence coincide,

$$R = \frac{\sin(i-r)}{\sin(i+r)} \quad \ldots\ldots (3)$$

(where i and r denote the angles of incidence and refraction).

From equations (2) and (3) we see that as we proceed towards grazing incidence the dark bands will become narrower. Denoting the distance between the centre of a dark line and the part where the brightness has half the maximum value by d, the "half-width," we have

$$\frac{(1-R^2)^2}{4R^2 \sin^2 \frac{\bar{d}}{2}} = 1,$$

for nearly grazing incidence. This reduces to $d = \frac{1}{R} - R$ and (by equation 3) to

$$\bar{d} = \frac{8\mu}{2\mu^2 - 1} i' \quad . \quad . \quad . \quad . \quad . \quad . \quad (4)$$

Here $i' = \frac{\pi}{2} - i$, (the angle the beam makes with the plane of the mica): $\bar{d}$ is expressed as a phase difference, the difference in phase between adjacent dark lines being 2π if i' be measured in radians.

Observed and calculated values of $\bar{d}$ were compared and found to be in agreement until i' reached the value $0{\cdot}8°$ (for smaller values the width of the lines was limited by the resolution of the spectroscope).

For nearly grazing incidence the intensity of the spectrum near any dark band may be written

$$\frac{\text{constant}}{1 + \left(\frac{\bar{d}}{d}\right)^2}, \quad . \quad . \quad . \quad . \quad . \quad . \quad (5)$$

where $\bar{d}$ is the distance from the centre of the band expressed as a phase difference. If two sets of equally intense banded spectra were superposed, the bands being nearly coincident, it can be shown that any complex band would have a bright centre if the phase difference between the two components exceeded $\frac{2}{\sqrt{3}}\, d$. The intensity at the centre of the complex band would then

be 25 per cent. of that of the bright part of the spectrum.

From equation (1) we have $\frac{\partial t}{\partial n}=\frac{\lambda}{2\sqrt{\mu^2-1}}$, and hence the difference in thickness that would just not give bands that are lighter in the centre is

$$\triangle t=\frac{\frac{2}{\sqrt{3}}d}{2\pi}\times\frac{\lambda}{2\sqrt{\mu^2-1}}=\frac{4}{\pi\sqrt{3}}\cdot\frac{\mu\lambda}{(2\mu^2-1)\sqrt{\mu^2-1}}\cdot i', \quad . \quad (6)$$

(where i' is measured in radians).

If $\mu=1{\cdot}6$ and $\lambda=5{\cdot}8\times10^{-5}$ cm., the equation becomes

$$(\triangle t \text{ cm.})=2{\cdot}3\times10^{-7}\times(i' \text{ degrees}).$$

So far no account has been taken of the finite resolving power of the spectroscope itself. For a chosen spectroscope the resolving power is directly proportional to the width of the portion of the collimator lens that is flooded with light. That is to say, it is proportional to the focal length, f, of the collimator lens and to the angle, θ, of the beam. It is not feasible to increase the focal length much. As to the angle of the beam, it cannot exceed twice the mean glancing angle i'.

To get all the light that left the mica at grazing angles of from 0 to $2i'$ to enter the spectroscope (so that θ equals twice the mean grazing angle) the mica was used in some of the experiments as the slit, the slit itself being used only as a stop. The collimator lens, of $f=-20$ cm., was replaced by one having $f=-30$ cm. The effective width of the slit, about 1/20 mm., was small enough not to limit the resolution. Under these circumstances, for small values of i' the width of the dark lines is inversely proportional to i', being determined by the resolution of the spectroscope. For larger values of i' the width of the line is directly proportional to i'. Hence there is an optimum value of i'. This optimum value was estimated theoretically, in the present experiments, for the case where the 7th, 8th, and 9th bands were observed for a piece of mica of thickness $17{\cdot}6\times10^{-5}$ cm. The approximate predictions were (i' mean)$=0{\cdot}35°$, angle of beam $\theta=0{\cdot}7°$, and "half-width" of dark line $d=1{\cdot}1°$.

The optimum values found experimentally were $i'=0{\cdot}8°$, $\theta=0{\cdot}8°$, and $\bar{d}=1{\cdot}2°$.

The theory of the resolution that has been given above was thus verified experimentally, and it was also found that the mica laminæ had no variations in thickness of as much as 8 Å.U. (apart from the small number of sudden steps in the cleavage). The test has a stringency about fifty times that of the third Baron Rayleigh's experiments.

In experiments where the observations are just not affected by the limited resolution of the spectroscope, it was found that the centre of the dark bands had a brightness of not more than 1/10th of that of the continuous spectrum (a neutral wedge being used for the comparison). The constancy in thickness of the mica to an accuracy of 12 Å.U. must therefore have extended to enable at least twenty successive reflexions at the back face : that is to say for a length of at least $5{\cdot}7\times10^{-3}$ cm. along the lamina. The angle between the two faces of the mica must therefore be less than 4″. This constancy in thickness must apply to at least half of the mica from which light is entering the spectroscope, so the angle is likely to be considerably less than 4″. (It was previously shown that the angle was of the order 1/20″ or less.)

In conclusion it may be noticed that these experiments have tested the constancy of the effective thickness of the mica lamina ; the *total* effect of irregularities at the two surfaces and in the interior of the mica has been shown to be equivalent to irregularities of not more than 8×10^{-8} cm., and probably not more than 2×10^{-8} cm., at one surface of the mica.

It gives me pleasure to thank Prof. J. A. Crowther, in whose laboratories these experiments were carried out, for the continued interest he has taken in the work. My thanks are also due to Mr. J. S. Burgess, the laboratory steward, for his help in making apparatus.

Department of Physics,
University of Reading.

April 3rd, 1933.

XXXIII. *The State of Polarization of Downcoming Wireless Waves of Medium Length.* *By* J. A. Ratcliffe, *M.A.*, *and* F. W. G. White, *M.Sc.*, *Cavendish Laboratory, Cambridge* *.

Summary.

An apparatus is described by means of which the state of polarization of a downcoming wireless wave may be directly delineated on the screen of a cathode-ray oscillograph, even in the presence of a strong ground-wave. The apparatus is used to investigate the downcoming waves from some of the B.B.C. transmitting stations, and these waves are found, in general, to be elliptically polarized with left-handed sense of rotation. This is shown to agree with Appleton's magneto-ionic theory, and the conditions are deduced under which a right-handed rotation would be expected. From the observed variations of the state of polarization it is suggested that rapid fading is due to an interference mechanism.

Contents.

(1) Introduction.
(2) Apparatus.
(3) Adjustments.
(4) Effect of Ground Reflexions.
(5) Determination of Sense of Rotation.
(6) Results and Theoretical Discussion.

(1) *Introduction.*

In 1928 Appleton and one of the present authors [1] investigated the polarization of medium waves by a "frequency change" method, while, more recently, in collaboration with E. L. C. White, the polarization of waves shorter than the magneto-ionic critical wave-length has been investigated by a "pulse" method [2]. Both these methods necessitate the use of an experimental transmitter, and if such a transmitter is available they yield very complete information. The necessity for a controlled transmitter, however, has the disadvantage that the possible sites for the sender are limited, and thus there are difficulties in the way of a research involving the investigation of different directions of propagation.

* Communicated by Prof. E. V. Appleton, F.R.S.

such as would be theoretically interesting. In the present paper a new method of investigating the state of polarization of downcoming wireless waves is described, which may be used in conjunction with any transmitter sending continuous waves, modulated or "keyed" *. The method may therefore be used to investigate the waves arriving from stations situated in different directions and at different distances. The apparatus may be used on any wave-length, but in the present series of experiments attention has been confined to "medium" waves (200 to 500 m.) for the following reasons :—

(1) A fairly complete investigation of the short wave region has been made by the pulse method;

(2) there are several conveniently situated broadcasting stations in this range of wave-lengths;

(3) it seemed desirable to compare the present method with that previously used by Appleton and Ratcliffe, and, in particular, to investigate the rapid variations which they had encountered.

In order to simplify the necessary assumptions as to the trajectory of the wave, the experiments were confined to stations which were not more than a few hundred kilometres distant from the receiver. Several lines of evidence point to the fact that, under these conditions, it is legitimate to visualize a "ray" type of propagation, with possible multiple reflexions, with angle of incidence determined roughly by the geometrical conditions and the known (approximate) height of the reflexion. Because of the short distances involved, the ground ray was always present on the wave-lengths used. This fact complicated the apparatus, in that it was necessary to provide for its suppression; but, on the other hand, it provided a very useful datum from which the apparatus could be calibrated in the daytime (when the atmospheric ray was absent).

(2) *Apparatus.*

The apparatus consists in essentials of two mutually perpendicular loop aerials connected, through two separate amplifiers, to the opposite pairs of plates of a cathode-ray oscillograph. One of the loops is in the plane of

* A preliminary account of this method has already been published[3].

propagation, and is combined with a vertical aerial so that the ground ray is suppressed, but so that an e.m.f. is induced in it by the vertical electric field (which we will call the normally polarized component) of the downcoming wave. The e.m.f. in the other loop (perpendicular to the plane of propagation) is due to the horizontal electric field (abnormal component) of the downcoming wave. If the phases and amplitudes are properly maintained through the amplifiers, the relative phases and amplitudes of the e.m.f.'s in the two aerial systems may be deduced from the oscillograph pattern, and the state of polarization of the downcoming wave may be determined.

The suppressed ground-ray aerial system is essentially similar to that described by Appleton and Ratcliffe [6]. The circuit used is shown in fig. 1. The vertical aerial is a short rod (1·7 m. long) situated along the axis of the loop, which is arranged to rotate round it. The variable mutual inductance M, and the vertical aerial tuning condenser C, are fixed to the loop, so as to rotate with it, and are contained in a metal screening-box. Antenna effect in the loop is eliminated by arranging the circuit to be electrically symmetrical, as shown in the figure.

The loop aerial which is perpendicular to the plane of propagation (the "perpendicular loop") also rotates about the vertical aerial as axis, and is provided with a fine adjustment device, so that its plane can be brought perpendicular to that of the suppressed ground-ray loop. It is tuned by means of a split condenser so as to eliminate antenna effect. The leads from both aerials to the amplifiers consist of flexible shielded cable.

Since the aerial systems are in close proximity, and since both amplifiers are connected to the same oscillograph, it is especially important to guard against interaction effects, which may be due to any of the following causes:—

(1) coupling between the two aerial systems;

(2) coupling between the two output circuits, by way of the electrode capacities of the oscillograph tube;

(3) coupling between the output of one amplifier and the aerial of the other.

Coupling between the aerials is eliminated by the

arrangement described above *. The coupling between the output circuits is found to vary with the type of oscillograph used; with some it is negligible. When present it is eliminated by using a "neutrodyne" arrangement suggested to us by Mr. E. L. C. White. In order to prevent interaction between the output end of one amplifier and the input end of the other, the fre-

Fig. 1.

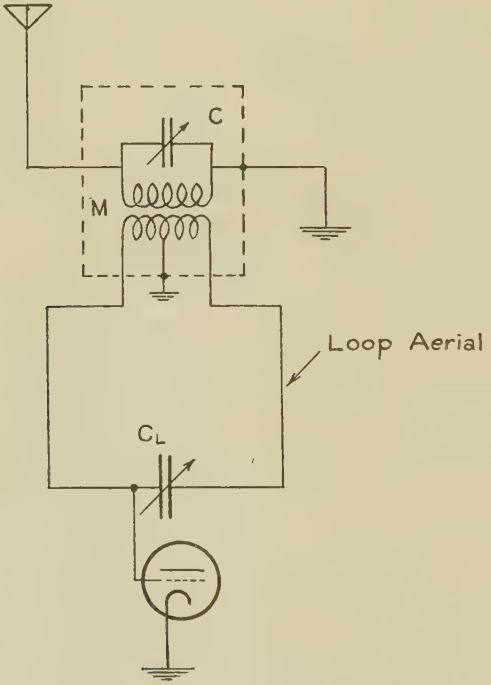

Suppressed ground-ray aerial system.

quency is changed half-way through the amplifiers. The heterodyning oscillation is fed from a common oscillator through screen grid separator valves into the two amplifiers. It has been pointed out by Merritt [4] that the phase relations are not disturbed by an arrangement such as this.

* This coupling is discussed by Appleton and Ratcliffe [2].

(3) *Adjustments.*

Let the downcoming wave be incident at an angle i in the plane of propagation, and let it have normal and abnormal field components given by (E_1, H_1) and (E_2, H_2) respectively. These field components are of the form $E_1 = E_{10} e^{j(pt+\varphi_1)}$ and their positive directions are taken to be orientated as in fig. 2, which is viewed looking along the ray. Let the electric and magnetic field of the ground wave be given by (E_0, H_0). Let E_L represent the e.m.f. induced by the wave in the loop circuit of the suppressed ground-ray system, and let E_A represent the e.m.f. in the vertical aerial, so that, when the ground wave alone is present,

$$E_L = \alpha \frac{dH_0}{dt} = jp\beta E_0$$

and

$$E_A = \gamma E_0,$$

Fig. 2.

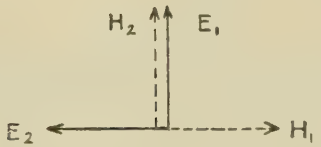

Field components viewed along positive direction of ray.

where α, β, and γ are circuit constants. These circuit constants are essentially real: in what follows we shall denote such constants by Greek letters, while Roman letters will be used to denote circuit constants which may be complex. If Z_L and Z_A are respectively the complex impedances of the loop and the equivalent series circuit of the aerial, it may be shown that the loop circuit current (i_L) is given by

$$i_L = \frac{E_L - \frac{jpM}{Z_A} E_A}{Z_L + \frac{p^2M^2}{Z_A}} = \frac{jpE_0 \left\{ \beta - \frac{M}{Z_A}\gamma \right\}}{Y},$$

where $Y = Z_L + \frac{p^2M^2}{Z_A}$ is a constant of the circuits. If,

now, the value of M is adjusted so that $\beta = \frac{M}{Z_A}\gamma$, the ground ray is completely suppressed. It will be noticed that this condition involves the fact that Z_A should be real, *i. e.*, the equivalent series aerial circuit should be tuned, but it is quite independent of Z_L, *i. e.*, of the tuning of the loop circuit. For the downcoming wave reference to fig. 3 shows that the induced e.m.f.'s are given by

$$E_L = \alpha \frac{dH_1}{dt}(1+K_1) = jp\beta E_1(1+K_1),$$

$$E_A = \gamma E_1(1+K_1)\sin i,$$

Fig. 3.

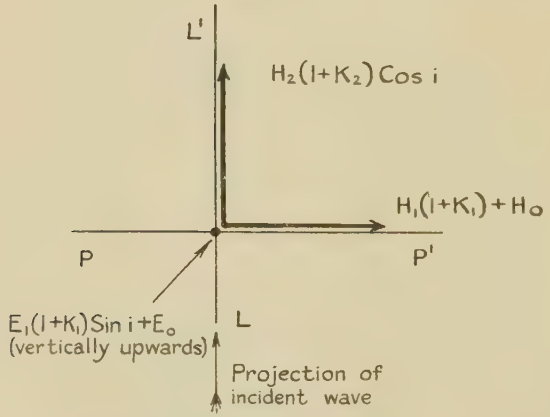

Ground-plan of fields.

K_1 being the reflexion coefficient of the ground for the normally polarized component. The resulting loop current is

$$i_L = \frac{jpE_1(1+K_1)\left\{\beta - \frac{M}{Z_A}\gamma \sin i\right\}}{Y},$$

and under conditions such that the ground ray is suppressed, we have

$$i_L = \frac{jpE_1(1+K_1)\beta(1-\sin i)}{Y} = jpXE_1(1+K_1)(1-\sin i),$$

X being a new circuit constant,

The e.m.f. in the perpendicular loop is given by

$$E_P=\eta\frac{d}{dt}H_2(1+K_2)\cos i=jp\zeta E_2(1+K_2)\cos i$$

and $$i_P=jpZE_2(1+K_2)\cos i,$$

where η, ζ, and Z are circuit constants, and K_2 is the reflexion coefficient for the abnormal component.

If the amplifiers are arranged to give linear amplification the e.m.f.'s e_1 and e_2 applied to the plates of the oscillograph are given by

$$e_1=jpX'E_1(1+K_1)(1-\sin i)e^{j(\omega-p)t}$$

and $$e_2=jpZ'E_2(1+K_2)\cos i\,e^{j(\omega-p)t},$$

where X′ and Z′ are new circuit constants, and the factor $e^{j(\omega-p)t}$ is due to the frequency change in the amplifier, ω being the new angular frequency. If the circuits are adjusted so that $\frac{X'}{Z'}$ is real, then the phase difference between the two electric vectors $E_1(1+K_1)$ and $E_2(1+K_2)$, acting on the aerial systems, is the same as that between the oscillograph e.m.f.'s, and this phase difference may be deduced from the nature of the oscillograph pattern. In order to adjust the circuits so that this condition is satisfied, use is made of the ground ray in the daytime, when no downcoming ray is present. The suppressed ground-ray loop is placed in the plane of propagation and the ground ray is suppressed, so that $\beta=\frac{M}{Z_A}\gamma$; the whole aerial system is then rotated through 90° in an anticlockwise direction as seen from above, so that, with the previous notation (see fig. 3),

$$\left.\begin{aligned}E_L&=0\\E_A&=\gamma E_0\end{aligned}\right\}.$$

$$\therefore\quad i_L=-jpXE_0,$$

giving $$e_1=-jpX'E_0,$$

and $$E_P=-\eta\frac{dH_0}{dt}=-jp\zeta E_0,$$

giving $$i_2=-jpZE_0 \quad\text{and}\quad e_2=-jpZ'E_0.$$

If, now, the amplifiers and their associated circuits are arranged so as to give a straight line on the oscillograph screen, it is known that $\frac{e_1}{e_2}$ is real, and hence that $\frac{X'}{Z'}$ is real, as required.

In order to carry out the calibration when using transmissions in which the ground ray in the daytime is much stronger than the downcoming ray at night, the amplifier gains are reduced by means of volume controls acting on variable screen-grid valves. It is found possible to arrange the gain controls so as not to affect the phases, and the method works quite well.

The above-mentioned method of calibration involves rotating the aerial system, and in order to be quite sure that this did not produce any disturbing effect it was checked by making use of an independent local oscillator arranged so as to send a ground wave in a direction perpendicular to the plane of propagation of the main signal. The effect of this local signal on the receiver was then the same as if the receiving system had been rotated through 90° and the main signal had been used, as in the calibration method described, but with the advantage that the receiving aerial system had not been altered in any way. The local transmitter was placed about $1\frac{1}{2}$ wavelengths away from the receiver, so that the phase relation between the electric and magnetic fields should be sensibly that of a radiation field. It was essential to work this transmitter on the same wave-length as the main transmitter; this was accomplished by the operator at the local transmitter listening, on a telephone line, to the signal received some distance away by a small receiver, and adjusting the local transmitter to give zero beat frequency with the main transmitter*. This check showed the method of adjustment to be quite reliable, and in future work it was dispensed with.

(4) *Effect of Ground Reflexions.*

The reflexion coefficients K_1 and K_2 are given by the expressions

$$K_1 = \frac{\sqrt{\epsilon}\cos i - \cos r}{\sqrt{\epsilon}\cos i + \cos r} \quad \text{and} \quad K_2 = -\frac{\cos i - \sqrt{\epsilon}\cos r}{\cos i + \sqrt{\epsilon}\cos r},$$

* To avoid any possibility of interference with the broadcast transmissions, these check observations were made during a very useful daily period of half-an-hour in the mornings during which the broadcasting station was found to emit an unmodulated carrier.

where i is the angle of incidence, r is the (complex) angle of refraction, and ϵ is the complex dielectric constant of the ground given by $\epsilon=\epsilon_0-\frac{2j\sigma}{f}$, where ϵ_0=true dielectric constant (e.s.u.), σ=conductivity (e.s.u), and f=wave frequency. The quantity $\frac{1+K_1}{1+K_2}$ which occurs in the above analysis is given by

$$\frac{1+K_1}{1+K_2}=\frac{\cos i\sec r+\sqrt{\epsilon}}{\sec i\cos r+\sqrt{\epsilon}}.$$

For the frequencies with which we are here concerned the approximate values of ϵ_0 and σ are known to be 10 and 10^8 e.s.u. respectively. The disturbing effect of the ground can be shown to become greater as the wave-length is decreased, so that if this effect can be shown to be negligible for a wave-length of 150 m., shorter than any wave-length used in these experiments, then the effects can be neglected here.

For 150 m. wave-length ϵ is found to be equal to $10-100j$. Using this value it is found that the value of $\cos r$, given by $\cos r=\sqrt{1-\frac{\sin^2 i}{\epsilon}}$ is approximately 1 for all values of $\sin i$; thus even when $\sin i=1$ it is found that $\cos r=1-0{\cdot}005j$. Then, writing the approximate value $\cos r=1$ in the equation, and putting $\sqrt{\epsilon}=7{\cdot}4-6{\cdot}7j$, we find

$$\frac{1+K_1}{1+K_2}=\frac{\cos i+7{\cdot}4-6{\cdot}7j}{\sec i+7{\cdot}4-6{\cdot}7j}=Re^{-j\delta},$$

where

$$R=\sqrt{\frac{6{\cdot}7^2+(7{\cdot}4+\cos i)^2}{6{\cdot}7^2+(7{\cdot}4+\sec i)^2}},$$

and

$$\delta=\tan^{-1}\frac{6{\cdot}7}{7{\cdot}4+\cos i}-\tan^{-1}\frac{6{\cdot}7}{7{\cdot}4+\sec i}.$$

The values of the phase difference δ and the amplitude ratio R introduced by the ground reflexion for various angles of incidence are plotted in fig. 4. It is seen that even with an angle of incidence of 60° the phase difference is only 5° and the amplitude ratio is 0·9, and that for

smaller angles of incidence, such as occur in the experiments described, the phase difference is less and the amplitude ratio is more nearly unity, so that we are justified in neglecting completely the effect of the ground and writing $\frac{1+K_1}{1+K_2}=1$.

(5) *Determination of the Sense of Rotation.*

The pattern obtained on the oscillograph screen by the above method enables the magnitude of the phase dif-

Fig. 4.

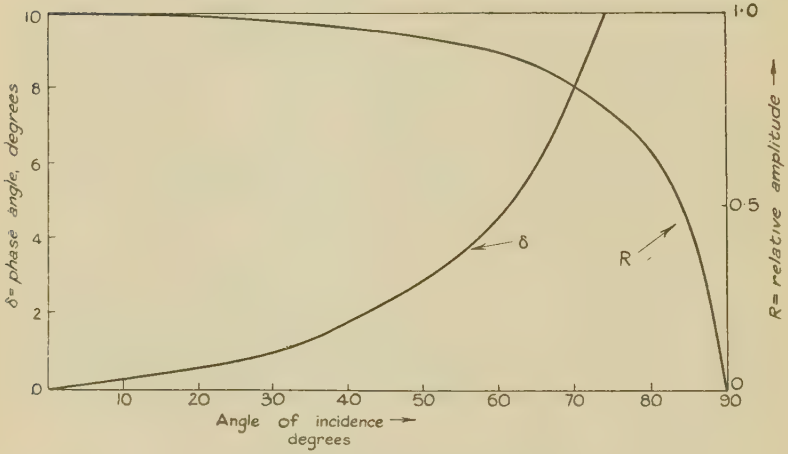

Effect of ground reflexion.

ference between $E_1(1+K_1)$ and $E_2(1+K_2)$ to be determined, but it gives no information as to its sign, *i. e.*, it leaves the sense of description of the ellipse unspecified. Information as to the sign of the phase difference is obtained by observing the effect of slightly detuning one of the aerial circuits. Thus suppose that, in the daytime, a straight line is obtained in a certain quadrant (the "calibration quadrant") when the calibration adjustment is made, *i. e.*, when $\frac{X'}{Z'}$ is a positive real quantity. Then

at night, with the aerial system in the normal position, we have, writing now $\frac{1+K_1}{1+K_2}=1$,

$$\frac{e_1}{e_2}=\frac{X'}{Z'}\frac{E_1}{E_2}\frac{(1-\sin i)}{\cos i},$$

and, if E_1 and E_2 are in phase e_1 and e_2 will be in phase, and we shall have a straight line in the calibration quadrant. If, however, the phase of E_1 differs from the phase of E_2, then an elliptical pattern is produced. If, now, a readjustment of the condenser C_L of the loop circuit of the suppressed ground-ray system is made, the phase of the current in this circuit, and hence of the e.m.f. e_1, will be altered; an increase in the capacity of C_L will produce a retardation of the phase of e_1 and *vice versa*. Suppose that, in the original wave ϕ_1 is greater than ϕ_2 by an angle less than $\frac{\pi}{2}$, then an increase in the capacity of C_L will decrease the phase angle ϕ_1 and will make the elliptical pattern approximate more closely to the straight line in the calibration quadrant. The above-mentioned condition, $0<(\phi_1-\phi_2)<\frac{\pi}{2}$, corresponds to a downcoming wave with a left-handed sense of rotation (looking along the direction of propagation). We therefore have the rule that if an increase of C_L causes the ellipse to approximate more closely to the straight line in the calibration quadrant, then the wave is left-handed, and *vice versa*.

(6) *Results and Theoretical Discussion.*

The method has been used to investigate the state of polarization of the downcoming wave received at Cambridge from the following stations of the B.B.C. :—

TABLE I.

Station.	Wave-length m.	Bearing (magnetic) (East of North.)	Distance km.
London Regional..	356	211°	60
London National ..	261	211°	60
Northern National .	301	334°	200
Midland Regional..	399	287°	86

It is found that the elliptical pattern on the oscillograph screen varies continually both in size and in shape, but that it corresponds nearly always to a left-handed sense of rotation. The elliptical pattern varies through all possible shapes, so that it is difficult to specify its behaviour in detail, but the following general statements can be made, and apply to reception from the above-mentioned stations :—

(i.) When the signal is strong the pattern is generally approximately circular and corresponds to a left-handed sense of rotation. It is unusual to observe straight lines or narrow ellipses with a strong signal.

(ii.) When the signal is weak or only moderate in strength the patterns are complicated, straight lines and narrow ellipses being frequently observed ; the direction of rotation is still predominantly left-handed, but there are occasions on which a right-handed sense is observed.

When using the "frequency change" method Appleton and Ratcliffe could only make deductions when conditions were reasonably constant and when the "fringes" obtained were "simple," *i. e.*, did not show complications due to the presence of multiply reflected waves. Their results, therefore, should agree with those recorded under (i.) above, and this is, in fact, found to be the case. They accounted theoretically for their results by assuming that, since the downcoming ray was inclined to the earth's magnetic field at only a small angle, the waves would behave approximately as in the longitudinal case of the magneto-ionic theory. It is now possible to extend their theory so as to avoid this assumption. Appleton[5] has shown that the absorption coefficient K, in the general case of propagation at any angle to the imposed magnetic field, is given by the expression

$$\frac{kc}{p} = \frac{z}{2x}\,\frac{(\mu^2-1)^2}{\mu}\left\{1+\frac{y_T^2}{2\left(1-\frac{2x}{3}\right)^2} \mp \frac{y_T^4}{2\left(1-\frac{2x}{3}\right)^2\sqrt{y_T^4+4y_L^2\left(1-\frac{2x}{3}\right)^2}}\right\},$$

where

$x=\dfrac{4\pi Ne^2}{mp^2}$, N=number of electrons per c.c.

e, m=electronic charge, mass.

p=angular frequency of wave.

$y_T=\dfrac{H_T e}{pmc}$, H_T=component of earth's magnetic field perpendicular to the wave normal.

$y_L=\dfrac{H_L e}{pmc}$, H_L=component of earth's magnetic field along the wave normal.

$z=\dfrac{\nu}{p}$, ν=frequency of electronic collisions.

c=velocity of light.

μ=refractive index.

This expression applies only to the case where $z<<1$; for the present purpose we will assume that it will be approximately true over most of the region where the absorption takes place. The upper sign corresponds to the extraordinary wave and the lower sign to the ordinary wave. The characteristic polarizations of the two waves which make up the wave incident at the receiver are probably determined at the last point in their trajectory at which they undergo differential absorption. There are several reasons for believing that this point is situated beneath the region where the waves are deviated appreciably, so that we may write $x<<1$ in the above expression. With this assumption we may take μ to be approximately equal to unity, and, inserting Appleton's expression for (μ^2-1), we arrive at the following approximate expression for K:

$$\frac{kc}{p}=z2x\left\{\frac{1}{2-y_T^2\mp\sqrt{y_T^4+4y_L^2}}\right\}^2\left\{1+\frac{y_T^2}{2}\mp\frac{y_T^4}{2\sqrt{y_T^4+4y_L^2}}\right\}$$

$$=zx\left\{\frac{1}{2-y_T^2(1\pm R)}\right\}^2\left\{2+y_T^2\left(1\mp\frac{1}{R}\right)\right\}. \qquad (A)$$

Where $R=\sqrt{1+\dfrac{4y_L^2}{y_T^4}}$,

and is always greater than unity.

We will further write

$$\{2-y_T^2(1\pm R)\}^2=P$$

and $$\left\{2+y_T^2\left(1\mp\frac{1}{R}\right)\right\}=Q,$$

so that $$\frac{Kc}{p}=zx\frac{Q}{P},$$

and we will denote by P_0, P_ϵ; Q_0, Q_ϵ the values of P and Q corresponding to the lower and upper signs respectively.

An examination of the equations reveals the following facts:

(i.) $Q_0>Q_\epsilon$ for all values of y_T^2 and of R.

(ii.) If $y_T^2>2$, then $P_0<P_\epsilon$ for all values of R.

(iii.) If $y_T^2<2$, then $P_0>P_\epsilon$ for all values of R.

(iv.) For a given value of y_T^2; $\frac{Q_0}{Q_\epsilon}$ has its greatest value when R=1.

(v.) For a given value of y_T^2; $\frac{P_0}{P_\epsilon}$ is most nearly unity when R=1.

From (i.) and (ii.) we see that if $y_T^2>2$, then $K_0>K_\epsilon$ for all values of R. From (i.) and (iii.) we see that for $y_T^2<2$ the two factors P and Q produce opposite effects on the value of the ratio $\frac{K_0}{K_\epsilon}$, and it is impossible, without further calculation, to decide which factor is the more important. To investigate this point we note from (iv.) and (v.) that the effect of Q is most marked compared with the effect of P when R=1. If, therefore, we find a critical value of y_T^2, such that, with R=1, $\frac{Q_0}{Q_\epsilon}<\frac{P_0}{P_\epsilon}$, then $K_0<K_\epsilon$, and this relation will hold, even more pronouncedly, when R has a value greater than unity. Putting R=1 we find $K_0=K_\epsilon$ at the critical value

$$y_T^2=\frac{2+\sqrt{10}}{3}=1\cdot72.$$

Thus for $y_T^2<1\cdot72$, $K_\epsilon>K_0$ for all values of R, and for $y_T^2>2\cdot0$, $K_\epsilon<K_0$ for all values of R. For y_T^2 between $1\cdot72$ and $2\cdot0$ the relative magnitudes of K_ϵ and K_0 depend on the value of R.

It is of interest to find for what conditions the differential absorption is most marked. Remembering that

R>1 it is seen that the first factor becomes infinite for the upper sign when $\frac{2}{1+R} = y_T^2$, so that for this condition $K_\epsilon = \infty$. A little reduction shows that this condition is the same as

$$y_T^2 + y_L^2 = 1 \quad \text{or} \quad p = \frac{e\sqrt{H_T^2 \cdot H_L^2}}{mc} = \frac{He}{mc},$$

where H is the total magnetic field. This value of p

Fig. 5.

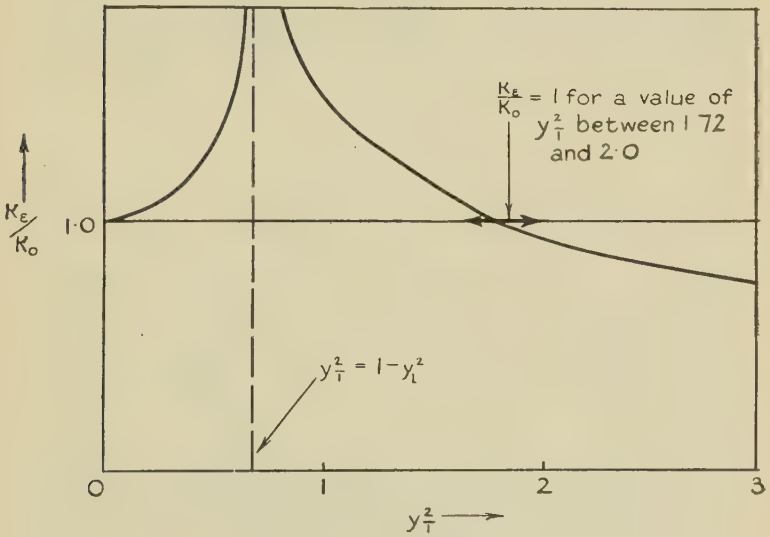

Ratio of absorption coefficient.

corresponds to the magneto-ionic critical wave-length of 214 m. It is now possible to sketch the curve of fig. 5 to indicate the relative values of K_0 and K_ϵ for different values of y_T^2.

To compare the experimental results with the theory we make the assumption that the wave travels through the absorbing region without appreciable deviation, and calculate the direction of travel in the absorbing region on the supposition of a sharp reflexion at a height of 100 km. (E region). The angle between the ray and the earth's magnetic field is calculated, and the value of y_T^2 is found, both for the upgoing and the downcoming

ray. The values are exhibited in Table II. If the two magneto-ionic components maintain their identity during their rapid deviation at the highest point of their trajectory, then both the absorption in the upgoing and that in the downcoming wave should be taken into account; if they do not, probably only that in the downcoming wave should be considered. From the present point of view it is sufficient to notice that all the values of y_T^2 are less than 1·72, so that for all the waves, in both parts of the trajectories, the extraordinary wave is the more absorbed, and we should expect the downcoming wave to be predominantly left-handed *. This is in agreement with the experimental results. In view of the very rapid changes in the shape of the observed polarization figures it has

TABLE II.

Station.	Angle between ray and magnetic field.		y_T^2.	
	Upgoing.	Down-coming.	Upgoing.	Down-coming.
London Regional ..	145°	20°	0·91	0·324
London National ..	145°	20°	0·49	0·174
Northern National..	154°	67°	0·395	1·68
Midland Regional ..	153°	38°	0·719	1·32

not seemed profitable to make a detailed comparison with the shapes to be expected theoretically; it is, however, clear that the "average" shapes are not inconsistent with those predicted by theory.

In order to obtain an estimate of the intensities of the two magneto-ionic component waves on arrival at the receiver, let us suppose that their attenuation takes place in a region where x can be supposed very small compared with unity, *i. e.*, where the wave velocity is not much different from that in free space, and that the collisional friction factor z varies throughout this region. The values of K_ϵ and K_0 will therefore vary, but from equation (A) we see that the ratio $\frac{K_\epsilon}{K_0}$ will be constant.

* In some recent experiments using the Daventry National transmitter ($\lambda = 1559$ m., $y_T^2 = 20$), Mr. R. Witty has found a large proportion of the extraordinary component in the downcoming wave.

If, then, ds represents an element of the path through the absorbing region, and if we assume that the wave incident on the region contains the two magneto-ionic components with equal amplitude E, then the amplitudes E_ϵ and E_0 on emergence will be given by

$$E_\epsilon = Ee^{-\int K_\epsilon ds} \quad \text{and} \quad E_0 = Ee^{-\int K_0 ds},$$

so that

$$\frac{E_0}{E_\epsilon} = e^{-\int (K_0 - K_\epsilon) ds} = e^{-\left(1-\frac{K_\epsilon}{K_0}\right)\int K_0 ds} = \left(\frac{E_0}{E}\right)^{\left(1-\frac{K_\epsilon}{K_0}\right)}.$$

This result shows that the relative amplitude on emergence is equal to $\frac{E_0}{E}$ raised to a constant power, so that when the overall emergent signal is small $\left(\frac{E_0}{E} << 1\right)$ the two component waves emerge with very different amplitudes, whereas when the overall signal is large $\left(\frac{E_0}{E}$ approaching unity$\right)$ the two waves have more nearly equal amplitudes. This deduction has been confirmed in the short wave experiments described by E. L. C. White and one of the present authors [2]; this confirmation lends support to the truth of the hypotheses involved in the above theoretical treatment. According to this reasoning it would be expected that, in the present experiments, when the received signal is large the two components would be nearly equal in intensity, and the oscillograph pattern would alter in shape and might change its direction of rotation, whereas when it became small due to absorption the ordinary component would be much stronger than the extraordinary and the pattern would be steady and always of one sign of rotation. Now, the observations (i.) and (ii.) listed above are in direct contradiction to this expectation. It seems, therefore, that the amplitude variations are not due in the main to absorption effects, but must be due to interference effects between two or more downcoming waves, which have travelled by different paths*. Even in the hours of

* Some recent experiments seem to indicate that we must not exclude the possibility of waves arriving simultaneously from a large area of the ionosphere by a process of irregular reflexion. Such a process might produce "lateral deviation" effects which might alter the responses of the two aerial systems, and so might be responsible for the rapid changes of shape of the oscillograph pattern.

darkness there must be sufficient absorption to make the ordinary component much the stronger, and this component gives the large steady pattern with left-handed rotation. When this ordinary component is reduced in intensity by destructive interference, without the extraordinary component being so reduced (as is possible since their optical paths will be different), a smaller signal is received in which the right-handed component is relatively more important, so that rapidly changing shapes and occasional right-handed polarization are observed. The deduction from the experiments is, therefore, that the more rapid variations of intensity of the downcoming wave are due to interference effects and are not due to absorption. This supports a suggestion, put forward on quite different grounds, by Appleton and Ratcliffe [6].

In conclusion, we wish to express our gratitude to our colleagues, Messrs. J. L. Pawsey and R. Witty, for the very considerable help they have given us during the progress of the work.

References.

(1) E. V. Appleton and J. A. Ratcliffe, Proc. Roy. Soc. A, cxvii. p. 576 (1928).
(2) J. A. Ratcliffe and E. L. C. White, Phil. Mag. xvi. p. 125 (1933).
(3) J. A. Ratcliffe and F. W. G. White, 'Nature,' cxxix. p. 364 (1932).
(4) Merritt, U.S. Patent 1,510,792.
(5) E. V. Appleton, Journ. I. E. E. lxxi. p. 642 (1932).
(6) E. V. Appleton and J. A. Ratcliffe, Proc. Roy. Soc. A, cxv. p. 315 (1927).

XXXIV. *Proofs of some Formulæ for the Hypergeometric Function. By* T. M. MacRobert, *Professor of Mathematics in the University of Glasgow* *.

§ 1. *Introductory.*

THE formulæ for the analytical continuation of the hypergeometric function $F(\alpha, \beta; \gamma; z)$ are usually established by means of contour integrals. The advantage of that method is that no restrictions need be placed on the values of the constants α, β, γ, except such as are

* Communicated by the Author.

necessary for the existence of the functions. In this paper it is shown that certain formulæ, (1) and (18) below, can be proved without contour integration for restricted values of the constants, and that the restrictions can then be removed by means of recurrence formulæ. There is then no difficulty in establishing the relations between the integrals of the hypergeometric equation, valid in different parts of the z-plane. It is also pointed out that the method can be employed to prove important formulæ for the Legendre Functions.

§ 2. *Recurrence Formulæ.*

In Gauss's 'Collected Works,' iii. pp. 130 and 133, a set of 23 recurrence formulæ for the hypergeometric function is given. On pp. 143 and 147 of the same volume he employs one of these formulæ in proving his well-known theorem

$$\mathrm{F}(\alpha, \beta; \gamma; 1) = \frac{\Gamma(\gamma)\Gamma(\gamma-\alpha-\beta)}{\Gamma(\gamma-\alpha)\Gamma(\gamma-\beta)}, \quad . \quad . \quad . \quad (1)$$

where $\mathrm{R}(\gamma-\alpha-\beta)>0$, and γ is not zero or a negative integer.

The following recurrence formulæ can be easily verified. All that is necessary is to show that the coefficient of z^n in each equation has the value zero:

$$\gamma\mathrm{F}(\alpha, \beta-1; \gamma; z)-\gamma\mathrm{F}(\alpha-1, \beta; \gamma; z) + (\alpha-\beta)z\mathrm{F}(\alpha, \beta; \gamma+1; z) = 0. \quad (2)$$

$$\gamma(\alpha-\beta)\mathrm{F}(\alpha, \beta; \gamma; z)-\alpha(\gamma-\beta)\mathrm{F}(\alpha+1, \beta; \gamma+1; z) + \beta(\gamma-\alpha)\mathrm{F}(\alpha, \beta+1; \gamma+1; z) = 0. \quad (3)$$

$$\gamma(\gamma+1)\mathrm{F}(\alpha, \beta; \gamma; z)-\gamma(\gamma+1)\mathrm{F}(\alpha, \beta; \gamma+1; z) - \alpha\beta z\mathrm{F}(\alpha+1, \beta+1; \gamma+2; z) = 0. \quad (4)$$

$$\gamma\mathrm{F}(\alpha, \beta; \gamma; z)-(\gamma-\alpha)\mathrm{F}(\alpha, \beta+1; \gamma+1; z) - \alpha(1-z)\mathrm{F}(\alpha+1, \beta+1; \gamma+1; z) = 0. \quad (5)$$

$$\gamma\mathrm{F}(\alpha, \beta; \gamma; z)-(\gamma-\beta)\mathrm{F}(\alpha+1, \beta; \gamma+1; z) - \beta(1-z)\mathrm{F}(\alpha+1, \beta+1; \gamma+1; z) = 0. \quad (6)$$

$$\gamma(\gamma-\alpha-\beta z)\mathrm{F}(\alpha,\beta;\gamma;z)-\gamma(\gamma-\alpha)\mathrm{F}(\alpha-1,\beta;\gamma;z)$$
$$+\alpha\beta z(1-z)\mathrm{F}(\alpha+1,\beta+1;\gamma+1;z)=0. \quad (7)$$

$$\gamma(\gamma-\beta-\alpha z)\mathrm{F}(\alpha,\beta;\gamma;z)-\gamma(\gamma-\beta)\mathrm{F}(\alpha,\beta-1;\gamma;z)$$
$$+\alpha\beta z(1-z)\mathrm{F}(\alpha+1,\beta+1;\gamma+1;z)=0. \quad (8)$$

$$\gamma\mathrm{F}(\alpha,\beta;\gamma;z)-\gamma\mathrm{F}(\alpha,\beta+1;\gamma;z)$$
$$+\alpha z\mathrm{F}(\alpha+1,\beta+1;\gamma+1;z)=0. \quad (9)$$

$$\gamma\mathrm{F}(\alpha,\beta;\gamma;z)-\gamma\mathrm{F}(\alpha+1,\beta;\gamma;z)$$
$$+\beta z\mathrm{F}(\alpha+1,\beta+1;\gamma+1;z)=0. \quad (10)$$

$$\gamma\{\alpha-(\gamma-\beta)z\}\mathrm{F}(\alpha,\beta;\gamma;z)-\alpha\gamma(1-z)\mathrm{F}(\alpha+1,\beta;\gamma;z)$$
$$+(\gamma-\alpha)(\gamma-\beta)z\mathrm{F}(\alpha,\beta;\gamma+1;z)=0. \quad (11)$$

$$\gamma\{\beta-(\gamma-\alpha)z\}\mathrm{F}(\alpha,\beta;\gamma;z)-\beta\gamma(1-z)\mathrm{F}(\alpha,\beta+1;\gamma;z)$$
$$+(\gamma-\alpha)(\gamma-\beta)z\mathrm{F}(\alpha,\beta;\gamma+1;z)=0. \quad (12)$$

$$\gamma(\gamma+1)\mathrm{F}(\alpha,\beta;\gamma;z)-\gamma(\gamma+1)\mathrm{F}(\alpha,\beta+1;\gamma+1;z)$$
$$+\alpha(\gamma-\beta)z\mathrm{F}(\alpha+1,\beta+1;\gamma+2;z)=0. \quad (13)$$

$$\gamma(\gamma+1)\mathrm{F}(\alpha,\beta;\gamma;z)-\gamma(\gamma+1)\mathrm{F}(\alpha+1,\beta;\gamma+1;z)$$
$$+\beta(\gamma-\alpha)z\mathrm{F}(\alpha+1,\beta+1;\gamma+2;z)=0. \quad (14)$$

$$\gamma\mathrm{F}(\alpha,\beta;\gamma;z)-(\gamma-\beta)\mathrm{F}(\alpha,\beta;\gamma+1;z)$$
$$-\beta\mathrm{F}(\alpha,\beta+1;\gamma+1;z)=0. \quad (15)$$

$$\gamma\mathrm{F}(\alpha,\beta;\gamma;z)-(\gamma-\alpha)\mathrm{F}(\alpha,\beta;\gamma+1;z)$$
$$-\alpha\mathrm{F}(\alpha+1,\beta;\gamma+1;z)=0. \quad (16)$$

Formulæ (11), (12), (13), (14), (15), and (16) are Gauss's formulæ (4), (11), (19), (20), (12), and (5) respectively. The first two of these are quoted incorrectly in the 'Collected Works.'

§ 3. *Gauss's Theorem.*

Theorem (1) can be deduced from the formula

$$\int_0^1 \lambda^{\beta-1}(1-\lambda)^{\gamma-\beta-1}(1-\lambda z)^{-\alpha}\,d\lambda=\mathrm{B}(\beta,\gamma-\beta)\mathrm{F}(\alpha,\beta;\gamma;z), \quad (17)$$

where $\mathrm{R}(\beta)>0$, $\mathrm{R}(\gamma-\beta)>0$.

This formula can be established by expanding $(1-\lambda z)^{-\alpha}$, where $|z|<1$, in powers of z, and integrating term by term. If $\mathrm{R}(\gamma-\alpha-\beta)>0$, the hypergeometric function converges absolutely when $z=1$ (Gibson, 'Advanced Calculus,' p. 174), and the integral then becomes

$$\int_0^1 \lambda^{\beta-1}(1-\lambda)^{\gamma-\alpha-\beta-1}d\lambda = \mathrm{B}(\beta, \gamma-\alpha-\beta).$$

Hence, if $\mathrm{R}(\gamma-\alpha-\beta)>0$, $\mathrm{R}(\beta)>0$, $\mathrm{R}(\gamma-\beta)>0$,

$$\mathrm{F}(\alpha, \beta; \gamma; 1) = \frac{\Gamma(\gamma)\Gamma(\gamma-\alpha-\beta)}{\Gamma(\gamma-\alpha)\Gamma(\gamma-\beta)}.$$

The restrictions $\mathrm{R}(\beta)>0$, $\mathrm{R}(\gamma-\beta)>0$ can be removed by the method of induction. Assume that the formula holds when $n<\mathrm{R}(\beta)\leqq n+1$, where n is an integer. Then, if $n-1<\mathrm{R}(\beta)\leqq n$, it follows from (13) and (1) that, if γ is not zero or a negative integer and $\mathrm{R}(\gamma-\alpha-\beta)>0$, $\mathrm{R}(\gamma-\beta)>0$,

$$\begin{aligned}\mathrm{F}(\alpha, \beta; \gamma; 1) &= \frac{\Gamma(\gamma+1)\Gamma(\gamma-\alpha-\beta)}{\Gamma(\gamma-\alpha+1)\Gamma(\gamma-\beta)} \\ &\quad - \frac{\alpha(\gamma-\beta)}{\gamma(\gamma+1)} \frac{\Gamma(\gamma+2)\Gamma(\gamma-\alpha-\beta)}{\Gamma(\gamma-\alpha+1)\Gamma(\gamma-\beta+1)} \\ &= \frac{\Gamma(\gamma)\Gamma(\gamma-\alpha-\beta)}{\Gamma(\gamma-\alpha)\Gamma(\gamma-\beta)}.\end{aligned}$$

Hence, by induction, the formula holds if $\mathrm{R}(\gamma-\alpha-\beta)>0$, $\mathrm{R}(\gamma-\beta)>0$, where γ is not zero or a negative integer.

Again, suppose that the formula holds if

$$n<\mathrm{R}(\gamma-\beta)\leqq n+1,$$

where n is an integer, and assume that

$$n-1<\mathrm{R}(\gamma-\beta)\leqq n.$$

In formula (2) replace α by $\alpha+1$, and it becomes

$$\begin{aligned}\mathrm{F}(\alpha, \beta; \gamma; z) &= \mathrm{F}(\alpha+1, \beta-1; \gamma; z) \\ &\quad + \frac{\alpha-\beta+1}{\gamma} z\mathrm{F}(\alpha+1, \beta; \gamma+1; z).\end{aligned}$$

Hence, if $\mathrm{R}(\gamma-\alpha-\beta)>0$ and γ is not zero or a negative integer,

$$\begin{aligned}\mathrm{F}(\alpha, \beta; \gamma; 1) &= \frac{\Gamma(\gamma)\Gamma(\gamma-\alpha-\beta)}{\Gamma(\gamma-\alpha-1)\Gamma(\gamma-\beta+1)} \\ &\qquad + \frac{\alpha-\beta+1}{\gamma}\frac{\Gamma(\gamma+1)\Gamma(\gamma-\alpha-\beta)}{\Gamma(\gamma-\alpha)\Gamma(\gamma-\beta+1)} \\ &= \frac{\Gamma(\gamma)\Gamma(\gamma-\alpha-\beta)}{\Gamma(\gamma-\alpha)\Gamma(\gamma-\beta+1)}(\gamma-\alpha-1+\alpha-\beta+1) \\ &= \frac{\Gamma(\gamma)\Gamma(\gamma-\alpha-\beta)}{\Gamma(\gamma-\alpha)\Gamma(\gamma-\beta)}.\end{aligned}$$

Thus formula (1) holds provided that $\mathrm{R}(\gamma-\alpha-\beta)>0$ and that γ is not zero or a negative integer.

§ 4. *The Four Forms of the Hypergeometric Function.*

If the integral in (17) is transformed by the substitution $\lambda=1-\mu$, it becomes

$$(1-z)^{-\alpha}\int_0^1 \mu^{\gamma-\beta-1}(1-\mu)^{\beta-1}\left(1-\mu\frac{z}{z-1}\right)^{-\alpha}d\mu,$$

and this, if $|z/(z-1)|<1$, has the value

$$\mathrm{B}(\gamma-\beta, \beta)(1-z)^{-\alpha}\mathrm{F}\left(\alpha, \gamma-\beta; \gamma; \frac{z}{z-1}\right).$$

Hence it follows that, if $\mathrm{R}(\beta)>0$, $\mathrm{R}(\gamma-\beta)>0$, and γ is not zero or a negative integer,

$$\mathrm{F}(\alpha, \beta; \gamma; z) = (1-z)^{-\alpha}\mathrm{F}\left(\alpha, \gamma-\beta; \gamma; \frac{z}{z-1}\right). \quad (18)$$

The series on the right converges if $\mathrm{R}(z)<\frac{1}{2}$, and, consequently, the R.H.S. gives the analytical continuation of the hypergeometric function over that half-plane.

The restriction $\mathrm{R}(\gamma-\beta)>0$ will now be removed. Suppose that (18) holds for $n<\mathrm{R}(\gamma-\beta)\leq n+1$; then, if $n-1<\mathrm{R}(\gamma-\beta)\leq n$, it follows from (16) that, if $\mathrm{R}(\beta)>0$ and γ is not zero or a negative integer,

$$\gamma F(\alpha, \beta; \gamma; z)$$

$$= (\gamma-\alpha)(1-z)^{-\alpha} F\left(\alpha, \gamma-\beta+1; \gamma+1; \frac{z}{z-1}\right)$$

$$+\alpha(1-z)^{-\alpha-1} F\left(\alpha+1, \gamma-\beta+1; \gamma+1; \frac{z}{z-1}\right)$$

$$= (1-z)^{-\alpha}\left\{(\gamma-\alpha) F\left(\alpha, \gamma-\beta+1; \gamma+1; \frac{z}{z-1}\right)\right.$$

$$\left.+\alpha\left(1-\frac{z}{z-1}\right) F\left(\alpha+1, \gamma-\beta+1; \gamma+1; \frac{z}{z-1}\right)\right\}$$

$$= (1-z)^{-\alpha}\gamma F\left(\alpha, \gamma-\beta; \gamma; \frac{z}{z-1}\right),$$

by (5).

Thus the formula holds for all values of $\gamma-\beta$.

Again, suppose that the formula holds for

$$n < R(\beta) \leqq n+1;$$

then, if $n-1 < R(\beta) \leqq n$, from (5)

$$\gamma F(\alpha, \beta; \gamma; z) = (\gamma-\alpha)(1-z)^{-\alpha} F\left(\alpha, \gamma-\beta; \gamma+1; \frac{z}{z-1}\right)$$

$$+\alpha(1-z)^{-\alpha} F\left(\alpha+1, \gamma-\beta; \gamma+1; \frac{z}{z-1}\right)$$

$$= (1-z)^{-\alpha}\gamma F\left(\alpha, \gamma-\beta; \gamma; \frac{z}{z-1}\right),$$

by (16). Hence the formula holds for all values of β, provided only that γ is not zero or a negative integer.

By interchanging α and β in (18) we derive the formula

$$F(\alpha, \beta; \gamma; z) = (1-z)^{-\beta} F\left(\beta, \gamma-\alpha; \gamma; \frac{z}{z-1}\right). \quad (19)$$

Again, on equating the right-hand sides of (18) and (19) and replacing β by $\gamma-\beta$ and z by $z/(z-1)$, the equation

$$F(\alpha, \beta; \gamma; z) = (1-z)^{\gamma-\alpha-\beta} F(\gamma-\alpha, \gamma-\beta; \gamma; z) \quad (20)$$

is obtained. Equations (18), (19), and (20) give the four forms of the hypergeometric function.

§ 5. *The Analytical Continuation of the Hypergeometric Function.*

It is now possible, by employing a method given long ago by Kummer (*Crelle*, xv. 1836, p. 56), to establish the formulæ for the analytical continuation of the hypergeometric function, without employing contour integration. The details of the method are merely indicated here; they are given more fully in § 6, in the proof of a formula for the Legendre Functions.

In the region common to the two domains $|z|<1$, $|z-1|<1$,

$$F(\alpha, \beta; \gamma; z) = AF(\alpha, \beta; \alpha+\beta-\gamma+1; 1-z) + B(1-z)^{\gamma-\alpha-\beta}F(\gamma-\alpha, \gamma-\beta; \gamma-\alpha-\beta+1; 1-z), \quad (21)$$

where A and B are constants, since the three functions satisfy the hypergeometric equation. To make the functions uniform, a cross-cut is taken along the x-axis from 1 to 2.

Now, if $R(\gamma-\alpha-\beta)>0$, if $\gamma-\alpha-\beta$ is not a positive integer, and if γ is not zero or a negative integer, this gives, when $z=1$,

$$F(\alpha, \beta; \gamma; 1) = A. \quad . \quad . \quad . \quad . \quad . \quad (22)$$

Again, if, further, $R(\gamma)<1$, (21) becomes, when $z=0$,

$$1 = AF(\alpha, \beta; \alpha+\beta-\gamma+1; 1) + BF(\gamma-\alpha, \gamma-\beta; \gamma-\alpha-\beta+1; 1). \quad (23)$$

On substituting in (22) and (33) from (1), and solving for A and B, we find that

$$F(\alpha, \beta; \gamma; z) = \frac{\Gamma(\gamma)\Gamma(\gamma-\alpha-\beta)}{\Gamma(\gamma-\alpha)\Gamma(\gamma-\beta)} F(\alpha, \beta; \alpha+\beta-\gamma+1; 1-z) + \frac{\Gamma(\gamma)\Gamma(\alpha+\beta-\gamma)}{\Gamma(\alpha)\Gamma(\beta)} (1-z)^{\gamma-\alpha-\beta} \times F(\gamma-\alpha, \gamma-\beta; \gamma-\alpha-\beta+1; 1-z), \quad (24)$$

where $R(\gamma-\alpha-\beta)>0$, $R(\gamma)<1$, and the constants are such that the functions exist.

The restrictions $R(\gamma-\alpha-\beta)>0$, $R(\gamma)<1$ can be removed as follows. When $R(\gamma-\alpha-\beta)>0$, $R(\gamma)>1$, transform the functions on the right of (21) by means of (20) and multiply by $z^{\gamma-1}$ before making the substitutions $z=0$ and $z=1$. It is sufficient to *verify* that the values of A and B found above still hold. For $R(\gamma-\alpha-\beta)<0$, $R(\gamma)<1$, transform the function on the left of (21) by means of (20) and multiply by $(1-z)^{\alpha+\beta-\gamma}$ before substituting. For $R(\gamma-\alpha-\beta)<0$, $R(\gamma)>1$, transform all the functions and multiply by $z^{\gamma-1}(1-z)^{\alpha+\beta-\gamma}$ before substituting. The border line cases $R(\gamma-\alpha-\beta)=0$ and $R(\gamma)=1$ can be deduced from considerations of continuity.

In deriving the formula for the region $|z|>1$ a cross-cut is taken along the x-axis from $-\infty$ to $+\infty$, and it is assumed that the amplitudes of z, $z-1$, and $1-z$ all have their principal values. Formula (24) is then applied to the R.H.S. of (18), and (18) is applied to the functions so obtained. The resulting expression for $F(\alpha, \beta; \gamma; z)$ when $|z|>1$ is

$$\frac{\Gamma(\gamma)\Gamma(\beta-\alpha)}{\Gamma(\gamma-\alpha)\Gamma(\beta)} e^{\pm i\pi\alpha} z^{-\alpha} F\left(\alpha, \alpha-\gamma+1; \alpha-\beta+1; \frac{1}{z}\right)$$

$$+\frac{\Gamma(\gamma)\Gamma(\alpha-\beta)}{\Gamma(\gamma-\beta)\Gamma(\alpha)} e^{\pm i\pi\beta} z^{-\beta} F\left(\beta, \beta-\gamma+1; \beta-\alpha+1; \frac{1}{z}\right), \quad (25)$$

where the upper or lower sign is taken according as $I(z) \gtrless 0$, the constants being such that the functions all exist.

§ 6. *A Legendre Function Formula.*

The method outlined in § 5 may also be employed to prove the important formula

$$Q_n^m(z) = \frac{\Gamma(m+n+1)\Gamma(m-n)}{2\Gamma(m+1)}$$

$$\times \left\{ \left(\frac{z+1}{z-1}\right)^{\frac{1}{2}m} F\left(-n, n+1; m+1; \frac{1+z}{2}\right) \right.$$

$$\left. - e^{\mp m\pi i} \left(\frac{z-1}{z+1}\right)^{\frac{1}{2}m} F\left(-n, n+1; m+1; \frac{1-z}{2}\right) \right\},$$

. . . (26)

where

$$Q_n^m(z) = \frac{\Gamma(m+n+1)\Gamma(\frac{1}{2})}{2^{n+1}\Gamma(n+\frac{3}{2})} \frac{(z^2-1)^{\frac{1}{2}m}}{z^{m+n+1}} \times F\left(\frac{m+n+1}{2}, \frac{m+n+2}{2}; n+\tfrac{3}{2}; \frac{1}{z^2}\right), \quad (27)$$

a cross-cut being taken along the x-axis from $-\infty$ to $+\infty$ to make the functions uniform. Formula (26) was given by Hobson (Phil. Trans. clxxxvii. A, 1896, p. 460). He established it by means of contour integrals. [For the definition given in (27) see Phil. Mag. ser. 7, xiv. p. 650.]

Since all the functions on the right of (26) and (27) satisfy Legendre's Associated Equation in the region common to the domains $|z-1|<2$, $|z+1|<2$, and $|z|>1$,

$$\frac{1}{z^{m+n+1}} F\left(\frac{m+n+1}{2}, \frac{m+n+2}{2}; n+\tfrac{3}{2}; \frac{1}{z^2}\right) = \frac{A}{(z-1)^m} F\left(-n, n+1; m+1; \frac{1+z}{2}\right) + \frac{B}{(z+1)^m} F\left(-n, n+1; m+1; \frac{1-z}{2}\right). \quad (28)$$

If $R(m)>0$, apply (20) to the function on the left, and multiply by $(z^2-1)^m$; then

$$z^{m-n-1} F\left(\frac{-m+n+2}{2}, \frac{-m+n+1}{2}; n+\tfrac{3}{2}; \frac{1}{z^2}\right) = A(z+1)^m F\left(-n, n+1; m+1; \frac{1+z}{2}\right) + B(z-1)^m F\left(-n, n+1; m+1; \frac{1-z}{2}\right).$$

Here put $z=1$ and apply (1); thus

$$\frac{\Gamma(n+\frac{3}{2})\Gamma(m)}{\Gamma\left(\frac{m+n+1}{2}\right)\Gamma\left(\frac{m+n+2}{2}\right)} = A 2^m \frac{\Gamma(m+1)\Gamma(m)}{\Gamma(m+n+1)\Gamma(m-n)},$$

and therefore, since (Gibson, 'Advanced Calculus,' p. 253)

$$\Gamma(m+n+1)\Gamma(\tfrac{1}{2})=2^{m+n}\Gamma\left(\frac{m+n+1}{2}\right)\Gamma\left(\frac{m+n+2}{2}\right),$$

$$\mathrm{A}=2^n\frac{\Gamma(n+\frac{3}{2})\Gamma(m-n)}{\Gamma(\frac{1}{2})\Gamma(m+1)}.$$

Again, put $z=-1$ and apply (1); thus

$$e^{\mp i\pi(n+1)}\frac{\Gamma(n+\frac{3}{2})\Gamma(m)}{\Gamma\left(\frac{m+n+1}{2}\right)\Gamma\left(\frac{m+n+2}{2}\right)}$$

$$=\mathrm{B}2^m\frac{\Gamma(m+1)\Gamma(m)}{\Gamma(m+n+1)\Gamma(m-n)},$$

whence

$$\mathrm{B}=-e^{\mp n\pi i}2^n\frac{\Gamma(n+\frac{3}{2})\Gamma(m-n)}{\Gamma(\frac{1}{2})\Gamma(m+1)},$$

according as $\mathrm{I}(z)\gtrless 0$.

Thus (26) holds if $\mathrm{R}(m)>0$. When $\mathrm{R}(m)<0$ the same results may be obtained by transforming the functions on the right of (28) by means of (20) before substituting for z. The case $\mathrm{R}(m)=0$ follows from considerations of continuity. The constants m and n must be such that the functions exist.

XXXV. *The Distribution of the Ionizing Particles of the Penetrating Radiation in Relation to the Magnetic Meridian.* *By* J. P. T. Viljoen *and* B. F. J. Schonland, *The University of Cape Town**.

ASSOCIATED with the penetrating or cosmic radiation are electrified particles of very high energy. Several writers have examined the influence which the earth's magnetic field should have upon the path of such particles, and it has been shown that a fast downward-moving electron or proton, provided that it is not a secondary ray produced in the lower atmosphere, may have its path so bent that it is unable to reach certain parts of the earth's surface at all. The forbidden region

* Communicated by the Author.

extends from the magnetic equator outwards as the energy of the particle decreases. A. H. Compton * and his co-workers and Clay and Berlage † have recently reported a variation in the total intensity of the radiation with magnetic latitude which is to be explained on these lines. The effect does not, however, disclose the sign of the charge upon the particles.

An examination of the nature of these curved paths shows that for negatively charged particles there should be a predominance in the number arriving from the east of the vertical plane through the magnetic meridian, and for positive particles a predominance from the west ‡. It has therefore been suggested that a comparison in the numbers of particles from these two directions should reveal an asymmetry in the distribution from which the sign of their charge could be determined. It appears that there should also be a difference in the numbers from north and south but only of the second order compared to that between east and west §.

A comparison of the distribution on the two sides of the meridianal plane has been made by Rossi || in Florence (mag. lat. 44° N.), who found that the asymmetry was less than his mean counting error of 1·5 per cent. An approximately symmetrical distribution of the same nature has been reported by Skobelzyn from Paris ¶.

The comparison described in the present paper included the north and south directions as well as the east and west. It was thought that the situation of Cape Town at the lower end of the African continent made the north–south comparison of additional interest in connexion with the possibility that some of the particles originate in thunderstorms. A repetition of Rossi's east–west comparison was thought desirable in view of the different magnetic latitude. Cape Town lies in magnetic latitude 31° S. and in a region where it appears ** that the total penetrating ray ionization alters fairly rapidly with latitude.

* A. H. Compton, Phys. Rev. xli. pp. 111 and 681 (1932).
† Clay and Berlage, *Naturwiss.* xxxvii. p. 687 (1933).
‡ Rossi, Phys. Rev. xxxvi. p. 606 (1930). Lemaître and Vallarto, Phys. Rev. xliii. p. 87 (1933).
§ Lemaître and Vallarto, Phys. Rev. xliii. p. 87 (1933).
|| Rossi, *Acad. d. Lincei*, Atti xiii. p. 47 (1931).
¶ Skobelzyn, *C. R.* cxciv. p. 118 (1932).
** Compton, Sc. Monthly, xxxvi. p. 75 (1933).

§ 1. *Apparatus and Experimental Arrangement.*

The particles were counted by means of the coincident impulses they produced in passing through two separate Geiger-Müller tube-counters. The counters were each 15·1 cm. long and 4·1 cm. in initial diameter, and they were mounted with their axes horizontal and 8·0 cm. apart. One counter was 5·5 cm. higher above the ground than the other, so that the combination as a coincidence counter was responsive to fast-moving particles from directions included between two planes at angles of 14° 8′ and 70° 42′ with the horizontal, and comprised within a

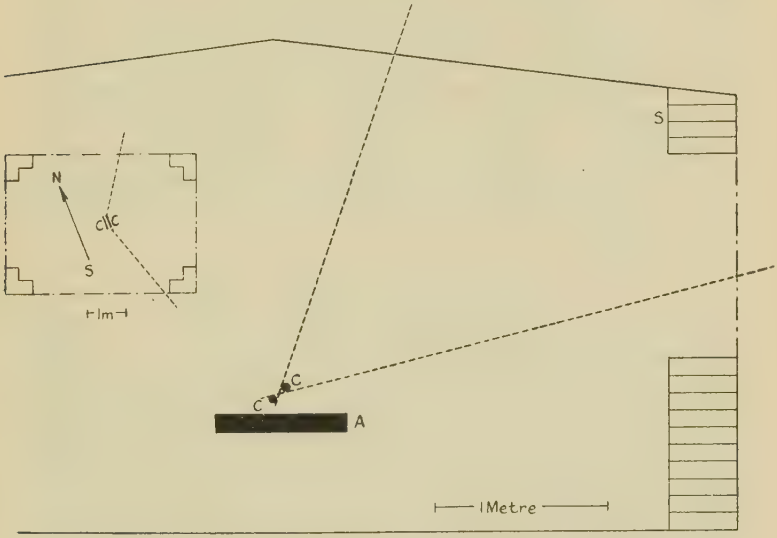

Section of room facing north (concrete beam, S, carried right round the room). Inset: plan.

cone of half-angle 61° 43′ (see figure). The arrangement could be rotated about a vertical axis to alter the relation between the cone of receipt of the rays and the magnetic meridian.

The counters were mounted on a wooden turntable, and their central wire electrodes were connected to a pair of ebonite-insulated slip-rings placed directly above the centre of the turntable. The counter impulses were led by spring contacts from these slip-rings to the coincidence counting circuit. This was of the type described

by Bothe*, using a double-grid valve. The amplifier was placed in a tin-covered screening-box, and the coincident impulses were finally registered on a mechanical counter operated by a thyratron.

In directional measurements it is essential to avoid interference with the paths of the particles such as can be caused by solid obstacles. The experiments were carried out in a room in the tower of the Department of Physics which offered conditions approximating very closely to those prevailing in the open air. The room, which was 50 metres above ground-level, measured 4·6 by 3·2 metres, and was 2·6 metres high. The roof was of tiles 5 cm. thick and the walls were fitted with large glass windows all round. The plan and sectional views given in the figure show that very little solid obstruction was offered to the particles and that what existed was symmetrically placed with respect to the counters at the centre. The counters, CC, were mounted on top and at the centre of a large iron shield, A, 70 cm. square and 10 cm. thick, which provided a screen against radiations from below.

§ 2. *The Counters.*

The Geiger-Müller counters were filled with dry argon at a pressure of 2 cm. of mercury and were of the sealed type already described by us†. To avoid spontaneous discharges and to obtain a constant counting efficiency from them it was necessary to keep the applied potential constant within a few volts. The accumulator battery supplying this potential was kept at a fairly constant temperature in a closed room.

The rapid changes in temperature of the tower during the summer heat produced changes in the pressure of the gas in the counters which led to alterations in their efficiency even at constant voltage. The turntable and counters were therefore placed inside a cubical wooden box, 50 cm. inside, with walls 2 cm. thick, placed N.-S. and E.–W. This was kept at a constant temperature of 30° C. by means of a toluene thermostat and electric heating.

The frequency of the accidental coincidences registered by the arrangement was found by separating the counters

* Bothe, *Zeit. f. Phys.* lix. p. 1 (1929).

† Schonland and Viljoen, Proc. Roy. Soc. A, cxl. p. 314 (1933).

a distance of 50 cm. from one another in an almost horizontal direction and arranging for the 10 cm. iron screen to be between them. It was then found in the course of several counts lasting 60 minutes that the accidental effect amounted to 0·22 coincidences per minute. Since each counter gave approximately 100 impulses per minute, the resolving power of the arrangement was $1{\cdot}1\ 10^{-3}$ secs.

§ 3. *Measurements.*

(a) *North-South.*

The first set of observations was concerned with the relation between the numbers of the particles coming in from the north and from the south. These were made between September 20th and November 20th, 1932. The procedure adopted was as follows:—The counters were turned "north," *i. e.*, with their axes along the magnetic east–west line, and with the upper counter to the north of the lower one, and a count made for a time t minutes. They were then rapidly rotated through 180°, and a count made in the "south" position for a time $2t$ minutes. They were then replaced in the north position for a further t minutes. These constituted one complete set of readings, and prevented any steady change in counting efficiency from affecting the comparison in the two directions. In some of the earlier observations t was 30 minutes, but for the majority it was 15 minutes, so that a complete set took one hour. The results are shown in Table I.; in the first group of observations the counter temperature was not controlled, but in the second group the counters were mounted in the constant temperature box described above.

It is evident that the results disclose no significant difference between the north and south directions. The difference found amounts to 0·4 per cent., less than of the probable error of 1·5 per cent. in the counting. The observations were all made between 7 and 19 hrs. G.M.T. A comparison of the counts made at different times of day shows no significant variation.

(b) *West-North-East.*

The second series of observations compared the numbers of particles coming in from the west, north, and east directions. In this case the procedure was to measure

with the arrangement facing west for 10 minutes, north for 10 minutes, east for 20 minutes, north for 10 minutes, and finally west for 10 minutes. The whole set of readings thus took one hour.

The results are shown in Table II. The measurements were made between Nov. 22nd and Dec. 24th, 1932, and the counters were kept at constant temperature throughout.

TABLE I.

North-South Comparison.

Group.	Time of observation.	Count from north.	Count from south.
1.....	3600 min.	6209	6136
2.....	2460 ,,	3159	3194
Total count.	6060 ,,	9368	9330
Accidental coincidences calculated.		667	667
Systematic coincidences.		8701 ± 29.5	8663 ± 29.4

Difference: north–south 38 ± 132, *i. e.*, 0.39 ± 1.52 per cent.

TABLE II.

Period of observation.	Count from west.	Count from north.	Count from east.
3600 min.	3239	3325	3195
Accidental coincidences calculated.	264	264	264
Real coincidences.	2975	3061	2931

Difference: north–west 86 ± 78 or 2.9 ± 2.6 per cent.
north–east 130 ± 77 ,, 4.3 ± 2.6 ,,
west–east 44 ± 77 ,, 1.5 ± 2.6 ,,

The accuracy of this comparison is not as great as that of the previous one, for the number of particles counted in each direction is smaller. The difference between the numbers counted from east and from west is less than the mean error of 2·6 per cent. in the counting. On the other hand, the count from the north shows an excess over both the east and west counts, the difference being 1·7 and 1·1 times the mean error in the two cases. Further

observations would be neccssary before accepting either figure as significant. The general indications to be drawn from the results are briefly discussed in the next section.

That the efficiency of the counters remained very constant over the observations can be seen from the following analysis of the records. The table contains the totals of 180 twenty-minute counts, and the average number of coincidences in each was 54·2. If the counting efficiency had remained absolutely constant over the whole period the mean deviation of individual counts from this value should have been $\sqrt{54{\cdot}2}$ or 7·4. The actual mean deviation of the 180 separate counts was 10·1, and if 12 counts made on a day when the counting rate was known to be above normal be eliminated, the mean deviation of the remaining 168 becomes 7·9. Thus the precautions taken to maintain a constant counting efficiency were successful.

These observations were made between 8 and 16 hrs. G.M.T. from Dec. 5th to Dec. 15th.

§ 4. *Discussion.*

Summarizing the results of the previous section, it may be said that a comparison of the numbers of particles from the four points of the compass shows: (*a*) no significant difference between the north and south directions; (*b*) no significant difference between the east and west directions; (*c*) small defects from east and west as compared with north and south. Of these the easterly defect is the larger (1·7 times the mean error in the experiment).

It may be concluded from (*a*) that whatever contribution distant thunderstorms can make to the penetrating radiation, it is not of a nature involving a direct passage of radiation to the apparatus from the thundercloud region; for the continent of Africa to the north was active from the thunderstorm aspect during the observations, while the Antarctic seas to the south could hardly have been of any consequence in this respect.

From (*b*) one could infer either that particles from neither the east nor the west are affected by an amount greater than the experimental error, or that a small effect is present which lowers the number from both directions by approximately the same amount. This latter view is supported by (*c*), from which it would follow that the particles carry charges of both signs, with the positive ones

more abundant than the negative. This is in accord with the Wilson chamber experiments of Kunze, who found the ratio of positively- to negatively-charged particles causing tracks in a Wilson cloud-chamber to be 1·5*.

This conclusion as to sign rests upon the question of the significance of the north-east defect. A more definite conclusion of another kind follows from the smallness of the defects observed. This could be explained if the energies of all the particles were very high, much higher than 5×10^9 *e*-volts†, but such an explanation contradicts evidence that 5×10^9 *e*-volts represents the upper limit of energy of the majority of the particles‡. The smallness of the defects must thus be due to the fact that any charged particles of extra-terrestrial origin are accompanied by a larger number of secondary particles generated in the atmosphere as a result of the absorption of some radiation which is not affected by the earth's magnetic field.

§ 5. *Summary.*

An investigation of the direction of arrival of the ionizing particles associated with the penetrating radiation has been made at sea-level in Cape Town (mag. lat. 31° S.). The numbers of particles from magnetic north, south, east, and west were compared by means of a coincidence counter.

The differences found were (1) north-south, $0\cdot4\pm1\cdot5$ per cent.; (2) west-east, $1\cdot5\pm2\cdot6$ per cent.; (3) north-west, $2\cdot9\pm2\cdot6$ per cent.; (4) north-east, $4\cdot3\pm2\cdot6$ per cent.

It is concluded that any charged particles of extra-terrestrial origin are accompanied by a larger number of secondary particles generated in the atmosphere by some radiation which is not affected by the earth's magnetic field.

The north-east difference suggests that the majority of the primary particles are positively charged.

Our thanks are due to Prof. A. Ogg for providing many facilities for this work, to Dr. E. C. Halliday for help with the proofs, and to the Research Grant Board for a grant with which to purchase thyratrons.

* Kunze, *Zeit. f. Phys.* lxxx. p. 559 (1933).

† Rossi, *loc. cit.* Both this and the following explanation were suggested by Rossi in 1931, but the evidence which leads us to adopt the second was not used by him.

‡ Schonland, Proc. Roy. Soc. A, cxxx. p. 37 (1930).

XXXVI. *Determination of the J-discontinuity by a Condition of Matter.* (*J-Phenomenon.*—Part X.) *By* Prof. C. G. Barkla, *F.R.S., and* Dr. J. S. Kay, *M.A., University of Edinburgh* *.

EXPERIMENTS upon the J-phenomenon have fallen into two classes:

I. Those in which the principal object has been the investigation of the laws governing the phenomenon—when it occurs;

II. Those in which the object has been the investigation of the conditions favourable to its occurrence.

The investigations described below are a selection only of a large number of experiments lasting over a period of about three years in which between one and two hundred J-discontinuities were not only observed but examined and measured. The principal points established, and with which we propose at present to deal, are the following:—

(1) With a given form of apparatus working in a given way, the occurrence or non-occurrence of the discontinuity depends entirely upon some state of the substance experimented upon and used to scatter and to transmit the radiations. Thus any suspicions that might be held regarding the peculiarities of the apparatus or of the radiation used are entirely removed. Specimen A gives the discontinuities; specimen B gives no trace of them, though it is placed in the same position as specimen A and exposed to the same radiation. The importance of this result must be emphasized. It is the simplest and most direct answer to any suggestion of the phenomenon being due solely to a special form of apparatus, or even to a particular constitution of the stream of radiation.

(2) With a given scattering and transmitting substance, there are certain conditions of excitation of the X-ray tube which are most favourable to the appearance of the J-discontinuity; in fact, certain energy-time or energy-wave-length relations may be essential. This has previously been shown when the excitation is by means

* Communicated by the Authors.

of an induction coil with mercury jet interrupter and by many experiments, the results of which have not been published. In the experiments described below it has been observed that, in the case of excitation of the high vacuum X-ray tube by an alternating E.M.F. from a transformer, certain voltages are more favourable to the occurrence of the discontinuity than either lower or higher voltages. This has been seen by several observers working in this Laboratory, but a more exhaustive investigation with various forms of apparatus is desirable.

(3) The experimental conclusion that the discontinuity occurs at a certain average absorbability, to a first approximation, has been tested under new conditions, and has been further verified.

The critical values of μ/ρ in our experiments were found in the neighbourhood of 3·2 and 2·2.

[It has, however, already been shown * that an alteration of the current through a high vacuum tube produces a small systematic displacement of the position of a discontinuity, that is of the average absorption coefficient at which it occurs, though enormous changes in intensity obtained otherwise produce no appreciable displacement.]

Experiments.

The following account is as brief as possible consistent with giving an intelligible description of experimental results. It indicates all that is essential for our present purpose.

In these particular experiments X-ray tubes of the high-vacuum type were excited directly from a transformer working at 50 cycles per second and producing peak-voltages up to 90 kilovolts. As in many previous experiments, the method adopted was that illustrated in fig. 1. A beam of primary X-radiation fell upon a scattering substance S in the form of a slab with its face at an angle of 45° with the axis of the radiation. Narrow pencils of the primary rays were allowed to pass through small apertures in a lead screen into the electroscope E_1. Scattered radiation from the slab S passed through much larger apertures into electroscope E_2.

* Barkla and Watson, Phil. Mag., Nov. 1926.

Apertures were adjusted to give comparable deflexions in the two electroscopes. Let the ratio of the ionizations observed in the secondary and primary electroscopes be S_0/P_0. By placing sheets of aluminium of equal thickness in the paths of both primary and secondary beams the ionizations were reduced to S and P, and the ratio S/P was observed. Owing to the Compton increase of wave-length on scattering (for the modified radiation) the scattered radiation should be more absorbable on the whole than the primary, and S/P should fall continuously with an increase in the thickness of aluminium placed in the two paths.

Fig. 1.

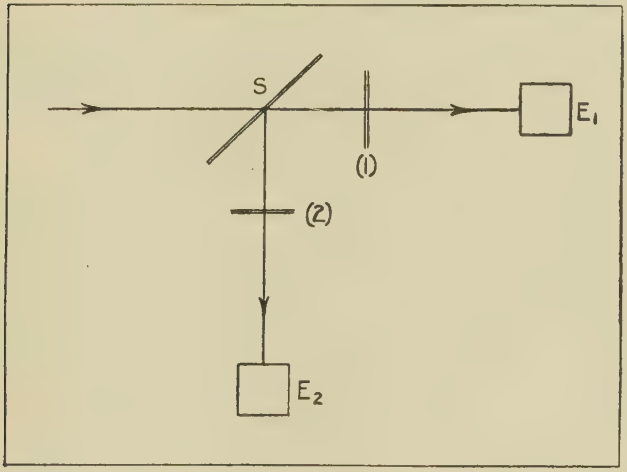

This may be said to be usually the case—at least, under the conditions obtaining in the vast majority of experiments that have been performed. The decrease of S/P with increasing thickness of aluminium is of considerable magnitude, as it should be according to the Compton theory and according to spectroscopic measurements, combined with a knowledge of the relation between absorption and wave-length. The magnitude, too, is of the right order, though as we have previously pointed out (Barkla and Khastgir *), when the wave-length is varied the difference in absorbabilities of scattered and primary radiations does not in general vary in such a way

* Phil. Mag., Oct. 1927.

as to correspond to Compton's change as given by the expression

$$\lambda_s = \lambda_p + \frac{h}{mc}(1-\cos\theta),$$

i. e.,

$$\lambda_s = \lambda_p + k,$$

but to a very precise law $\left(\frac{\mu}{\rho}\right)_s = \left(\frac{\mu}{\rho}\right)_p + k'$ when correctly interpreted. This is totally different from Compton's law if we accept the known relationship between wave-length and absorbability.

It is a remarkable fact that measurements of wave-length should show a constant increase in wave-length λ, produced by scattering, while experiments on absorbability show, within limits, a constant increase of absorption coefficient μ/ρ. These results can only be in agreement for one particular wave-length and absorbability.

Dealing, however, with the progressive absorption of both primary and scattered beams, we *frequently* find these two radiations to be equally absorbable, as shown by the constancy of S/P with increasing thickness of intercepting aluminium. In this case the fall in the ratio S/P takes place by jumps, as though the difference in absorbability were latent, and that it only became evident when certain critical average constitutions of the beam were attained by the filtering process.

The two well-marked cases are thus those in which

(1) The scattered radiation is continuously more absorbable than the primary, as shown in fig. 2, specimen A. No discontinuity appears.

(2) The difference between scattered and primary radiations appears solely (or partially) as a sudden fall of the relative ionization from one level to another (see fig. 2, specimen B).

Unlike many of the cases previously described, our experiments usually showed some initial difference in absorption of primary and scattered radiations, even though the discontinuity appeared by further absorption. In the only cases tested, the discontinuity was a fall in ionization produced by the scattered radiation.

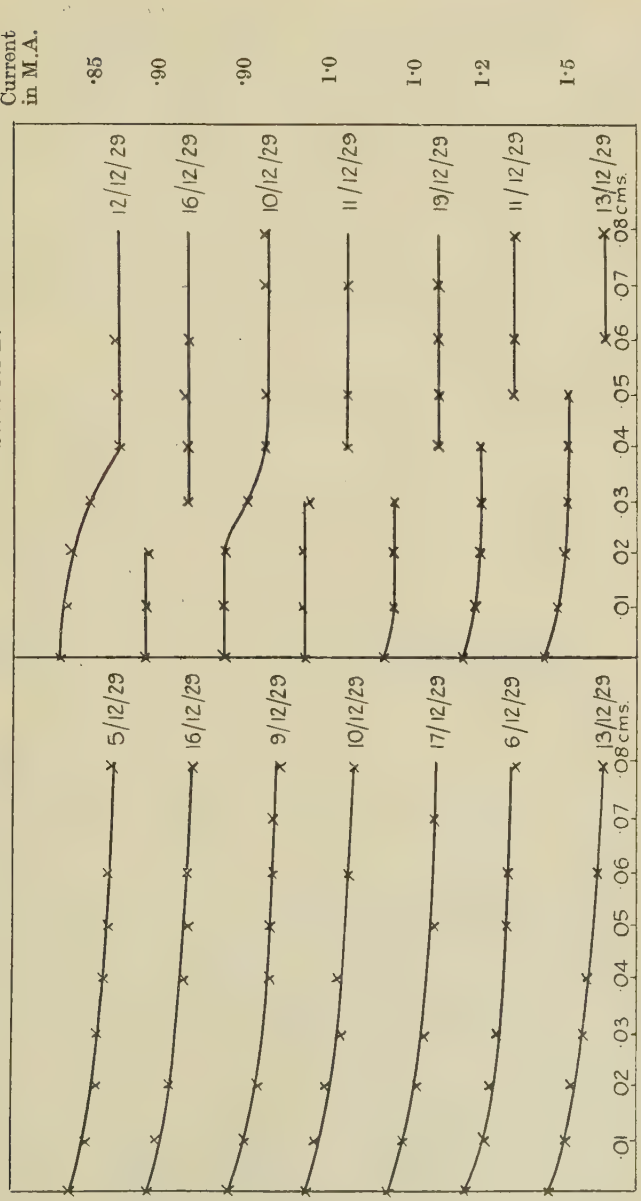

Fig. 2.—Contrasting results obtained with two scatterers, each 100 sheets paper.

State of the Scattering and Transmitting Substance.

In a series of experiments on the filtering of the scattered and primary radiations when 100 sheets of filter paper A were used as the scattering substance, no discontinuity was observed for quite a long period. A new scatterer B consisting of 100 similar sheets not previously exposed to the radiation was then used and discontinuities were regularly observed. The two scatterers were then used alternately, sometimes on the same day, and it was found that while the discontinuities occurred quite regularly with the new scatterer B, there was still no evidence of the discontinuity when the old scatterer A was used.

When using the first—the original scattering sheets—the results obtained were invariably those as shown in fig. 2 (A), in which a gradual decrease in the value of S/P is found with equal additions of absorbing aluminium in both beams. This, of course, is the result so frequently obtained, and indicating an increase in absorbability by scattering. During the same period, December 1929, when the scatterer B was placed in the same position, the curves all without exception showed a discontinuity, or in a few instances, a very rapid localized fall. Variation in the closeness of packing of the sheets of paper produced no observable effect on the type of result obtained.

Curves of fig. 2 were those obtained in the series of experiments lasting over a period of several weeks. The dates are shown with each curve. The results have been arranged not in the order of date, but of the current through the X-ray tube, as this shows a systematic displacement of the discontinuity. This is probably due in part to the fall of potential and consequent increase in the average absorbability, but largely to the absolute variation (found by Barkla and Watson) of the value of μ/ρ at the critical point when the current through the tube is increased. The peak potential was approximately 60 kilovolts.

These curves, characteristic of the two specimens, persisted until the Christmas vacation of 1929. When work was resumed after the vacation, no discontinuity could be found with either of the scatterers, and for a long period results of the one normal type (A) only could be obtained.

Experimental results similar to the above, and showing the effect in an equally definite manner, were also obtained

with two scatterers of paraffin wax 11 mm. in thickness. One scatterer, which had been in use for several years, was found to be giving the discontinuities with remarkable consistency. Another slab of paraffin of exactly the same dimensions was then made, but on testing the radiations as before, no discontinuity was ever found. Fig. 3 shows a typical series of results obtained with these two scatterers.

The three curves were obtained using scatterers B, A, B in the order shown. In this case the X-ray tube was kept running continuously throughout the whole

Fig. 3.—Showing results obtained with two specimens of paraffin wax as scatterers, experimented upon in the order B, A, B.

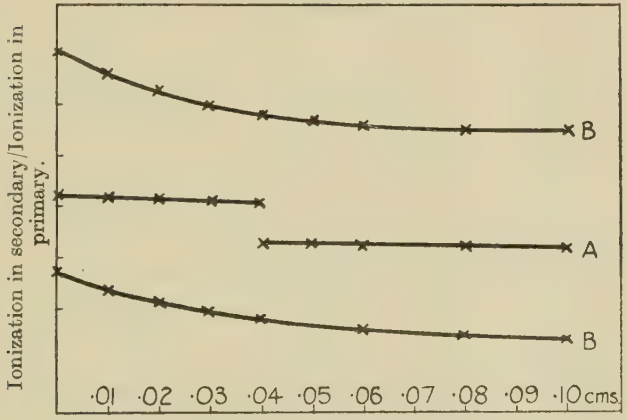

series of observations, and both the exciting potential and the current through the tube were kept constant.

We also give in fig. 4 the results obtained with these two specimens over a long period. One specimen, A, gave the discontinuities, with one exception, dated 25/2/31, and one other of a total of eleven, *i. e.*, nine of the eleven experiments with A, gave discontinuities; specimen B consistently gave the continuous slope. Such results showed that the discontinuity was dependent upon some state of, or in, the scattering and transmitting substance--paraffin wax in this case.

In order to make the test as stringent as possible, it was decided not to take the full series of observations with one substance before proceeding to experiment

Fig. 4.—Contrasting results obtained with two scatterers of paraffin wax 11 mm. thick.

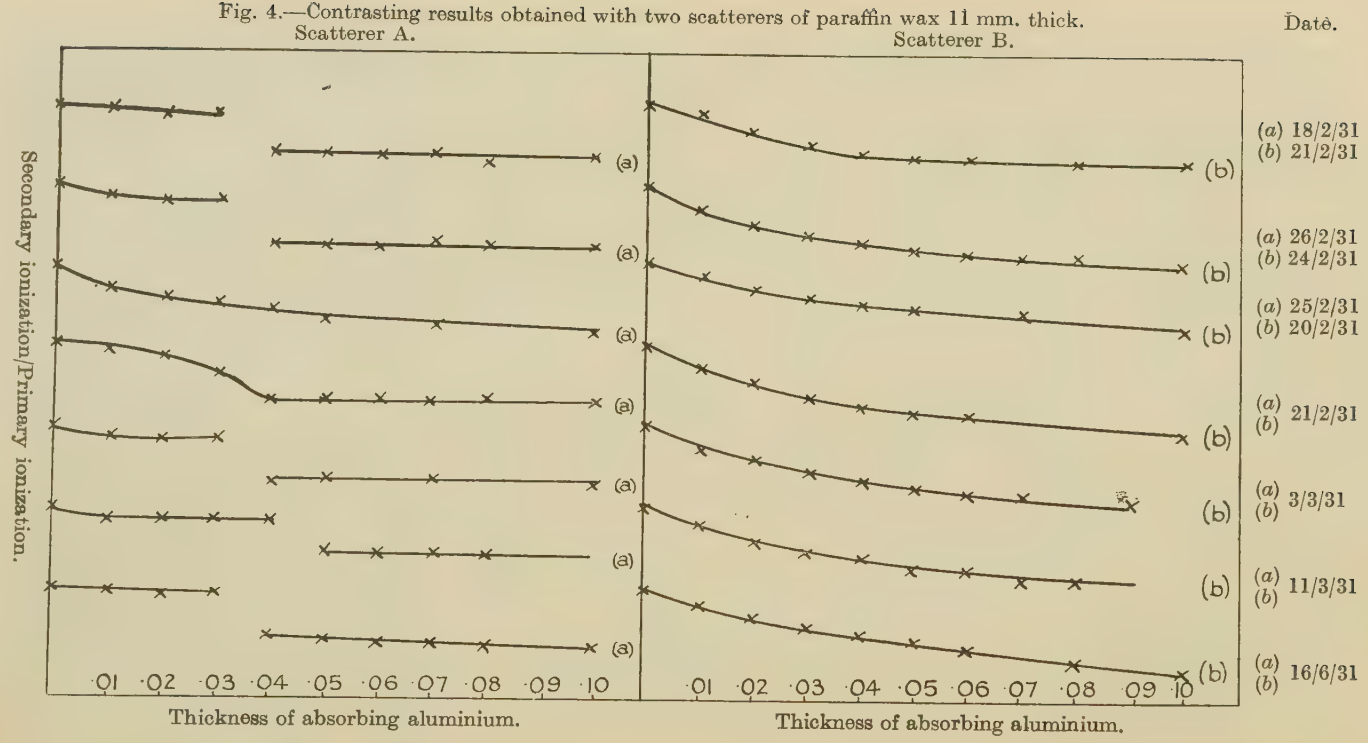

upon the other substance, but to experiment upon the two substances alternately throughout the whole of the absorbing or filtering process.

A stand was made into which the slabs of paraffin wax fitted tightly, and it was arranged that with the slab in position it made an angle of 45° with the axis of the primary beam. The two scatterers could then be placed alternately in this stand, and replaced very accurately in their original positions. On testing the value of S/P before a scatterer had been removed, and after it had been removed and replaced, it was found that the values were accurately the same. Thus it was possible to take

TABLE I.

Thickness of aluminium filter in cm.	S/P. Scatterer B.	S/P. Scatterer A.
—	·97	·93
·01	·94	·91
·02	·91	·90
·03	·89	·89
·04	·88	·89
·05	·865	·83
·06	·86	·83
·07	·85	·83
·08	·84	·82

readings with the two scatterers A and B alternately in the same position, for the same thickness of absorbing aluminium, then proceed to the next thickness of aluminium and again take readings with B and then A, and so on throughout the whole experiment. Thus the two filtering curves showing the variation of S/P with thickness of absorbing aluminium were obtained simultaneously, or, to be precise, by alternate readings with the two scatterers through the whole series. Again, while no trace of a discontinuity could be observed in the absorptions with the new scatterer in position, a pronounced break was obtained with the old scatterer.

Table I. and fig. 5 show the results obtained in this

particular experiment. The numbers by the curves show the order in which the observations were taken for the first three points; the procedure was continued throughout the whole experiment.

After the completion of the experiment, observations in the neighbourhood of the discontinuity was again made. As the figures in Table II. show, the discontinuity was

Fig. 5.—Showing results obtained concurrently with two scatterers (paraffin). Order of observation shown by numbers.

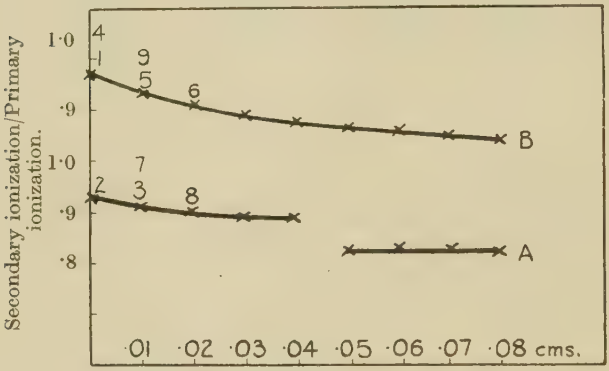

Thickness of absorbing aluminium.

TABLE II.

Thickness of aluminium.	S/P. Scatterer A.	
·06	·83	·83
·05	·83	
·04	·89	·89
·06	·83	

persisting in precisely the same place—for a thickness of filtering aluminium between ·4 and ·5 mm.

It should be observed that apart from the J-discontinuity of about 7 per cent. in magnitude, there is no irregularity in the series greater than about 1 per cent. This may be seen to be substantially true for all series recorded in this paper: it indicates the magnitude of the possible error.

Thus while the discontinuity was found when specimen A was used, no trace of such an effect was observable when specimen B was in the same position, with the same apparatus and with precisely the same working conditions.

After this contrast in results had persisted for several weeks, during which no indication of a discontinuity was ever obtained with specimen B, the discontinuities which had been obtained with specimen A so consistently began to appear less frequently—indeed, it became quite rare, and further investigations of this character were abandoned for the time. The characteristic curves as shown in fig. 4 were, however, occasionally obtained over a period of several months. The latest pair of curves on the figure is dated 16/6/31.

These experimental results seem to be of the greatest importance because they show, without a shadow of doubt, that the occurrence of the discontinuity is dependent upon some state of the scattering (and transmitting) substance. This, of course, does not mean that particular radiations or sequences of radiations are not essential, but that with the right type of radiation the phenomenon depends upon some state of, or in, the substance which cannot be observed by ordinary methods. Nor can it be attributed to any particular crystalline structure or arrangement of the crystals in such a structure, for the phenomenon was observed equally definitely when the radiating and transmitting substance was in the form of 100 separate sheets of paper.

Many questions naturally arise regarding these experimental results. For instance, does the *effect* of a highly localized state spread throughout the whole scattering and transmitting substance? Such points will be discussed in other papers; some of them are at present under investigation.

Influence of Exciting Potential.

In earlier papers it has been shown that the details of the method of excitation of an X-ray tube have considerable influence on the results obtained in these absorption experiments. Barkla and Miss Mackenzie * found, for instance, that in certain experiments in which the potential was applied by an induction coil with

* Phil. Mag., Nov. 1926.

mercury interrupter, that as the frequency of interruption was increased, the character of (S_2/S_1, t) curves changed regularly from the normal continuous slope to the horizontal lines with discontinuities, and back again to the continuous slope. Thus the whole range of results described was obtained by merely changing the speed of the interrupter. In these experiments, S_1 and S_2 were, however, the ionizations produced by two scattered beams making angles of 60° and 120° with the primary beam.

Many other series of unrecorded experiments have also shown the importance of the character of the whole stream of radiation from the tube, though not in so direct and simple a manner

In our experiments we find that, when the excitation of the X-ray tube is by a transformer with constant frequency of alteration, the voltage applied has a very definite influence on the *probability* of occurrence of the discontinuities. In these experiments the current through the high vacuum tube was kept constant, and the method of experiment was one of two types.

In one series a definite peak voltage was applied to the tube and the progressive absorption experiment was performed in the usual manner—taking three observations for each thickness of absorbing aluminium. When this was completed, another voltage was applied and the whole absorbing process was again gone through. Thus a number of curves, each giving S/P for various thicknesses t of aluminium traversed by both beams was obtained.

In the other series with the particular thickness t of absorbing aluminium, measurements of S/P were made with various exciting potentials, and the process was repeated for each thickness of absorbing aluminium.

Thus by the former procedure one (S/P, t) curve was obtained at a time, while by the other procedure corresponding points were taken on all the curves for different voltages before proceeding to the next thickness of absorbing aluminium. In this second case, however, a short interval was necessary between each pair of observations to permit the tube to arrive at a steady state appropriate to the changed voltage.

It was soon apparent that a peak potential of about

60 kilovolts was definitely the most favourable for the occurrence of absorption discontinuities.

In our investigation of the influence of the applied potential on the probability of occurrence of the J-discontinuity, the following numbers of experiments were made :—

Exciting potential in kilovolts.	Number of experiments performed.	Number of discontinuities obtained.	Percentage number of discontinuities obtained.
20	4	0	—
30	2	0	—
40	14	3	21
50	19	7	37
60	21	15	71
70	9	3	33
80	4	0	—

The number of experiments performed with the lower and higher voltages was not sufficiently great to allow us to attach much weight to the proportion showing the discontinuities; but it was found that over short periods the discontinuity occurred in the region of a 60 k.v. potential, while it did not occur for lower and higher voltages.

In the above table the number of discontinuities includes those cases in which well-marked rapid changes in S/P were obtained which did not develop into actual breaks in the curve. Frequently, of course, the break is so abrupt as to give two distinct levels for one thickness of absorbing aluminium, the value jumping from one to the other.

Altogether in the course of this particular work some 200 experiments were made with a peak potential of 60 kilovolts. The proportion of discontinuities obtained was approximately 37 per cent.; but of the total number many were obtained for verification when the conditions were found to be unfavourable, so that a simple mean does not correctly represent the probability of obtaining discontinuities—say, on different days.

Influence of Exciting Potential on the Position of a Discontinuity.

From an enormous number of experiments upon a discontinuity which could be easily identified, it has been consistently observed that the discontinuity depends not upon any particular constituent, but upon the beam as a whole. The various methods of testing such a conclusion cannot even be summarized here: reference should be made to earlier papers. The effect of altering the constitution of a beam by changing the potential applied to the X-ray tube by a transformer had, however, not previously been published.

With regard to the critical nature of the radiation at which a discontinuity occurs, to a first approximation it has been found sufficient to measure the average absorption coefficient for the whole of a complex heterogeneous beam, by calculating the value of μ/ρ in aluminium from the results of an experiment in which the ionization produced by the beam in a short air electroscope was reduced by aluminium by about 50 per cent. This is, of course, an arbitrary method, for we do not know what weight should be attached to the various constituents of the beam. But every experiment by which the constitution of the beam—the energy distribution in its spectrum—has been changed, has shown a corresponding change in the position of the discontinuity. When a higher (or lower) potential has been applied to the tube, the radiation either primary or scattered required less (or more) filtering to bring it to the critical penetrating power.

In our experiments we found that precisely the same law held when the potential applied by a transformer was changed. When the voltage applied was reduced, the resulting radiation was on the average more absorbable, and it required more filtering to bring it to the critical average absorbability. When the voltage was increased, the critical condition was obtained by a smaller amount of filtering.

This is illustrated in fig. 6, which shows (S/P, t) curves for the three peak voltages 40, 50, and 60 kilovolts. These three curves were again taken concurrently, as shown by the numbers indicating the order in which the points were obtained.

Such a displacement as that shown in fig. 6 was found on each of the four occasions on which the experiment was made, in which the discontinuity was actually shown.

Summary.

(1) Experiments described show that an absorption discontinuity is dependent on some state of, or in, the particular substance used to scatter and transmit the

Fig. 6.—Illustrating the systematic displacement of a discontinuity by changing the potential applied to the X-ray tube.

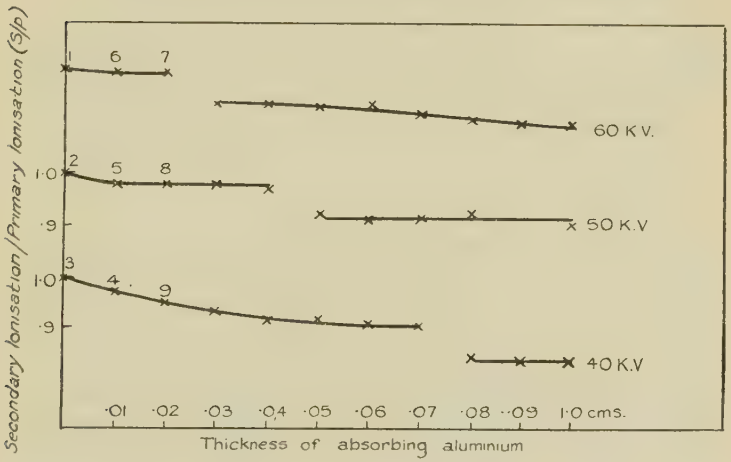

Thickness of absorbing aluminium.

radiations experimented upon, every other condition remaining the same.

This we regard as conclusively established.

(2) Experiments strongly indicate that, with a given apparatus, certain voltages applied by the transformer to the X-ray tube are more favourable to the occurrence of a discontinuity in the absorption of the resulting radiation—other conditions remaining the same.

Such a conclusion, however, is necessarily based on a very limited number of observations with one form of apparatus. While it is of some practical interest, it only suggests one of a number of possible causes.

(3) The systematic displacement of a discontinuity by a change of voltage applied to the X-ray tube by a transformer, has been found to fully confirm previous conclusions as to the critical state of the radiation at a discontinuity being determined by an average constitution of the heterogeneous beam, and not by any particular constituents or small group of constituents.

A discussion of the above results would be unprofitable without full consideration of all the body of evidence obtained from other investigations. Further communications will shortly be made.

XXXVII. *Intensity Distribution in the Spectrum of Beryllium Oxide. By* R. C. Johnson, *M.A., D.Sc., and* E. Gordon Dunstan, *B.Sc., University of London, King's College* *.

[Plate X.]

Introduction.

SINCE the provision of a theoretical basis for the distribution of intensities within the bands of a system by Condon in 1926 very little experimental work has been done which might provide a quantitative test of the theory. There is little doubt as to the general validity of the Franck-Condon † theory, but the fact remains that, with the exception of Elliott's work ‡ on the α-system of boron monoxide, Johnson & Tawde's paper § on the Swan system of C_2, and one or two papers from the Utrecht School most of the illustrations of the theory have been of the nature of eye-estimates. These are notoriously unreliable, whether made directly on a spectrum or from a photographic plate, and may easily be in error by several hundred per cent. In the present paper we have made quantitative observations of the $'\Sigma \rightarrow {}'\Sigma$ system of BeO. Data of the gross structure of this system are given by Jevons ‖, and references

* Communicated by the Authors.

† Phys. Rev. xxviii. p. 1182 (1926).

‡ "The Optical Determination of the Relative Abundance of Isotopes" (Dissertation, Utrecht, 1930).

§ Proc. Roy. Soc. cxxxvii. p. 575 (1932).

‖ Proc. Roy. Soc. cxxii. p. 218 (1929).

to earlier work may be found in his paper. Fine structure analysis of six of the strongest bands has been made by Jenkins and Rosenthal *. The system is degraded towards the red and lies entirely within the visible part of the spectrum.

Experimental Procedure.

The bands were obtained by exciting metallic beryllium in an arc between pure carbons, and for purposes of intensity measurements were photographed on a Hilger constant deviation prism spectrograph with Ilford rapid process panchromatic plates. Experience had shown us that with these conditions an exceptionally clear background accompanied a well developed band-system, and that there need be little error due to grain effects. Blackening-intensity curves of the usual kind were derived by using a step-slit and a Tungsten spiral filament-lamp run under constant conditions as a source of continuous spectrum. The procedure has been given in a paper by Read & L. W. Johnson†, and also in a paper on the Swan system of C_2 to which reference has already been made. Care was taken to ensure that the band-system and the continuous calibration spectrum were recorded on the plate for the same time. This was ensured by using a Compur shutter between the source and slit. Owing to the wide variation of intensity of the bands of the system it was found necessary to take several plates, of which some were exposed a longer time for the benefit of the weaker bands. Correlation of the plates was made by measuring a number of bands of intermediate intensity common to different plates. In addition the plates were always fogged before exposure, so as to bring them into a condition represented by the linear part of the blackening-intensity curve. Neglect of this precaution may be a source of considerable experimental error, especially at the more refrangible end of the spectrum.

Microphotometric records were obtained of the band-system and of the calibration spectra opposite each band-head. The rapid variation of the sensitivity of the plate made necessary a separate curve for each band-head. The intensities were all obtained on a relatively correct scale from a knowledge of the energy : wave-length

* Phys. Rev. xxxiii. p. 163 (1929).
† Phil. Mag. xi. p. 1152 (1931).

distribution in the continuous spectrum of the lamp. This had been previously determined by means of a quartz monochromator, thermopile, and sensitive galvanometer.

Peak intensities have everywhere been measured, and to this procedure valid objections can be made. The only really satisfactory method is based upon completely resolved bands, in which case the intensities of all the component lines can be summed and a quantity which is really proportional to the weight of the band obtained. The difficulties in the way of this kind of investigation are immense. The necessarily high resolving power will for many band spectra involve very long exposures, and this implies exposure of the standard lamp for an equal time. Following this the computation of intensities for many hundreds of lines is a formidable undertaking. An alternative, and probably fairly reliable, procedure is the comparison of corresponding lines of the various bands. All the methods based upon unresolved band-heads are open to some valid criticism, and under these circumstances we have felt that reasonably accurate data based upon peak intensities are at least a great advance upon the widespread eye-estimates, which have no quantitative value. The comparative ease with which the former can be obtained is perhaps some justification for this class of work.

Potential Energy Functions.

In order to derive the Condon parabola of maximum probability of transition use has been made of both the expressions for potential energy of Morse * and Rydberg †. Morse's function is

$$U(r)=D(1-e^{-a(r-r_e)})^2,$$

where D is the energy of dissociation given approximately by $\frac{\omega_e^2}{4x_e\omega_e}$ and $a=(8\pi^2 c x_e \omega_e \mu/h)^{\frac{1}{2}}$, the unit in both cases being $(\text{cm.})^{-1}$.

The band origins are given by

$$\nu=21254{\cdot}05+1370{\cdot}81(v'+\tfrac{1}{2})-7{\cdot}76(v'+\tfrac{1}{2})^2 -1487{\cdot}45(v''+\tfrac{1}{2})+11{\cdot}87(v''+\tfrac{1}{2})^2.$$

* Phys. Rev. xxx. p. 825 (1927).
† *Zeit. f. Phys.* lxxiii. p. 376 (1931).

From this we have calculated for the upper and lower states respectively :

$$D' = 60549, \quad a' = 16{\cdot}337 \times 10^7, \quad (r_e' = 1{\cdot}358 \times 10^{-8} \text{ cm.}).$$
$$D'' = 46599, \quad a'' = 20{\cdot}207 \times 10^7, \quad (r_e'' = 1{\cdot}327 \times 10^{-8} \text{ cm.}).$$

The resultant potential energy curves are shown in fig. 1. Using Condon's graphical method the parabola

Fig. 1.

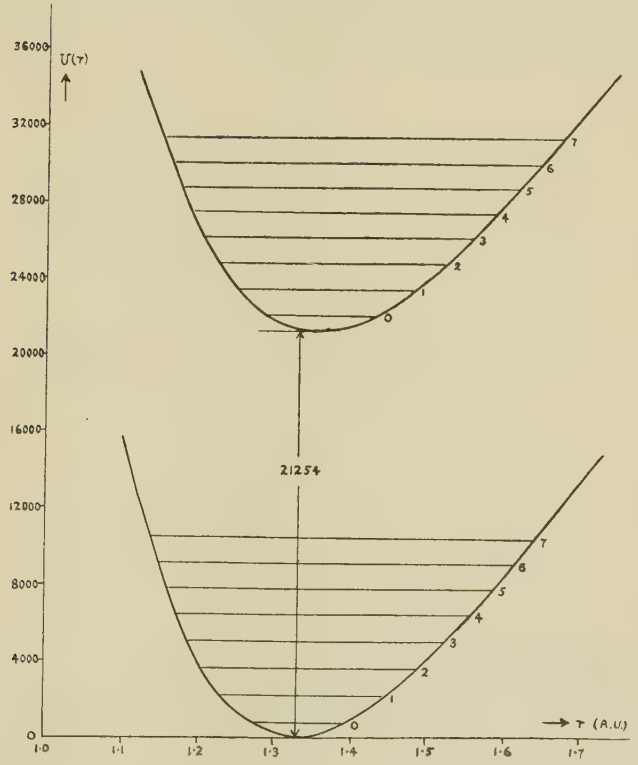

representing maximum probability of transition has been derived and superposed in its correct position upon the data of fig. 2.

The Rydberg function is $U(r) = D(ax+1)e^{-ax}$, where $x = r - r_e$, and the constants D and a have their previous significance. Here, however, the energies $U(r)$ are measured downwards from the energy level of dissociation as the zero. We have plotted this function and derived

a parabola as in the first case. For the sake of brevity these data are not included in the paper. In the few cases in which it has been tested Rydberg's expression appears to have given rather better agreement than Morse's function. In the present case the difference between them was very small and consisted largely in a closer approximation of the lower arm of the parabola towards the diagonal line of the system, *i. e.*, a narrower parabola was found. This appears to agree better with the exceptionally strong (0, 0) sequence which is a notable feature of the system (*vide* Pl. X.).

Fig. 2.

v' \ v''	0	1	2	3	4	5	6	7	8
0	·72	·24	·04						
1	·05	·55	·36	·04					
2		·07	·49	·39	·05				
3			·09	·30	·54	·07			
4				·09	·32	·58			
5					·10	·30	·60		
6						·14	·23	·63	
7							·22		·79

Transition probabilities.

In the table the experimental values of the intensities are given on a relatively correct scale, taking the (0, 0) band as 100. The intensity of a transition is proportional to ν^4, to the population of the initial state, and to the transition probability. Each intensity has therefore been divided by a number proportional to ν^4, and these results are placed in the table below the intensities. The sum of these values (I/ν^4) for each v'' progression is placed adjacent to the corresponding v', and is proportional to the population of the initial state. By dividing the (I/ν^4) values by the appropriate population values we have therefore numbers proportional to the transition probabilities. These values are given in fig. 2.

Discussion.

A striking feature of the intensity distribution is the strong development of the (0, 0) sequence, the members of higher v values being much stronger than is usual in systems having vibrational constants of this order of

Values of I and (I/ν^4).

Weight.	v'' / v'	0.	1.	2.	3.	4.	5.	6.	7.	8.
	0.	100	25·5	3·3						
68·67		49·2	16·6	2·87						
	1.	7·4	57·9	28·3	2·5					
52·95		2·85	29·1	18·8	2·20					
	2.		7·3	40·9	24·7	2·2				
42·46			2·86	20·9	16·7	2·0				
	3.			6·1	15·2	20·8	2·2			
26·69				2·44	7·95	14·3	2·0			
	4.				4·7	12·2	17·1			
20·24					1·94	6·50	11·8			
	5.					4·0	9·3	14·5		
16·76						1·67	4·99	10·1		
	6.						2·8	3·7	7·8	
8·67							1·17	2·02	5·48	
	7.							2·1		4·4
3·99								·89		3·1

magnitude. The Condon parabola deduced by using Morse's function agrees well on the low frequency side of the (0, 0) sequence. This is the side corresponding to $r > r_e$. The agreement is not so good on the high frequency side, but perhaps adequate in view of the limitations of the experimental method. The slightly better apparent agreement of Rydberg's function has already been mentioned. It should, however, be re-

membered that the potential energy curves are rather sensitive to small changes in the constants D and a.

In the paper on the Swan bands of C_2 to which we have already referred certain effective temperatures are discussed. The distribution of molecules in the initial vibrational states is assumed to be one of thermal equilibrium amongst themselves at an effective temperature T, so that the population of a state of vibrational quantum number v is given by $N_v = N_0 \exp\left(-\frac{E_v}{KT}\right)$. Hence

$$hc[\omega_e'(v'+\tfrac{1}{2}) - \omega_e' x'(v'+\tfrac{1}{2})^2] = KT \log_e\left(\frac{N_0}{N_{v'}}\right).$$

In the case of BeO

$$1370{\cdot}81(v'+\tfrac{1}{2}) - 7{\cdot}76(v'+\tfrac{1}{2})^2 = 1{\cdot}6083 \log_{10}\left(\frac{N_0}{N_{v'}}\right).$$

Plotting vibrational energy against $\log_{10}\left(\frac{N_0}{N_{v'}}\right)$ a straight-line graph has been obtained verifying that there is a statistical distribution of the thermal type. From this graph an effective temperature of 5900° abs. has been obtained. This is, of course, very much higher than the true temperature of the arc. We have endeavoured to account for the high effective temperature by assuming that the kinetic energy of the Be and O atoms at the arc temperature, together with the dissociation energy (D′) which may be imagined liberated in the production of the molecule in its initial electronic state, give rise to the BeO molecule with an energy (kinetic, vibrational, and rotational) appropriate to the effective temperature. We have not, however, been able to secure any quantitative agreement with this theoretical view. The effective temperatures we have calculated have been higher than those deduced from experiment.

If any correlation could be found of the "effective" temperatures derived experimentally by a study of the intensity distribution in the gross structure of band systems and the real temperature of the source, a very interesting field of investigation in astrophysics is opened up.

We wish to thank Prof. Fowler for allowing us to make use of the Cambridge microphotometer of the Imperial College.

XXXVIII. *The Thermal Expansion of Zinc by the X-Ray Method.* *By* Prof. E. A. Owen, *M.A., D.Sc., and* John Iball, *Ph.D., University College of North Wales, Bangor* *.

WHEN a cast specimen of zinc is rolled the crystals tend to take up a definite orientation in the material. Transmission X-ray photographs through thin sheets show that the hexagonal units gradually turn until after severe rolling the basal planes become parallel to the surface of rolling. Since the thermal expansion along the hexagonal axis is different from that at right angles to this direction, the value of the linear coefficient of thermal expansion of a zinc rod will depend upon whether the crystals composing it are orientated at random as in a cast specimen, or whether they all take up approximately the same orientation as in a heavily rolled specimen. This accounts for the range of values given for the mean coefficient of linear expansion of this material cited in some published tables.

To measure the expansion along and at right angles to the hexagonal axis two methods have mainly been employed, namely, the direct measurement of the expansion of a single crystal, and the measurement of the crystal parameters from X-ray spectra of the material taken at different temperatures. From measurements over several ranges of temperature on single crystal rods of zinc, Gruneisen and Goens † found that the coefficient of expansion showed a marked difference in the two directions mentioned. Values were determined for each direction over temperatures ranging between 20° C. and 100° C. McLennan and Monkman ‡, from X-ray spectrum photographs, taken at room and liquid air temperatures, found that the values of the coefficient of expansion along the two principal axes decreased with temperature while the ratio between them remained constant. The main results are summarized in Table I., which includes also the values recorded by Bridgman §.

There seem to be but few published data on the coefficients of expansion of zinc in the two directions at

* Communicated by the Authors.
† *Zeit. f. Physik.* xxix. p. 141 (1924).
‡ Trans. Roy. Soc. Canada, xxiii. p. 255 (1929).
§ Amer. Acad. Proc. lx. p. 305 (1925).

temperatures well above room temperature. Freeman, Sillars, and Brandt * find the average value of the coefficient of linear expansion of zinc from the measurement of X-ray powder photographs over a range of temperature between 20° C. and 300° C. to be $3{\cdot}93\times10^{-5}$.

In the present investigation X-ray spectrum photographs were taken with a Muller camera when the specimen was maintained at various temperatures ranging from room temperature up to 400° C. The method, though not capable of yielding accurate values of the thermal coefficient of expansion, gives definite information regarding any change in structure that may take place

TABLE I.

Temperature range.	Coefficient of linear expansion.	Direction in ref. to hex. axis.	Observer.
°C.	$\times10^{-5}$.		
−20 to +20	6·43	∥	Gruneisen and Goens.
	1·25	⊥	
+20 to +100	6·39	∥	
	1·41	⊥	
−190 to +18	4·95	∥	McLennan and Monkman.
	1·13	⊥	
20	5·74	∥	Bridgman.
	1·26	⊥	

should an allotropic modification exist at high temperature as recorded by some workers. Information on this point was desired in view of further measurements on this element to be made with the precision camera.

Method of mounting the Specimen.

Fine filings of zinc were prepared and annealed *in vacuo* at 300° C. for about one hour. The filings were always mounted in a layer 0·07 mm. thick on a glass fibre 0·60 mm. in diameter. These dimensions of fibre and reflecting material had previously been found by experiment † to yield fine spectrum lines and to eliminate certain spurious lines at small angles of reflexion which appeared with fibres of a different thickness.

* U.S. Bur. Stand. Sci. Papers, No. 522 (1926).

† Owen and Pickup, Proc. Roy. Soc. A, cxxxix. p. 526 (1933).

The camera was calibrated with fibres coated respectively with aluminium, copper, and silver, the parameters of which were accurately known. From curves plotted on a large scale showing the relation of the arc length between corresponding lines in the spectrum to the true sines of the glancing angles, the correct parameter could be readily calculated. The only other correction to be made was that due to the shrinkage of the film; this was obtained from the measurement of fiducial marks recorded on the film, the actual distances apart of which on the camera had previously been accurately measured.

The structure of zinc being close-packed hexagonal, two parameters are to be found. These can approximately be determined by means of the usual "$\log \sin \theta$" graphs, but the scale of these graphs is not large enough to give accurate values. These curves, however, enable the lines in the photographs to be identified and an approximate value of the axial ratio to be found. From amongst the reflecting planes, those having a zero value for the Miller index l are chosen. These give a value of the parameter a independent of the axial ratio. Next, by taking a pair of planes and assuming a to be the same for each, a value of the axial ratio c is found. When a few pairs of planes have been treated in this way, the resulting mean value of the axial ratio is taken and the values of a worked out for all the planes represented on the film. This method is somewhat long and tedious, but it yields consistent results.

Powder Spectra at High Temperatures.

For this purpose a small furnace was mounted on the camera to heat the fibres during exposure. The furnace, which was of simple construction, consisted of a coil of nichrome wire approximately 20 mm. in length and 7 mm. in diameter, mounted on a slate slab which could be fixed to the camera. The coil was made in two sections, with a gap between them to allow a clear passage for the X-rays. The coil was arranged on its mounting so that the straight length of wire joining the two sections was on the side of the fibre remote from the slit. In this position it was completely shielded by the fibre from the direct beam. To adjust the coil finally on the camera a beam of light replaced the X-ray beam.

When taking photographs with the specimen at high temperature it was unnecessary to modify the method of mounting the powder on the fibre which was adopted at ordinary temperature, and since the powder was very fine, there was no need to oscillate the fibre during exposure. If the temperature of the fibres be raised too quickly, the adhesive used to fix the powder in position tends to distort the even surface of the powder; but by gentle initial heating to dry the fibre gradually, it was possible to obtain at the higher temperatures a fibre the surface of which showed no appreciable change. Once the camera is set with the coil in position so that the X-ray beam strikes the fibre symmetrically, there is no need to interfere further with the specimen.

Temperature Measurement.

To measure the temperature of the fibre at the point where the X-ray beam strikes it the fibre was replaced by a thermo-couple. The junction of the couple, which was approximately of the same thickness as the fibre, was placed at the same point on the axis of the coil as that at which the X-ray beam fell on the fibre when it was in position. The current through the coil necessary to raise the temperature of the junction to the desired temperature was registered on an open scale ammeter which could be read to 0·01 ampere. With the coil used, a current of 1 ampere at 20 volts, for example, was sufficient to maintain a temperature of 380° C. To maintain steady conditions a battery of cells of large capacity was employed to supply current to the coil. Having carried out a thorough investigation of the current-temperature relation, in the course of which a survey was also made of the variation of temperature at different points along and in the vicinity of the axis, the thermo-couple was removed and the specimen replaced in position. It may be mentioned that the variation of temperature along the axis of the coil over a range of 2 mm. on either side of the correct position was well within 10° C. The temperature on the axis of the coil was frequently checked in the course of the measurements.

Preliminary Tests.

The camera was tested with a sample of aluminium (99·5 per cent. pure), the parameter of which was

accurately known. The photograph taken at 400° C. gave sharp lines, the Kα doublet of copper radiation being clearly resolved at large angles of reflexion. The result of the measurement of this photograph is shown in Table II.

The first four lines in the photograph are not included in Table II. The parameters calculated from the various lines are in fair agreement, and represent the kind of agreement obtained with this camera when the fibre is at

TABLE II.

Sin θ from calibration curve.	Reflecting planes.	λ.	Calculated parameter (Å.).
0·3767	(200)	α	4·081
0·4810	(220)	β	4·085
0·5328	(220)	α	4·081
0·5645	(311)	β	4·081
0·5895	(222)	β	4·082
0·6246	(311)	α	4·082
0·6524	(222)	α	4·082
0·7421	(331)	β	4·081
0·7533	(400)	α	4·082
0·7608	(420)	β	4·083
0·8203	(331)	α	4·085
0·8330	(422)	β	4·085
0·8417	(420)	α	4·084
0·9212	(422)	α_1	4·088
0·9237	(422)	α_2	4·087
		Mean value	4·083

ordinary temperature. Taking the value 4·083 Å. for the parameter at 400° C., and the value 4·041 Å. at 20° C., the mean linear coefficient of thermal expansion for aluminium over this range of temperature is found to be $2{\cdot}74\times10^{-5}$, which is in satisfactory agreement with the value $2{\cdot}72\times10^{-5}$ given in the 'International Critical Tables' for aluminium of 99·1 per cent. purity, over the same range of temperature.

The amount of oxidation on heating aluminium is small, but it may be appreciable with zinc, and precautions have to be taken to prevent its occurrence. With this object

in view the fibre was surrounded during exposure with an atmosphere of nitrogen. A special support for the fibre, shown in the figure, was constructed for this purpose. The annular space round the centre pillar is supplied with gas through a side tube, and a column of nitrogen rises and surrounds the fibre. The nitrogen is dried by passing it through concentrated sulphuric acid, which also serves as an indicator of the flow of gas. The flow was kept constant during the exposure and was always very slow. Since the density of nitrogen does not

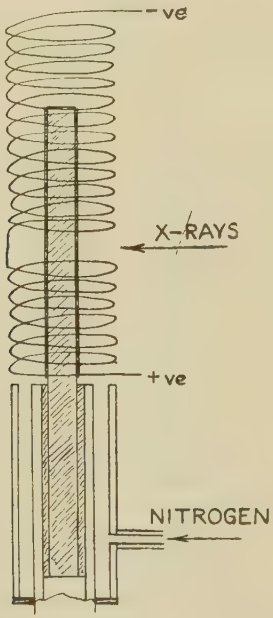

differ much from that of air, the former does not diffuse away rapidly. The arrangement proved satisfactory, the zinc, after several heating operations, presenting a clean surface.

The temperature variation inside the coil was again explored under the new conditions. To shield the camera from draughts it was enclosed in a box, the top of which was removed to allow the heated gas to escape.

The time required to obtain a photograph at a high temperature in the way described above is longer than at ordinary temperature. For, in addition to the usual nine or ten hours' exposure, from one to two hours are

necessary to raise the temperature to the required value and to reach a steady state.

Results.

Photographs were taken at room temperature with the precision camera and at 250° C., 350° C., and 400° C. respectively, with the powder spectrum camera.

To solve a photograph of a hexagonal structure obtained with the precision camera, reflexions from at least two sets of planes must appear on the film. With zinc as reflector, cobalt radiation gives three doublets, two fairly close in and one towards the end of the film; but the two inner doublets have the α_1 line of the one doublet very near to the α_2 line of the other. The lines were, however, well enough separated for measurement. Nickel radiation is more suitable, as it gives three Kα doublets which are quite separated.

To calculate the results it is necessary to know the approximate value of the axial ratio and the base side of the hexagonal cell. A powder spectrum photograph taken of zinc on which about 30 lines were measured, gave an axial ratio of 1·86 and a base side of 2·663 Å. From the ordinary graphs used to determine the axial ratio together with the positions of the lines in the precision camera photograph, all the reflecting planes in this photograph were identified.

The procedure after the identification of the planes corresponding to the lines in the photograph has already been described *. The maximum error in estimating the parameter of hexagonal lattices by this method is about 0·05 per cent. in axial ratio and 0·02 per cent. in base side.

Tables III. and IV. contain the results obtained respectively with cobalt and nickel radiation. To demonstrate the amount of change in base side which is caused by small changes in axial ratio, three different axial ratios are given with the respective values of the base side for cobalt radiation.

The value of the axial ratio which yields most consistent values of the base side with cobalt radiation is 1·856; this is confirmed by the photographs taken with nickel radiation. The mean values of the parameters of zinc are, therefore, axial ratio 1·856, base side 2·6590 Å.

The photographs of zinc at 250° C., 350° C., and 400° C.,

* Owen and Pickup, *loc. cit.*

taken with the powder spectrum camera showed well-defined lines even at the highest temperatures, and the agreement between the parameter values calculated from the lines recorded at these temperatures is as good as that obtained with this camera when the specimen is at ordinary temperature. In calculating mean values, about

TABLE III.

Zinc–Cobalt Radiation.

Sin θ.	Reflecting planes.	λ.	Base side. $c=1{\cdot}856$.	Base side. $c=1{\cdot}855$.	Base side. $c=1{\cdot}854$.
			Å.	Å.	Å.
0·98411	$(10\bar{1}5)$	α_1	2·6586	2·6598	2·6610
0·98624		α_2	2·6587	2·6599	2·6611
0·98719	$(11\bar{2}4)$	α_1	2·6586	2·6594	2·6601
0·98931		α_2	2·6587	2·6595	2·6602

TABLE IV.

Zinc–Nickel Radiation.

Sin θ.	Reflecting planes.	λ.	Base side. $c=1{\cdot}856$.
			Å.
0·95042	$(21\bar{3}0)$	α_1	2·6591
0·95266		α_2	2·6591
0·96517	$(21\bar{3}1)$	α_1	2·6589
0·96729		α_2	2·6591
0·97291	$(21\bar{3}3)$	α	2·6591
0·98277	$(20\bar{2}4)$	α_1	2·6589
0·98506		α_2	2·6589

half-a-dozen lines appearing at the smallest reflecting angles are omitted. Two temperatures only are cited; these suffice to show the degree of agreement obtained. The photographs were taken with copper radiation.

The structure of zinc at all the temperatures investigated is close-packed hexagonal, the same as at room temperature. There is, therefore, no evidence of an allotropic modification existing up to a temperature of 400° C. But although the structure remains the same at all

TABLE V.

Powder Spectrum Photograph of Pure Zinc; Sample at 250° C.

Sin θ.	Reflecting planes.	λ.	Parameter (axial ratio = 1·868).
0·4541	$(10\bar{1}2)$	α	2·666
0·5147	$(10\bar{1}3)$	β	2·670
0·5210	$(11\bar{2}0)$	β	2·667
0·5695	$(10\bar{1}3)$	α	2·670
0·5772	$(11\bar{2}0)$	α	2·664
0·5912	$(11\bar{2}2)$	β	2·666
0·6166	(0004)	α	2·670
0·6541	$(11\bar{2}2)$	α	2·666
0·6665	$(20\bar{2}0)$	α	2·668
0·6831	$(20\bar{2}1)$	α	2·668
0·7014	$(10\bar{1}4)$	α	2·666
0·7340	$(20\bar{2}2)$	α	2·666
0·8106	$(20\bar{2}3)$	α	2·668
0·8436	$(11\bar{2}4)$	α	2·670
0·8804	$(21\bar{3}0)$	α	2·668
0·8940	$(21\bar{3}1)$	α	2·667
0·9068	$(20\bar{2}4)$	α	2·670
0·9326	$(21\bar{3}2)$	α	2·668

Mean value of the parameter at 250° C. = 2·668 Å.

TABLE VI.

Powder Spectrum Photograph of Pure Zinc; Sample at 400° C.

Sin θ.	Reflecting planes.	λ.	Parameter (axial ratio = 1·884).
0·4511	$(10\bar{1}2)$	α	2·673
0·5109	$(10\bar{1}3)$	β	2·674
0·5196	$(11\bar{2}0)$	β	2·674
0·5654	$(10\bar{1}3)$	α	2·674
0·5751	$(11\bar{2}0)$	α	2·673
0·5875	$(11\bar{2}0)$	β	2·678
0·6152	$(20\bar{2}1)$	β	2·672
0·6510	$(11\bar{2}2)$	α	2·674
0·6636	$(20\bar{2}0)$	α	2·675
0·6807	$(20\bar{2}1)$	α	2·676
0·6947	$(10\bar{1}4)$	α	2·674
0·7297	$(20\bar{2}2)$	α	2·678
0·8050	$(20\bar{2}3)$	α	2·678
0·8386	$(11\bar{2}4)$	α	2·674
0·8782	$(21\bar{3}0)$	α	2·674
0·8907	$(21\bar{3}1)$	α	2·678
0·9288	$(21\bar{3}2)$	α	2·677

Mean value of the parameter at 400° C. = 2·675 Å.

TABLE VII.

Temperature of zinc.	Axial ratio.	Base side.	Height.	Atomic volume.
°C		Å.	Å.	Å^3.
20	1·856	2·659	4·93	15·11
250	1·868	2·668	4·99	15·36
350	1·880	2·674	5·02	15·52
400	1·884	2·675	5·04	15·62

temperatures, the axial ratio is found to change with the temperature, showing that zinc is anisotropic. The results are summarized in Table VII.

Approximate values of the thermal coefficients of linear expansion of zinc in the two directions, parallel and perpendicular to the hexagonal axis, and the mean volume coefficients calculated from the figures given in Table VII. are shown in Table VIII.

The values of the parameters at temperatures approaching the melting-point of zinc need to be further investigated by a more accurate method. A suitable camera for precision measurements at high temperatures has now been

Table VIII.

Temperature range.	Mean linear coefficient of expansion.		Mean volume coefficient.
	Perpendicular to hexagonal axis.	Parallel to hexagonal axis.	
° C.	$\times 10^{-5}$.	$\times 10^{-5}$.	$\times 10^{-5}$.
20–250	1·5	5·3	7·2
20–350	1·7	5·5	8·2
20–400	1·6	5·9	8·9

designed. The results obtained with it will be discussed in a later paper.

Summary.

The parameter of zinc has been measured at various temperatures ranging from 20° C. to 400° C. It is found that the crystal structure remains close-packed hexagonal even at the highest temperature. This is taken as evidence that no allotropic modification of zinc exists up to this temperature. From the values of the parameter and axial ratio, the mean thermal coefficient of linear expansion along and at right angles to the hexagonal axis, and the mean volume coefficient, are calculated for different ranges of temperature.

XXXIX. *Observations concerning Precision Weights.* By J. J. Manley, *M.A., D.Sc.Oxon., Fellow of Magdalen College, Oxford* *.

Introductory.

METROLOGISTS are familiar with the fact that when precision weights of any kind whatsoever are for a time retained in their boxes, they invariably acquire some kind of film. In some instances the films may be recognized by a decrease in the reflectivity of the polished surfaces; whilst in others their existence is discovered only by having recourse to direct weighing. In addition to the acquired films, which according to circumstances differ both in character and quantity, the presence of sundry spots may sometimes be noted. The spots, usually more or less circular in form, suggest a purely local corrosive action; and my own observations lead me to conclude that they occur chiefly upon weights which have been gilded.

Very small errors arising from the presence of films and a few diminutive spots, may be almost nullified by gently rubbing the affected weights with clean and dry soft linen or silk. A standard of precision amply sufficient for most purposes may thereby be ensured. It will, however, be noted that in following such a plan, we incur the risk of lessening the actual mass of the weight itself, the risk being the greatest in the case of gilded weights, this owing to the relative softness of gold. We are thus led to conclude that for all investigations demanding an accuracy of, say, 1/100–1/1000 mg., not only are such ultra-refinements as those described in former papers † essential, but precautions must also be taken to maintain, as nearly as may be, a strict constancy of the masses used for weighing; and to that end it is imperative that attention of the most critical kind be given to any plan evolved for storing and conserving idle weights. These considerations led me to examine the matter in detail by carrying out experiments (1) to ascertain the origin of the films found upon stored weights; (2) to determine their

* Communicated by the Author.

† Phil. Trans. A, ccx. pp. 387–415: also ccxii. pp. 227–260; Proc. Roy. Soc. A, lxxxvi. (1912); Proc. Phys. Soc. London, Aug. 1926 and Aug. 1927; see also Thorpe's 'Dictionary of Chemistry,' article "Balance."

influence upon the affected masses ; and (3) to discover means for maintaining the desired constancy in the masses of precision weights in general.

Apparatus.

For the investigation seven new 100 grm. precision weights were procured. Six were of brass, and the surface of each differed from those of the companion weights. The seventh weight was of "Nichrome," an alloy consisting of approximately 80 per cent. of nickel and 20 per cent. of chromium. The form of each weight was that of the standard pound of platinum. Three polished mahogany boxes were made for the weights. The seven cavities of the first box were lined with a white woollen felt of fine texture ; and those of the second with black velvet. The cavities of the third box were unlined. These boxes afforded opportunities for testing three distinctly different plans commonly followed in storing weights.

In addition to the weights named above, there were available other precision weights of brass. Some were gilded but others were heavily platinized. Experiments were also made with four standard weights of platinum-iridium, having the respective values of 10, 20, 20, and 50 grm.

All the weighings were carried out with a precision balance of the highest grade. And although details of the balance and its equipments have been published elsewhere, it appears necessary, on account of the smallness of the quantities now under consideration, to give a summary of the several devices and refinements introduced for ensuring accurate weighing. Accordingly we make mention of the following salient points ;—

(1) The beam, cantilever in form and having for all loads from 0–200 grm. an invariable sensitivity, is, by means of an auxiliary case, guarded against convection currents and their consequent effects.

(2) The pans and stirrups are completely enclosed by massive cylindrical walls of brass, polished without and blackened within.

(3) The arrestors are fitted with gold spheres which engage the gilded pans when the beam is brought to rest.

(4) The beam carries two stretched platinum wires, each of which is threaded through the eye of a rider. One rider is of gold and the other of aluminium wire. The former weighs 10 mg. and the latter 1 mg.

(5) The position of each rider is measured with a travelling-telescope operated by a micrometer screw having a large graduated head. By this device the weight values for the two riders are determinable to ·001 and ·0001 mg. respectively.

(6) Deflexions of beam are measured with the aid of a mirror fixed to the central knife-edge block, a vertical mm. scale, and a reading-telescope having its cross-threads situated at a distance of 4 m. from the mirror. The effective pointer of light is therefore 8 m.

(7) All objects contained in the pans are, prior to their being weighed, subjected to an appropriate washing with streams of dry and carbon dioxide-free air. The streams, supplied by an automatic apparatus, are led through the tops of the cylinders surrounding the pans and then directed downwards.

It may also be stated that all weighings were carried out only with a fully fatigued beam. Deflexions of the pointer were readable to 0·1 mm.; and the sensitivity S of the balance was high, being equal to 276 scale units (mm.). Hence a variation in weight equal to ·0004 mg. was measurable. We now describe the procedure adopted in experimenting with the seven 100 grm. weights.

Method of Experimenting.

First, the interior of the felt-lined box was brushed and loose particles removed. Secondly, the weights were thoroughly rubbed with warm silk and at once transferred to their respective cavities; the box was then closed and kept near the balance. Thirdly, a year having elapsed, each weight was in turn compared with a standard mass of 100 grm. For that purpose the weight to be tested was lifted with ivory forceps, lightly brushed with dry camel's hair, and then placed in one pan of the balance, the standard weight being in the other. Fourthly, the

brass cylinders surrounding the pans having been closed, and the two riders appropriately placed, streams of purified air were for some hours passed over the two weights. Fifthly, after the released beam had been duly fatigued, the weights were repeatedly compared at slightly different temperatures; then, with the aid of the temperature coefficient of the balance (newly determined for these experiments), all the weighings were reduced for a convenient standard temperature, and the mean value w_1, derived from the whole series, accepted as the true one.

Results. 1*st Series.*

TABLE I.

No.	Kind of weight.	Remarks.	Total mass of film.	Mass of film per 1 sq. cm.
1.	Brass, highly polished.	Decided film on crown.	$\cdot 111_3$ mg.	$\cdot 003_8$ mg.
2.	„ lacquered.	No film observable.	$\cdot 090_6$ „	$\cdot 003_1$ „
3.	„ oil-treated *.	„ „ „	$\cdot 091_1$ „	$\cdot 003_1$ „
4.	„ gilded.	Decided film on crown and sides. No corrosion spots.	$\cdot 321_6$ „	$\cdot 011_1$ „
5.	„ nickel-plated.	No film observable.	$\cdot 054_3$ „	$\cdot 001_9$ „
6.	„ chromium-plated.	„ „ „	$\cdot 013_4$ „	$\cdot 000_5$ „
7.	"Nichrome."	„ „ „	$\cdot 075_0$ „	$\cdot 002_6$ „

* This weight, highly polished, was first heated to redness and then suddenly plunged into boiled linseed oil. Subsequently it was washed (*a*) with turpentine and (*b*) with pure benzene. Finally, it was, like the others, rubbed with silk and stored in the box.

Sixthly, the weight was placed upon four layers of newly dried silk and thoroughly wiped with the same, scrupulous care being observed to avoid all direct contact between the weight and the hand. Then the weight was again lifted with the forceps, lightly dusted with the camel's-hair brush and at once replaced in the balance pan, and a second series of weighings undertaken. These were then reduced for the standard temperature and the new mean value, w_2, calculated. The mass of the film removed by wiping the weight is given by the difference $w_1 - w_2$.

Finally, the total area of the weight was measured, and the mass of the film per unit area of 1 sq. cm. calculated, and the experiment with the first weight thus terminated. Precisely similar measurements were then carried out with the other and six remaining weights. The results are given in Table I.

From the above table it will be seen that for the weights Nos. 1, 2, 3, and 7, the mass of the film per unit area approximates to the common value of ·003 mg.; whence it appears that within the limits of our observation, the film-forming power of each of these several weights is one and the same. The most pronounced film was acquired by the gilded weight and the least by the chromium-plated.

Origin of the Abnormal Films.

Our inquiry was now directed with the object of discovering the origin of the films; and to this end the box in which the weights had been kept for a year was scrutinized. It was then found that the hinges and iron screws were badly corroded. Viewed with a lens, the dark red substance upon the screws was seen to contain minute liquid globules, and the brass to be coated with a bluish-green incrustation. The screws and hinges of the velvet-lined box were similarly affected; but, in addition to the coloured compounds, tiny well-defined white prismatic crystals, as of zinc sulphate, were detected. Subjected to analysis the corrosion was found to contain not only the expected copper, iron, and zinc, but also chloride and sulphate. Hence the liquid globules mentioned above, consisted, in all probability, of deliquesced ferric chloride. It may here be added that the hinges and screws of the unlined box were unaffected, and that their appearance was perfectly normal.

Continuing the examination, the white felt lining of the box in which the weights had been stored was now removed and then soaked in water. A few hours later the water was filtered off and analysed. The analysis revealed the presence of sulphuric and hydrochloric acids. This surprising result led to an examination of samples of unused glue and white felt, both of which the maker of the weights kindly supplied. The following experiments were carried out with the glue.

Exp. I.—Water was distilled from a weak solution of glue. The clear distillate was acid and the presence of hydrochloric acid was affirmed by silver nitrate.

Exp. II.—Small pieces of glue were covered with water. Later, when these were swollen and presented a greyish-white and gelatinous appearance, the water was decanted and filtered and then analysed. Free hydrochloric and sulphuric acids were present but no phosphoric acid. Next, the glue was repeatedly washed by decantation; but, although the process was continued for some days, the glue remained acid.

Exp. III.—1 grm. of glue was dissolved in 10 c.c. of water and the solution evaporated to a jelly-like consistency. This operation was repeated first with other 25 similar portions of water and then with an additional 12 portions, each of 100 c.c. Thus there were in all 38 independent evaporations. During each evaporation the escaping vapours completely reddened litmus paper.

Exp. IV.—Two Jena glass dishes containing solutions, the one of silver nitrate and the other of blue litmus, were introduced into the box from which the lining had been removed, and the lid closed. Two days later the silver nitrate was distinctly opalescent and the litmus decidedly but not fully reddened.

Exp. V.—Some pieces of glue were first placed in a glass jar; then a Jena glass dish containing a 100-grm. gilt-brass weight of high and uniform reflectivity was introduced, the aluminium lid screwed on, and the jar left upon the balance bench.

Two days later the weight had lost much of its reflectivity, this owing to the formation of an irregular but decided film. When the experiment had been in progress for four days, most of the surface presented an appearance as of "frosted" gold. The mass of the film, determined in the manner already described, was 0·450 mg., or ·0149 mg. per 1 sq. cm.

The experiment was now resumed and continued for a total period of six weeks. The entire surface of the body of the weight with the exception of its base, which had lost but little of its original brightness, then appeared like dull "frosted" gold. A final measurement showed

that the mass of the film was 1·782 mg , and this was equal to ·0588 mg. per 1 sq. cm.

Exp. VI.—For this, the concluding experiment of the series, use was made of two newly-wiped weights, the one of platinum-iridium and the other of gilt-brass. The former weighed 50 grm. and had an area of of 6·94 sq. cm., whilst the latter weighed 20 grm. and possessed an area of 11 sq. cm. With these placed side by side, but not in contact, Exp. V. was repeated for the shorter period of eight days only. The mass of the film acquired by the platinum-iridium weight was ·0048 mg., whilst that of the gilt-brass weight was ·0379 mg. Hence in the first case the mass of the film per 1 sq. cm. was ·0007 mg., and in the second ·0034, the latter being almost five times greater than the former.

Discussion.

The result obtained with the gilt weight is important. It clearly shows that the abnormal film acquired by the gilt weight was chiefly due to chemical action ; otherwise it is difficult to understand why it was so far in excess of that found upon the chemically inert alloy of platinum and iridium. This conclusion receives confirmation from the results obtained with the chromium-plated weight, which was very perfectly coated (see Table I.).

The collective evidence of this series of experiments leaves no doubt as to the source whence abnormal films are derived ; also the experiments show, and that most clearly, why the hinges and screws of some boxes become so markedly corroded.

Further inquiry led to the discovery that, during the preparation of glue, use is made of lime, alum, sulphur dioxide, and hydrochloric acid. Now, although the final product may be freely washed, it would, from our own experiments (*vide supra*), appear very improbable that this in every case effects a *complete* removal of the several purifiers. Hence, as in the present instance, the finished and solid glue may still contain appreciable quantities of the highly corrosive compounds sulphuric and hydrochloric acids *, and these, when distributed with the glue

* Perhaps it is unnecessary to point out that any residual sulphurous acid is quickly oxidized to sulphuric acid, and that this by reacting with unremoved calcium chloride (itself deliquescent and damaging), gives rise to gaseous hydrochloric acid which then diffuses and attacks the weights.

over the undersurface of the lining of the box, readily attack certain weights. If these views are correct, we at once perceive why weights in general, and imperfectly gilded ones in particular, are affected in the way so frequently observed.

With regard to the gilded weight of Exp. V. it may be of interest to add that, on concluding the final weighing, the weight was first carefully re-polished and then examined with a powerful lens. It was then seen that the surface, previously film-covered, was now evenly dotted with minute pits. The handle, which throughout had retained its intrinsic brightness, was unpitted. It therefore appears that although the gilding of the handle was complete, that of the body was uniformly imperfect ; and, as a result, the main surface consisted of two interlaced nets, the one of brass and the other of gold. Whence it is seen that the chief area was made up of an infinitude of minute voltaic elements which, in the presence of gaseous hydrochloric acid, set up and maintained a maximum rate of chemical change with the production of the chlorides of zinc and copper.

Experiments with Glue.

The possible deleterious effects of glue having now been amply confirmed, an attempt was made to render the substance harmless.

For that purpose the glue was first treated with distilled water and then repeatedly washed and so changed to a semi-fluid gelatinous mass. As this continued acid, a slight excess of barium hydrate was added and the whole concentrated over a water-bath. During evaporation the glue became neutral, this owing to absorption of carbon dioxide from the air. When the glue was of normal consistency, and therefore ready for ordinary use, the porcelain containing-vessel was removed and protected with a glass cover. Some weeks later a fine mould or fungus had developed upon the surface and the glue when liquefied again gave an acid reaction *. On repeating the operations it was found that distinct

* Mr. W. H. Wilkins, mycologist in the Department of Botany at Oxford, informs me that certain fungi decompose glue with the production of oxalic, citric, and gluconic acids. The presence of any one of these acids would be harmful.

colonies of fungi appeared within five days. These abortive experiments were therefore ended, and others, in which the glue was avoided, were instituted.

Some Experiments in which the use of Glue was excluded.

To begin with, three polished wire triangles were arranged upon a clean glass plate. The first triangle was of gold, the second of nickel, and the third of brass.

Results. 2nd Series.

TABLE II.

Kind of weight.	Total mass of film.	Mass of film per 1 sq. cm.	Ratio: mass of 1st film (Table I.) / mass of 2nd film.
(1)	(2)	(3)	(4)
Nichrome	·0040 mg.	$\cdot 0001_4$ mg.	19
Brass, gilded	·0166 ,,	·0006 ,,	18
,, polished.....	·0050 ,,	·0002 ,,	19
,, chromium-plated ..	·0021 ,,	$\cdot 0000_7$,,	7
,, nickel-plated.....	·0205 ,,	·0007 ,,	2·7
,, lacquered	·0305 ,,	$\cdot 0010_5$,,	2·8

All the films were wholly invisible.

Next, six of the 100-grm. weights (Table I.) were again wiped with warm and dry silk ; then the gilt weight was stood upon the first triangle, the nickel-plated weight upon the second, and the plain polished brass weight upon the third. Thus, in so far as these three weights were concerned, all direct contact between them and some other substance chemically different was avoided. The chromium-plated weight was placed upon the bare glass ; but the nichrome and the lacquered brass weights were each introduced into an aluminium cell lined with unsecured and newly cleaned white woollen felt *. Finally,

* The felt was cleaned in the following way. First it was washed several times with distilled water and soap; then it was rinsed in distilled water only and dried. Finally, it was treated with successive portions of highly purified benzene and again dried. It was then ready for use.

each weight was covered with a small glass dome, and so protected from dust.

When the weights had been stored for eleven weeks, their new films were measured in the way already described. The results are set forth below.

From Table II. we find that our several experimental plans for storing weights are each and all superior to those usually employed; the relative superiority being in each case represented by the corresponding ratios given in column 4.

The more attenuated films acquired by the weights during this second series of experiments are to be regarded as the inevitable and normal gas-grown skins formed and retained in consequence of the contact of the weight with air. For any given weight the mass of such a skin per *apparent* unit area will vary with the degree or fineness of the polish imparted to the surface. Therefore the more mirror-like the appearance of the weight the less will be the *actual* area and the smaller the surface of the accompanying skin. Hence the advantage of a highly polished surface.

With the object of rendering our investigation more complete a third series of experiments was initiated and carried out, with the results recorded in Table III.

Six weights were used, and these were stored for appropriate periods under the differing conditions named in column (*b*).

Discussion.

From column (*e*) it will be seen that the results yielded by the weights 1–4 are very similar to those obtained with the weights used for the second series of experiments (Table II. col. 3). We therefore conclude that the plans adopted for storing those four weights were practically ideal.

With regard to the films found upon the weights Nos. (5) and (6), we note that their respective values are some 15 and 32 times greater than those accepted as unavoidable and normal. Whence it appears (α), that a weight, even when stored within fully seasoned mahogany, may in consequence become invested with an abnormal film or skin; and (β), that such a skin acquires a still greater thickness when woollen felt is interposed between the

weight and the wall of its wooden cell. This second and greater effect follows as a result of the superior absorptive power of the felt, which, in consequence, becomes impregnated with a relatively large amount of volatile matter obtained from the wood; and the weight, being in contact with it, is intensively affected*. The accuracy of this

Results. 3rd Series.

TABLE III.

Experiment.	(*a*) Weights.	(*b*) Storage cells.	(*c*) Time allowed for storing.	(*d*) Total mass of film.	(*e*) Mass of film per 1 sq. cm.
(1)	200 grm. gilt brass.	Glass jar having an aluminium lid. Interior covered with shellac varnish and then baked.	72 days.	·0057 mg.	$\cdot 0001_2$ mg.
(2)	„ „ „ „	Cell and lid of African blackwood. Unlined.	89 „	·0060 „	$\cdot 0001_3$ „
(3)	20 „ „ „	Cell and lid of old ivory. Unlined.	70 „	·0016 „	$\cdot 0001_5$ „
(4)	50 „ „ „	Cell and lid of brass lined with re-washed white woollen felt.	61 „	·0039 „	$\cdot 0001_9$ „
(5)	100 „ „ „	Cell and lid of old mahogany. Unlined.	56 „	·0706 „	·0022 „
(6)	50 „ plain polished brass.	Cell and lid of old mahogany lined with re-washed white woollen felt.	57 „	·0925 „	·0048 „

conclusion is borne out by the result obtained in Exp. (4) of Table III. For that experiment a portion of the same white woollen felt was used; but a cell of brass was substituted for that of mahogany. The acquired skin was thus reduced from ·0048 to ·0002 mg. We now review

* In connexion with this particular point, it may be recalled that the late Lord Rayleigh sometimes took advantage of the large absorptive power of wool, and established some degree of dryness in his laboratory by suspending therein one or more blankets.

the several ways in which a weight ideally stored, may, as the result of being wiped, exhibit temporary variations in mass.

First, we observe that a weight on being wiped is affected by

(1) the removal of dust and visible films ;

(2) the mutilation and temporary reduction of its normal gas-grown skin ;

(3) an inevitable rise in its temperature, together with the consequent variations, both in volume and buoyancy ; and

(4) the removal of exceedingly fine particles of the metal composing the weight.

In connexion with highly refined weighing, it is important that we examine in detail each of the above named points, and so in some measure obtain necessary information of a quantitative character.

Of Sundry Variations in the Effectiveness of a Weight.

Accordingly, a gilt brass weight of 200 grm. was first rubbed with dry silk and then stored for 15 hours within a glass jar lined with a coat of shellac and fitted with an aluminium lid. The weight was then lifted with forceps, lightly brushed with camel's hair, and transferred to the balance and counterpoised with a precisely similar weight which had also been wiped. Next, both weights were for some hours continuously washed with dry and carbon dioxide-free air and then compared. Finally, the experimental weight was again wiped with dry silk, and its relative value repeatedly determined at short intervals. The results thus obtained are correlated graphically in fig. 1.

During this experiment the temperature of the balance varied within the limits of 11·70° and 11·89° C., the mean temperature being 11·80° C. The temperature coefficient of the balance was equivalent to 9·4 telescopic scale divisions, and the sensitivity was 276 per 1 mg. Hence for a variation of $\pm 0{\cdot}1°$ C., the corresponding variation in the apparent mass was $\pm\ 0{\cdot}94/276 = {\cdot}0034$ mg., and therefore even the largest corrections were of a small order only.

On referring to the above extrapolated curve it will be seen that the weight on being wiped suffered, according to the evidence of the balance, (1) a transitory loss of 0·155 mg.; and (2) a permanent one of 0·021 mg. We also note (3) that, although on the cessation of wiping the weight rapidly recovered the major portion of its temporary loss, an additional three hours elapsed before a

Fig. 1.

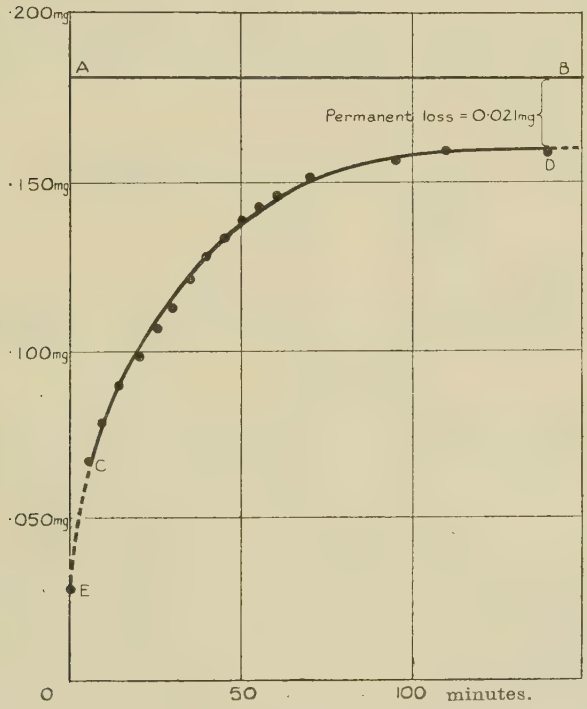

normal value was attained. The permanent loss here observed is the sum of the losses incurred by the removal of (*a*) dust, (*b*) an ordinary film of foreign matter, and (*c*) minute particles of the weight itself. In the present instance, the loss (·021 mg.) would, on account of the brief period allowed for the whole experiment, appear to be almost entirely due to the detachment of metallic particles from the gilded surface. We now describe the methods used for determining the apparent changes in

mass resulting from the unavoidable rise in the temperature of the weight. They were as follows.

Of the Influence of Temperature upon the Effectiveness of a Weight.

First, with the aid of a lathe, a block of highly polished brass, having the form and size of the 200 grm. weight, was prepared and given a vertical and central cavity which was just large enough to receive the bulb of the required thermometer. Secondly, the thermometer, readable to 0·01° C., having been inserted, and the filling of the cavity completed by adding two or three drops of water,

Fig. 2.

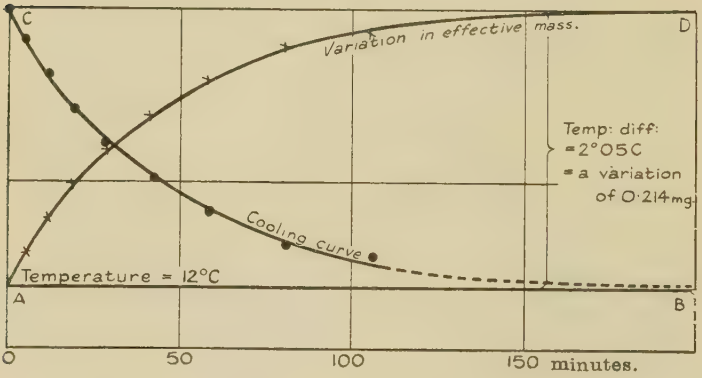

the block was warmed and then stood upon a cork within a tin cylinder the interior of which was blackened. The lid, perforated for the passage of the thermometer stem, was replaced, and the tin immersed in a thermostat adjusted for 12° C. Finally, observations were now carried out to determine the time taken by the block to cool from 14° to 12° C. The results of the experiment are shown by the graph CB, fig. 2.

Discussion.

On extrapolating this curve we find that for a weight of 200 grm. some three or more hours are required for the re-establishment of the original and lower temperature. Obviously these remarks are in a measure equally applicable to any other weight.

Next, we observe that, for given invariable conditions, the effective mass of a weight is constant and may be represented by a right line AB. But when, as a result of wiping, the temperature is increased 2° C. and the buoyancy of a 200 grm. weight thereby lessened, the effectiveness of the weight is temporarily increased by the calculable amount of 0·214 mg. During the ensuing continuous cooling there is a corresponding and unbroken growth in buoyancy, which results in an equivalent and uninterrupted decrease in the effectiveness of the weight. A graphic representation, AD, of the growth in buoyancy is obtained by inverting the cooling curve CB *.

For quantitative work in general these variations in the effective mass of a weight are almost, if not entirely, negligible. But for the correct solution of certain particular problems for which the quantities to be measured are in themselves excessively small, they must be fully considered and duly allowed for. In illustration of this mention may be made of researches dealing with (1) the mean density of the earth, and (2) with the question of the constancy of mass during chemical action.

On consulting papers dealing with problems involving refined weighing, we note that thermometers have sometimes been placed within the balance case for indicating the temperature of the object to be weighed. In such instances it is evidently assumed that the temperature of the air and that of the object are one and the same. This can seldom be true. Fortunately, very close approximations to the truth sufficient for most purposes, are thus obtainable when the variations in the temperature of the balance room are both slow and small, and numerous weighings, spread over a considerable time, are carried out. It may, however, be observed that in making precise allowances for changes in buoyancy resulting from variations in temperature, it is essential that we measure, not the temperature of the air at *any* convenient point within the balance case, *but that of the thin shell of air which envelops the object and is in actual contact with it.* In a future communication we shall hope to deal more completely with this important matter, and show how such determinations of temperature may be made.

* The curve CB represents not only the rate of cooling, but also the continuous decrease in the effectiveness of the weight.

We also hope shortly to be able to describe certain plans now being tested and perfected, whereby precision weights may be stored conveniently and in such a manner that the growth of films other than those we designate normal gas-grown skins, will be completely and permanently suppressed.

With regard to the change in the volume only of a 200-grm. brass weight resulting from a variation of $\pm 0{\cdot}1^\circ$ C., we observe that it corresponds to an alteration in buoyancy of $\pm{\cdot}00012$ mg. At present so small a quantity generally falls without the limits of the accuracy attainable in weighing, and is therefore entirely negligible.

The Gables,
Littledown Avenue,
Bournemouth.

XL. *Instability of Liquid Jets.* *By* E. Tyler, *D.Sc., M.Sc., F.Inst.P., Lecturer in Physics, College of Technology, Leicester* *.

[Plates XI,–XIII.]

Introduction.

IN attempting to explain the breaking up of a cylindrical column of liquid into drops, in the light of Savart's † results, Plateau ‡ has shown that any disturbance acting upon such a system produces alternate swellings and contractions, and when the "wave-length" of these appearances exceeds the circumference of the column, instability predominates with resolution into drop formation.

Rayleigh §, applying this criterion of instability to a liquid jet falling vertically, points out that the kind of disturbance most susceptible to the jet as it leaves the orifice is one which impresses upon it alternate swellings and contractions of wave-length equal to 4·51 times the initial diameter of the jet. Such a disturbance created at the orifice grows exponentially in amplitude as it

* Communicated by the Author.
† *Ann. Chim. Phys.* liii.
‡ 'Statique des Liquides,' p. 354 (1873).
§ 'Sound,' xi. p. 360.

travels down the jet and finally effects disruption in the "jet-length."

Provided the velocity of descent of the jet remains sensibly constant, there is very little change in the diameter of the column, the degree of instability remains constant, and the jet is resolved into drops separated by a common interval λ. The drops do not at once assume and retain the spherical form but execute a series of vibrations, being alternately compressed and elongated in the direction of the axis of symmetry.

The time of disintegration according to Rayleigh is dependent upon the initial amplitude of disturbance a_0, created at the orifice and the rate at which it grows.

Ignoring viscosity of the jet fluid it is expressible as $t=\frac{1}{y}.\log_e\frac{a}{a_0}.\sqrt{\frac{\rho d^3}{\sigma}}$, where a is the final amplitude of disturbance at the disruption point, ρ the density, and σ the surface tension of the liquid respectively, d being the diameter of the jet, and y a function of $\frac{\pi d}{\lambda}$, controlling the degree of instability. This function is a maximum when $\frac{\lambda}{d}=4{\cdot}51$.

If viscosity is considered, by dimensional reasoning it can be shown that $t=\frac{1}{y}.\log_e\frac{a}{a_0}\sqrt{\frac{\rho d^3}{\sigma}}.f\left(\frac{\sqrt{\sigma\rho d}}{\mu}\right)$, and experimental evidence suggests $f\left(\frac{\sqrt{\sigma\rho d}}{\mu}\right)$ to be of the form $1+\frac{1}{4095}.\left(\frac{\sqrt{\sigma\rho d}}{\mu}\right)^{\frac{3}{2}}$ in the case of capillary jets formed in air *.

Whether such jets break up into drops under the condition required for maximum instability is a matter of experimental investigation, and it was considered interesting to examine capillary jets from this point of view. Some recent work of a similar nature has been done by Haenlein † and others ‡, usually with wider nozzles than those used in the present work.

* Tyler and Watkin, Phil. Mag. xiv. Suppl. Nov. 1932.

† *Forschung. Ing. Wes.* ii. no. 4, pp. 139–149, April 1931.

‡ Weber, *Zeit. f. ang. Math. u. Mech.* xi. no. 2, pp. 136–154, April 1931. Reissner, *Zeit. f. ang. Math. u. Mech.* xii. p. 25 (1932).

Theoretical Consideration of Drop Formation.

Supposing V to be the velocity of the jet at the disruption point, N the frequency of drop formation, and λ the wave-length separation distance between the drops or swellings on the jet, then $V=N\lambda$.

Also if d and D be the diameters of the jet and corresponding spherical drop for a given nozzle, assuming continuity of the fluid and neglecting the size of Plateau's spherule, the relationship $\frac{\pi}{6}D^3N=\frac{\pi}{4}d^2V$ holds good, whereupon

$$\frac{\lambda}{d}=\frac{V}{Nd}=\frac{2}{3}\left(\frac{D}{d}\right)^3.$$

If λ be the same as the wave-length of disturbance effecting disintegration, then measurement of either the size and spacing of the drops together with the mean diameter of the jet, or the evaluation of the frequency of drop formation together with the corresponding speed and diameter of the jet, enables the degree of instability $\frac{\lambda}{d}$ to be computed and compared with the above theory.

Instantaneous spark photographs of jets permit measurement of λ, d, and D, whereas an experimental determination of $\frac{V}{Nd}$ suffices to give an alternate value of $\frac{\lambda}{d}$. The following investigations were undertaken with this object in view.

Spark Photographs of Liquid Jets formed in Air. Measurement of λ, d, *and* D.

The usual arrangement of obtaining spark photographs was employed (fig. 1), in which the discharge from a Leyden jar served as the illuminant.

Liquids such as mercury, anline, and coloured water were used by virtue of their marked differences in properties in respect of density, surface tension, and viscosity, and at the same time being more or less opaque.

Figs. 1–7 (Pls. XI.–XIII.) are typical exposures for jets of different diameters. In each case a series of exposures at different phases of resolution but at constant speed are exhibited.

The oscillatory motion of the drops is clearly evident. Accurate measurement of the diameter of the jet at various distances from the orifice revealed very little tapering. Incorporated in Table I. are the average values of λ, d, and D, obtained from the various plates and expressed as microscope readings, together with the deduced values of $\frac{\lambda}{d}$ and $\frac{2}{3}\left(\frac{D}{d}\right)^3$.

Fig. 1.

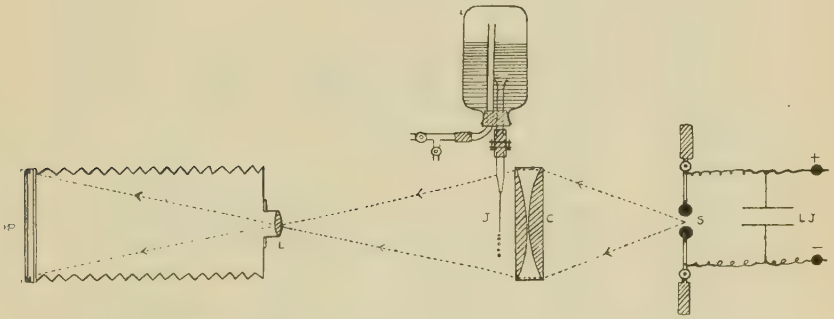

J=Liquid jet. S=Spark gap (1 cm.).
L=Camera lens. P=Photographic plate.
LJ=Leyden jar. C=Condenser lens (10″ diameter).

Frequency Measurement of Drop Formation.

Deduction of $\frac{V}{Nd}$.

Methods previously used for measuring the frequency of drop formation of a liquid jet under normal resolution comprise either the stroboscope or audible method in which the impact of the drops on either a stretched rubber membrane or piece of wood gives rise to sounds of audible pitch which, despite their impurity, can be estimated by tuning with a monochord.

Table I.

Results for Jets in Air. Average Measurements from Photographs.

Liquid jet.	Diameter of nozzle (actual) (mm.).	Mean speed of jet, V(cm./sec.).	Diameter of jet. Microscope readings, d (mm.).	$(\lambda)_{jet}$. Microscope readings (mm.).	$(\lambda)_{drops}$. Microscope readings (mm.).	Diameter of spherical drop. Microscope readings, D(mm.).	$\left(\frac{\lambda}{d}\right)_{jet}$.	$\left(\frac{\lambda}{d}\right)_{drops}$.	$\frac{2}{3}\left(\frac{D}{d}\right)^3$.
Mercury ..	·300	118	·410	1·938	1·940	·793	4·72	4·71	4·81
	·300	122	·386	1·730	1·790	·741	4·48	4·64	4·71
	·300	130	·420	2·060	2·030	·795	4·91	4·84	4·53
	·319	165	·342	1·500	1·670	·660	4·40	4·89	4·79
	·319	200	·383	1·790	1·720	·747	4·67	4·49	4·88
Water	·450	187	·485	2·290	2·300	·925	4·73	4·75	4·61
	·450	210	·446	2.110	2·090	·849	4·73	4·69	4·56
	·650	148	·543	2·600	2·480	1·090	4·78	4·58	4·76
Aniline....	·450	251	·491	2·250	2·280	·930	4·58	4·65	4·54
	·450	200	·452	2·040	2·040	·877	4·52	4·52	4·60
	·650	156	·677	3·180	3·260	1·270	4·71	4·82	4·43

Mean values ..... $\left(\frac{\lambda}{d}\right)_{jet}=4{\cdot}65$, $\left(\frac{\lambda}{d}\right)_{drops}=4{\cdot}69$, $\frac{2}{3}\left(\frac{D}{d}\right)^3=4{\cdot}66$.

With capillary jets the frequency of drop resolution is usually high, and analysis with the stroboscopic disk becomes less adaptable when it is required to investigate over a complete jet-length velocity curve. Other methods are therefore desirable, and the following have been successfully utilized.

In each case values of $\frac{V}{Nd}$ are obtained using water only for different nozzles.

Method and Results using Photo-Electric Cell.

As a consequence of the opacity and refractivity of the liquids employed, it is possible to utilize this property whereby the detached drops at the end of the jet cause an intermittent illumination of light falling on a photo-electric cell, by intercepting the incident light. Such effects will produce periodicity in the photo-electric currents which after valve amplification may be rendered audible. The arrangements adopted are shown in figs. 2 *a* and 2 *b*, the former giving the stronger sounds. Fig. 2 *c* shows the schematic diagram of the amplifier, which is one of the usual devices adopted in amplifying photo-electric currents.

The jet as it falls vertically is so adjusted to pass in front of a small aperture in an opaque screen, with only the drops moving past the aperture.

Light from a 40-watt auto-lamp (gas filled), with a straight horizontal filament and in line with the aperture, is focussed on the drops. A photo-electric cell of the vacuum type, suitably placed on the other side of the screen, receives the intermittent light by virtue of the periodic cutting off of the light by the drops.

The frequency of the light fluctuations received by the cell is the same as that of drop formation, and the resulting photo-electric currents, after passing through a two-valve amplifier, are converted into sound waves by the insertion of a loud speaker or telephones in the plate circuit of the last valve.

The pitch of the note heard is tuned to a similar note produced on a monochord calibrated afterwards with a 512 fork.

In view of the oscillatory motion of the drops, the variation in light-intensity falling on the photo-electric

Fig. 2 *a*.

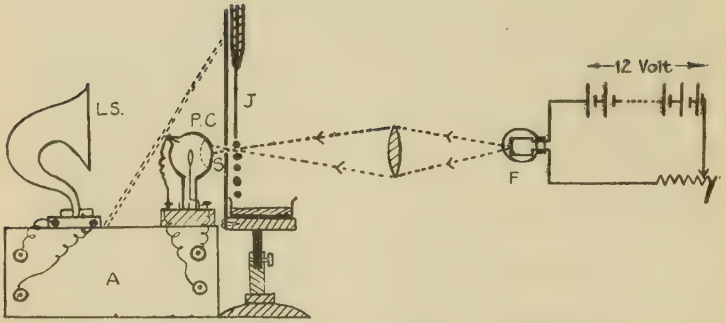

J=Liquid jet.
PC=Photo cell.
A=Amplifier.
LS=Loud speaker.
F=Filament source.
S=Aperture.

Fig. 2 *b*.

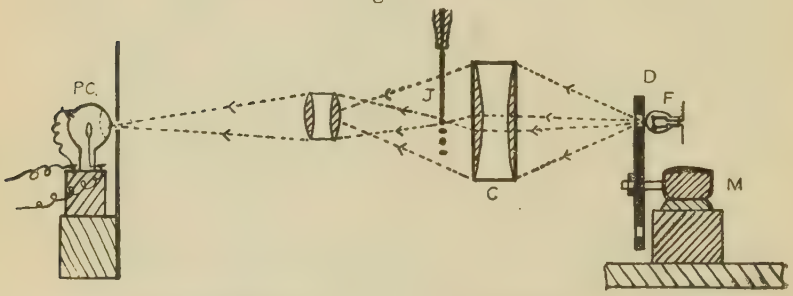

D=Stroboscopic disk.
C=Condenser lens.
M=Motor.
PC=Photo cell.
J=Liquid jet.

Fig. 2 *c*.

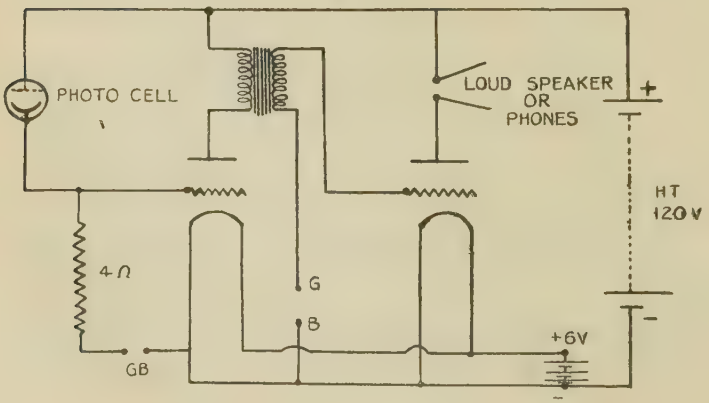

cell will not be of a simple form, and it is therefore to be expected that the quality of the tones heard will not be pure, although the pitch is easily tunable.

It is preferable to use an aperture slightly smaller in diameter than that of the drops, together with a filament

TABLE II.

Frequency of Drop Formation. Results for Liquid Jets in Air. (Photo-Electric Cell Method.)

Liquid jet.	Mean diameter of jet. d (mm.).	Mean velocity of jet. V(cm./sec.).	Frequency of drop formation N.	$\frac{V}{Nd}$
Water....	·500	116	512	4·52
		136	610	4·46
Water....	·650	161	517	4·79
		136	430	4·85
		146	517	4·35
		126	420	4·50
		171	560	4·70
		221	735	4·63
		231	795	4·46
		281	940	4·60
		196	686	4·40
Water....	·450	126	603	4·65
		220	1080	4·55
		168	795	4·71
		146	735	4·43
		272	890	4·70
Water....	·352	137	862	4·51
		188	1100	4·72
		220	1250	5·00
		180	1040	4·90
		185	1150	4·56
		240	1360	5·00
		205	1320	4·41

Average value of $\frac{V}{Nd}$ = 4·62.

source of light already mentioned, and also to work with the aperture just below the disruption point of the jet.

To enable larger apertures to be used, the magnification

method outlined in fig. 2 *b* was found satisfactory, although, as mentioned previously, the sounds produced are weaker in strength, due to the reduction in light-intensity at the greater working distance of the screen from the source of light.

The measurement of V and *d* for corresponding frequencies of drop formation was the same throughout ; V, by collecting the liquid in a given time and weighing, and *d* by direct measurement with microscope either of the actual jet or from the photographs.

The errors involved are of the same order as in the evaluation of the frequency of drop formation, and it was considered undesirable under such conditions of accuracy to adopt the precision method of Bohr * whereby the velocity of an element of the jet is obtained photographically.

A summary of results for jets of different diameters is included in Table II.

Method and Results using Flashing Neon Tube stroboscopically.

In this method the stroboscoping of a liquid jet is rendered possible by utilizing the intermittent illumination from a Neon tube of the G.E.C. television type with vertical plate, suitably coupled to a valve oscillator, of controllable frequency.

Since it is essential to have a good source of illumination, a specially designed oscillator is necessary †, and such an arrangement is shown in fig. 3.

The jet is allowed to fall vertically in front of the plate of the neon tube, and the frequency of flashing varied either by altering the resistance in the filament circuit of the valve, or by the bank of condensers, until the drops appear stationary.

A loud speaker included in the neon circuit, either in series or parallel with the lamp, served as a means of deducing the flashing frequency, which is, of course, a measure of the frequency of drop formation.

* Phil. Trans. ccix. A, p. 452 (1909).

† My thanks are due to Mr. C. R. Chadfield, of the Engineering Dept., Leicester College of Technology, for the loan of this.

The note audible in the speaker was tuned to a similar note produced on a monochord as in the previous method. The corresponding speeds and diameter of the jets for the various frequencies were also obtained at the same time.

Care must be taken to avoid interference between the sound waves emitted by the loud speaker and the jet, for it was observed that when the speaker was sounding

Fig. 3.

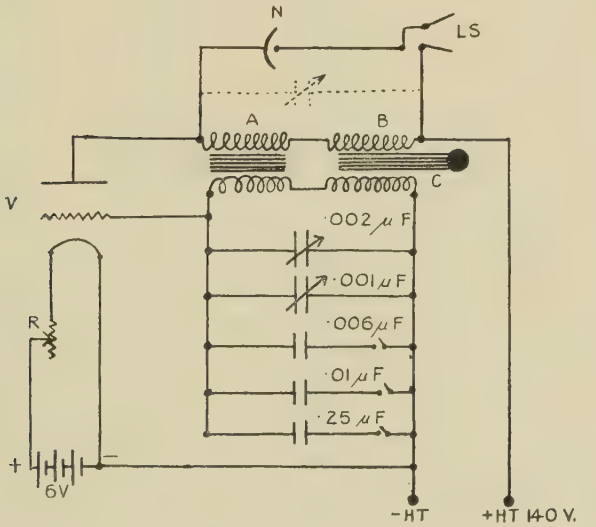

V=LS 5 valve. N=Neon tube, G.E.C. television type. LS=Loud speaker or phones. A = Power transformer, ML component, Coventry, Patent No. 33604/22. B=Variable core transformer, C=Variable core (stranded), Diameter 1·50 cm., length=15 cm.

strongly the jet, although forming at constant speed, became susceptible to certain tones more than others (*i.e.*, overtones of the speaker).

Usually the speaker was enclosed in a box and removed as far as possible from the jet.

In Table III. are results obtained by this method.

TABLE III.

Frequency of Drop Formation. Results for Liquid Jets in Air. (Stroboscopic Neon Tube Method.)

Liquid jet.	Mean diameter of jet. d (mm.).	Mean velocity of jet. V(cm./sec.).	Frequency of drop formation N.	$\frac{V}{Nd}$
Water....	·650	151	496	4·70
		147	496	4·56
		176	600	4·51
		221	790	4·30
		104	318	5·05
		*85	239	5·46
		110	375	4·51
		201	670	4·63
		*96	296	5·00
		196	670	4·51
		272	915	4·50
		131	410	4·75
Water....	·450	*115	512	5·00
		136	617	4·88
		184	895	4·57
		210	990	4·70
		164	795	4·58
		250	1260	4·41
		308	1510	4·53
		365	1760	4·60
		248	1205	4·59
Water....	·352	194	1160	4·75
		174	1002	4·84
		240	1460	4·67
		297	1880	4·50
		343	2150	4·53
		305	1880	4·60
Water....	·500	151	600	5·03
		*101	420	4·80
		129	600	4·30
		186	840	4·43
		245	1080	4·54
		288	1160	4·95

Average value of $\frac{V}{Nd}$ = 4·64.

* Below or near the lower critical velocity.

Method and Results using the Rotoscope and Stroboscopic Disk.

As a verification of the results obtained by the previous methods a few values of $\frac{V}{Nd}$ were obtained using both the Ashdown rotoscope * and the stroboscopic disk.

In the former method, frequencies up to 40,000 per minute may be measured with the displaced (ultra speed) shutter, and with special instruments frequencies up to 250,000 per minute are possible.

In the stroboscopic disk method 40 slits were used and the intermittent light illuminating the jet was projected on to a screen, on which was also formed an enlarged image of the jet.

The speed of the disk was adjusted until the detached drops appeared stationary. Instead of measuring the speed of the disk at this condition, which is the usual procedure adopted for evaluating the frequency of illumination, or in this case that of drop formation, the photo-electric cell amplifying device used earlier is employed.

The intermittent light produced by the rotating disk is allowed to fall on the cell giving rise to electrical impulses which after amplification are converted into sound waves of the same frequency. Thus to effect a deduction of the drop resolution frequency, the disk's speed is varied until an apparent stationary picture of the jet is formed, and at the same time the cell is exposed to the light fluctuations, and the resulting sound heard in the loud speaker is tuned to a similar note produced on a monochord. The pitch of this note is the same as that of the frequency of drop formation.

Table IV. includes results obtained by these methods from which if will be observed there is good agreement with the data obtained by the other methods.

Discussion of Results.

Referring to the summary of the average values of $\frac{\lambda}{d}$ and $\frac{V}{Nd}$ given in Table V., it will be observed there

* 'Notes on the Rotoscope,' pamphlet, A. J. Ashdown, Ltd., London, March 1919.

TABLE IV.

Frequency of Drop Formation. Results for Liquid Jets in Air. (Stroboscope and Rotoscope Method.)

Liquid jet.	Mean diameter of jet. d (mm.).	Mean velocity of jet. V(cm./sec.).	Frequency of drop formation N.	$\frac{V}{Nd}$.
Water	·650	116	380	4·71
		131	415	4·85
		123	403	4·70
		162	512	4·88
		200	700	4·41
		231	766	4·64
		*75	231	5·02
		98	310	4·86
		86	300	4·42
Water	·500	120	532	4·51
		112	470	4·76
		*102	405	5·02
		119	475	4·99

Average value of $\frac{V}{Nd} = 4·75$.

* Below or near the lower critical velocity.

TABLE V.

Summary of Average Results.

Method.	Photo cell.	Flashing neon tube.	Rotoscope and stroboscope.	Spark photographs. $\left(\frac{\lambda}{d}\right)_{jet}$.	Spark photographs. $\left(\frac{\lambda}{d}\right)_{drop}$.	Spark photographs. $\frac{2}{3}\left(\frac{D}{d}\right)^3$.
$\frac{V}{Nd}$.	4·62	4·64	4·75	4·65	4·69	4·66

is fairly good agreement with the theoretical value of $\frac{\lambda}{d}$, (4·51), and the results confirm the existence of maximum instability with such jets. The magnitude of λ given by

the photographs may be accepted as a reliable measure of the wave-length of disturbance producing maximum instability of the liquid jets. The discrepancy between theory and experiment is of the same order as the experimental errors involved.

Even with mercury jets where the effect of gravity might be expected to be greater than with lighter liquids, and so modify the degree of instability, maximum instability condition exists.

Any increase in the velocity of the jet due to gravity may be evaluated from elementary considerations.

As each element of the jet leaves the orifice, it is at once accelerated by gravity, and if V be the mean velocity of efflux near the orifice, its value is increased approximately to $V\left(1+\frac{gL}{V^2}\right)$ at the end of a jet of length L cm.

In the case of the mercury jets $\frac{gL}{V^2}$ may be as large as 10 per cent. at the upper critical point where turbulence occurs, suggesting that the increase in speed of the jet has a maximum value of about 10 per cent. in the limiting cases

The corresponding decrease in the diameter of the jet necessary to fulfil the condition Velocity $\times$ Area of cross-section of the jet is a constant, would involve a change of about 5 per cent.

The variations of these two quantities can be shown by dimensional reasoning to have opposite effects in controlling the wave-length of the disturbance, and therefore tend to maintain it constant.

With the less dense and more viscous liquids $\frac{gL}{V^2}$ is generally smaller than with mercury, thus producing less tapering and maintenance of constancy in the degree of instability.

It has been shown elsewhere * that with such jets formed in air the jet-length velocity curve is characteristic of two critical velocities at which discontinuity in the jet-length occurs.

* Smith and Moss, Proc. Roy. Soc. A, xciii. (1917); Tyler and Richardson, Proc. Phys. Soc. xxxvii. (Aug. 1925).

The lower critical velocity is an attribute of excessive drop formation disturbance gaining access at the nozzle, whereas the upper is due to turbulence within the jet prevailing over streamline motion. It is only over this range between the critical velocities that the ordinary theory of instability should be applied, and for experimental verification this was adhered to in the evaluation of $\frac{V}{Nd}$. For speeds less than the lower critical there is an apparent rise in the value of $\frac{V}{Nd}$, consistent with the photograph shown in fig. 1 (Pl. XI.), for mercury, since the drops are much larger and spaced further apart. The change in $\frac{V}{Nd}$ in this region is mainly due to the sudden reduction in the frequency of drop formation. This phenomenon is analogous to eddy formation behind obstacles in a stream of fluid at low Reynolds number *. The methods outlined for measuring the drop frequency resolution, by virtue of intermittent illumination, may well be adapted to other vibration problems, but preference must be given to the stroboscopic neon tube owing to its elasticity and accuracy in use.

Summary.

The degree of instability of capillary jets is examined experimentally. Spark photographs produced under varying conditions are included, from which measurement of the size and spacing of the drops formed at the end of the jet enables a comparison with theory to be made.

Methods suitable for determining the frequency of drop formation are described employing the use of (*a*) photo-electric cell, (*b*) flashing neon tube, and (*c*) stroboscope or rotoscope. A knowledge of such frequencies of resolution together with the corresponding diameter and speed of the jet permit a further comparison between theory and experiment. Such comparisons reveal satisfactory agreement.

* Tyler, Phil. Mag. xi. (April 1931); Bernard, *Comptes Rendus*, cxlvii. p. 839 (1908); Richardson, Proc. Phys. Soc. xxxvi. (1924).

XLI. *Emission from Oxide-coated Cathodes.*—II.

By M. Benjamin, *B.Sc.*, *and* H. P. Rooksby, *B.Sc.** (Communication from the Research Staff of the M.O. Valve Company, Limited, May 1933.)

[Plate XIV.]

Summary.

IT has been shown that in the case of an activated oxide cathode :—

(1) the constituent oxides can exist in all states ranging from a simple mixture to a homogeneous solid solution ;

(2) there exists a definite relationship between the physical state of the oxides and the thermionic emission obtained from them.

Introduction.

In a recent paper † the results of an investigation on the thermionic properties of oxide cathodes were described. It was stated that :

(1) The oxide coating on the activated cathode was a homogeneous solid solution of barium and strontium oxides.

(2) The thermionic emissions depended on the relative proportions of barium oxide and strontium oxide present in the solid solution.

Further investigation of the coated cathodes has shown that anomalous results are sometimes obtained. In these cases the oxide coating was a mixture of two solid solutions, one rich in barium and one rich in strontium. Fig. 1, *a* (Pl. XIV.) is an X-ray photograph of such a coating, and the existence of two phases is shown by the presence of pairs of lines corresponding to compositions 75 per cent. BaO/25 per cent. SrO and 11 per cent. BaO/89 per cent. SrO by weight respectively.

A large number of activated cathodes were examined, and it was found that the emissions were higher when the

* Communicated by C. C. Paterson, M.I.E.E.

† Phil. Mag. xv. p. 810 (April 1933).

coating was homogeneous than when it consisted of two or more phases. This result would be expected from the data given in our previous paper (fig. 4 *a*), which shows there is an optimum value in the composition-emission curve.

It appeared interesting, however, to follow in detail the changes in emission accompanying the formation of a homogeneous solid solution from the mixed oxides. Since the commencement of this work Burger * has shown that the mixed oxides from solid solutions when subjected to suitable heat treatment, although he has not followed the emission changes in detail.

Experimental †.

(i.) *Preparation of a Simple Mixture of Oxides.*

The cathode coatings described in our previous paper were solid solutions of carbonates, which on decomposition gave solid solutions of oxides. For the present experiments the cathodes were coated with a mixture of carbonates in order to obtain mixed oxides on decomposition. This was done by dipping in an aqueous suspension of equal proportions by weight of the two carbonates.

The cathodes used were 0·044 mm. diameter nickel wire, and the coating was sintered at 700° C. in CO_2 after each application. The wire was alternately dipped and sintered until the weight of coating was 2·5–3·5 mg. per 20 cm. length of wire. Coatings produced in this way were found to be simple mixtures of the carbonates, as shown by the X-ray pattern in fig. 1, *f* (Pl. XIV.), which should be compared with the pattern for the solid solution shown in fig. 1, *g* (Pl. XIV.).

The coated wires were then mounted in the apparatus previously described, the tubes evacuated, and the cathodes activated. After activation the cathodes were detached and subjected to X-ray examination. The X-ray photographs showed that the coating was practically a simple mixture of barium and strontium oxides. The initial flashing of the cathodes had probably produced a simple

* *Zeits. für Physik*, lxxx. p. 352 (1933).

† Full details of the apparatus used, the method of activation etc. appeared in the previous paper (*loc. cit.*).

oxide mixture, but during activation a slight degree of coalescence had occurred.

The X-ray photograph of a typical cathode is reproduced in fig. 1, *c* (Pl. XIV.), and in this the two phases are of equal intensity and have respectively compositions 91 per cent. BaO, 9 per cent. SrO, and 9 per cent. BaO, 91 per cent. SrO. The emission obtained was 1·2 ma.

Fig. 2 shows the curve relating composition with emission applicable to cathodes of this length. This curve is derived from fig. 4 *a* in the previous communication. The maximum emission to be expected when this coating is a homogeneous solid solution is about 6·5 ma. For the two phases present the emission expected

Fig. 2.

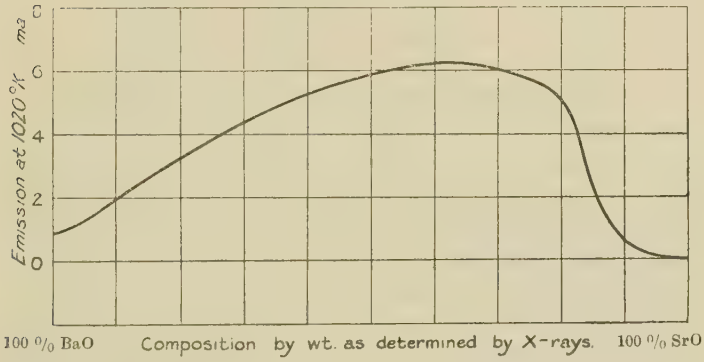

Relation between composition and emission.

would be the mean of 2·4 ma. and 0·4 ma. The 1·2 ma. obtained is in good agreement with the 1·4 ma. expected.

(ii.) *Conversion of Mixed Oxide Coatings to the Solid Solution State.*

The next step was to convert the mixed oxides to the homogeneous solid solution state and observe the emission changes.

Similar cathodes to those described in the previous section were mounted and treated as before. After the normal 15 minutes activation period the emission was

recorded. The activation was then continued, emission measurements being made at regular time intervals.

Column A of the Table gives the results for a typical cathode :—

Time (minutes).	Emission (ma.) at 1020° K. A.	B.	C.
0	0	0	0
15	1·1	2·5	1·9
20	1·8	3·95	—
25	1·95	4·0	2·95
30	2·1	4·0	—
35	3·4	3·7	4·2
40	4·7	4·1	—
45	4·85	4·8	4·2
60	5·6	4·9	4·5
75	5·8	4·8	4·8
85	5·8	4·9	5·2

It will be observed that the emission, which after normal activation period was 1·1 ma., gradually increases to a steady value of 5·8 ma.

The cathode was now detached for X-ray examination, and the photograph is reproduced in fig. 1, *d* (Pl. XIV.). On comparing it with fig. 1, *c* and 1, *b* it will be seen that the oxides, originally a simple mixture, now approach closely to a homogeneous solid solution.

This transformation has been accompanied by an increase in emission, and the final emission of 5·8 ma. compares favourably with the value of 6 to 7 ma. expected from this coating in the solid solution state. Actually fig. 1, *d* (Pl. XIV.) does reveal that the composition of the coating is not yet quite uniform : the lines are somewhat diffuse, indicating a small range of solid solutions spreading slightly to either side of the mean value. The most intense part of the lines correspond to a solid solution of composition 42 per cent. BaO, 58 per cent. SrO by weight, whilst there is a second peak of about one-quarter intensity corresponding to a composition 63 per cent. BaO, 37 per

cent. SrO by weight. Similar results were obtained with cathodes B and C.

It is necessary, however, to record one exception. This cathode gave an emission of 0·8 ma. after 15 minutes activation. Continued activation gave no increase in emission, and despite treatment for 100 minutes the final emission had decreased to 0·5 ma. X-ray examination revealed that the coating was still in the two-phase state, the compositions being 89 per cent. BaO, 11 per cent. SrO, and 15 per cent. BaO, 85 per cent. SrO, by weight respectively.

It is not possible to offer any explanation as to why the emission did not rise under conditions normally giving an increase. It is significant, however, that, consistent with no increase in emission, there is no evidence of any pronounced coalescence.

(iii.) *Additional Experiments.*

A carbonate coating which was a homogeneous solid solution containing equal proportions of the carbonates was prepared by a method independent of that described in the preceding communication. The cathodes were coated by dipping into an aqueous suspension of the double carbonate and then sintering the coating in CO_2 at 700° C. The emissions obtained from such coatings were always of the order of 6–7 ma., after 15 minutes activation. The X-ray pattern of a typical cathode is shown in fig. 1, *e* (Pl. XIV.), where it will be observed that the oxide coating is in the homogeneous solid solution state.

Discussion.

(*a*) For cathodes coated with BaO/SrO it is shown that a relationship exists between the physical state of the activated coating and the emission obtained from it. When the oxides are present as a simple mixture the emission is a function of the emissions obtainable from cathodes coated with each of the single oxides respectively. When partial coalescence of the oxides is made to occur the emission increases, because the compositions of the component phases have changed, and the new phases both have higher emissions than the pure oxides. The

actual emissions will be related to the compositions of the component phases and their proportions, and not to the composition of the coating as a whole. For an emission-composition curve of the shape shown it is probably true that the highest emission is obtained when only one phase, the solid solution, is present.

(*b*) It has been shown that the emission-composition curve has an optimum value. In the present state of knowledge it is impossible to state definitely why this should be the case. Becker * and Gehrts † have shown that practically nothing but free barium evaporates from a BaO/SrO cathode. This fact, together with the fact that SrO has a greater heat of formation than BaO, permits the inference that until the proportion of SrO becomes great it is free barium that is responsible for the thermionic activity. Reimann and Murgoci ‡, Becker and Sears §, Reimann and Treloar ||, and Fowler and Wilson ¶ have indicated independently that the activity is due to free barium dispersed through and adsorbed on the surface of the oxide. Becker and Sears § experimentally, and Fowler and Wilson ¶ theoretically, have shown that the concentration of barium dispersed through the coating will affect the A in Richardson's equation $I = AT^2\epsilon^{-\phi e/kT}$, and that the concentration of barium on the surface will affect the work function ϕ.

The experimental results described in this and the preceding paper indicate that barium dispersed through and adsorbed on the surface of BaO/SrO is a better emitter than barium dispersed through and adsorbed on the surface of BaO alone.

What effect the solid solution will have on the equilibrium concentration of free barium dispersed through the coating it is difficult to say. It may be, however, as Becker and Sears and others have indicated, that the surface layer of barium conforms to the lattice spacing of the underlying oxide. In this case the concentration of surface barium will increase as the solid solution becomes richer in strontium oxide, and thus lower the

* J. A. Becker, Phys. Rev. xxxiv. p. 1323 (1929).
† A. Gehrts, *Naturwissenschaften*, xx. p. 732 (1932).
‡ Phil. Mag. ix. p. 440 (1930).
§ Phys. Review, xxxviii. pt. 2, p. 2193 (1931).
|| Phil. Mag. xii. p. 1073 (1931).
¶ Proc. Roy. Soc. A, cxxxvii. p. 503 (1932).

work function. When the proportion of SrO becomes very large the presence of free strontium intermixed with the barium will raise the work function.

The Authors desire to tender their acknowledgment to the General Electric Company and the Marconiphone Company, on whose behalf the work was done which has led to this publication.

XLII. *Notices respecting New Books.*

The Metallic State. By W. Hume-Rothery. [Pp. xx+371.] (Oxford: Clarendon Press. Price 25*s.*)

DURING the past twenty years many powerful new experimental weapons have been employed in the struggle to solve the mysteries of the metallic state. The preparation of metal single crystals has advanced the problem a stage further, for ultimately the properties of polycrystalline metals must be explained in terms of the single crystallites. The methods of X-ray crystal analysis have made it possible to classify the alloys more systematically than could be done before the lattice structure was investigated. Very low temperatures, very high pressures, very great magnetic fields have revealed fresh properties, especially concerning the conduction of electricity in metals—the property of superconductivity, in particular, springs to the mind. As regards the theoretical aspect, neither the mechanical nor the electrical properties are very satisfactorily explained, even as regards single crystals, but advances have recently been made which solve some of the old difficulties. All this body of work, however, is scarcely represented in the English text-books, or books of reference, so that there is no doubt as to the need of a book like that now before us, which undertakes to give a systematic account of the present knowledge of the metallic state.

The author concerns himself mainly with the electrical and thermal properties of metals, having but little to say of the mechanical and magnetic aspects of the problem. He is particularly interested in the information afforded by the analysis of crystal structures, on the basis of which he classifies alloys into different types of solid solutions. There is a very interesting discussion of the types of crystal structure exhibited by metals in connexion with their places in the periodic table, and of the bearing which the regularities

thus revealed have on the metallic linkage and degree of ionization, if it may be so called, of the metallic atom.

The book is divided into two sections. The first is devoted to our experimental knowledge of the electrical conductivity and thermal conductivity of pure metals and of alloys, together with the thermoelectric properties, thermionic emission, and the contact potential. Considering the great quantity and, in many cases, complexity of the experimental results this digest and discussion are remarkably successful, and the references are extremely well chosen, the reader not being overwhelmed with a mass of material of secondary importance. Significant modern work is particularly stressed. In the second section the development of the electronic theory of conduction is discussed. The author, wisely, we think, starts with the original electron-gas theory of Drude, which, in spite of the well-known difficulties offered by the specific heats, to which the conduction electrons do not apparently contribute, remains the prototype of the electron theories. The way in which Sommerfeld's theory preserves the electron gas, but avoids this difficulty by introducing the Fermi-Dirac statistics and the allied conception of a degenerate gas, is well described, and the later modifications of this theory, as exemplified by that of Bloch, are also exposed. Between the new and the old type of theory we have other attempts, and Lindemann's theory, which has a characteristically clear physical conception behind it, receives well-merited attention. The author does not, however, claim too much for the modern theories, which, in spite of their complexity, fall very short of giving a satisfactory account of the phenomena, especially of the mysterious super-conductivity. Some introduction of a new physical conception is plainly needed.

The book is very clearly and attractively written, and presenting, as it does, a great body of interesting and important material of which no collected and critical account has hitherto been available in English, deserves a warm welcome.

E. Grimsehl. *A Textbook of Physics.* Edited by R. Tomaschek, Professor of Physics in the University of Marburg. Authorized translation from the VIIth German edition by L. A. Woodward, B.A. (Oxon.), Ph.D. (Leipzig). Vol. II. *Heat and Sound.* [Pp. xi+312.] (London & Glasgow: Blackie & Son. Price 12*s.* 6*d.* net.)

This is a treatise of physics suited for the degree standard. The most attractive feature of it consists of the biographical epitomes which are supplied in footnotes. These, in general,

give a very satisfactory summary of the main contributions of various investigators. Now and then, however, they are surprisingly short ; *e. g.*, the notice of Sir William Thomson (Lord Kelvin) consists of less than three lines.

The text and illustrations are both of high character, and the student who takes it as his textbook will obtain a very sound knowledge of physics. Only now and then in glancing through the pages do we find questionable matter. The description (p. 107) of the Joule-Kelvin effect is not at all up to date and it should be rewritten ; the latest date given is 1902. In one particular it is wrong. To say that "the heat produced by friction in the plug was so small as to be negligible" shows a lack of appreciation of the important part which this friction plays in the experiment.

Cinématique de la Relativité. E. Bauer. (*Actualités Scientifiques et Industrielles,* vol. xl. (Paris : Hermann & Cie. 1932. Price 7 frs.)

L'Inertie de l'Enérgie. F. Perrin. (*Ibid.* vol. xli. 1932. Price 6 frs.)

La Théorie Einsteinne de la Gravitation : les vérifications expérimentales. G. Darmois. (*Ibid.* vol. xliii. 1932. Price 7 frs.)

Le parallélisme absolue et la théorie unitaire du champs. E. Cartan. (*Ibid.* vol. xliv. 1932. Price 6 frs.)

La Relativité : Conclusion générale. P. Langevin. (*Ibid.* 1932. Price 6 frs.)

These short monographs are the reprints of lectures delivered at a conference on relativity in Paris in 1930. The object aimed at has been to give an account of the existing state of each branch of the theory rather than of original discoveries. Bauer and Perrin devote themselves to special relativity : the former to the Lorentz transformation, the latter to the variation of mass with velocity which arises therefrom. Darmois deals with the equations of the general theory and the deductions made from the "Schwarzschild solution" regarding the displacement of the perihelion of Mercury, the bending of light rays, and the spectral shift towards the red in the gravitational field of massive stars.

Cartan's contribution will be found of interest because of the short and clear account he gives of the theories of parallelism rather than for his description of Einstein's unified field theory of gravitation and electromagnetism, based on parallelism at a distance. The latter has to-day been discarded, even by its author. In the general conclusion, Langevin lays stress

on the change in the point of view regarding mechanics which has come about since the advent of relativity. Once looked upon as the simplest and easiest understood part of physics, to-day mechanics appears as the most complex.

The general impression made on the reader is that the contributors are all convinced that the aim of scientific enquiry is the "explanation" rather than the description of phenomena. As a result much space is devoted to such matters as the demonstration that Einstein's gravitational equations imply that gravitation is propagated by means of waves with the speed of light, or the deduction of the equivalence of mass and energy from different sets of physical principles.

Fondements de la Théorie de la Relativité générale.—Gravitation et Electricité—Structure cosmologique de l'espace. By A. Einstein. Translated by Maurice Solovine. (Paris: Hermann & Cie. 1933. Price 35 frs.)

The book contains translations into French of two of Einstein's most important papers already published elsewhere, together with a third in which he puts forward his views regarding the Expanding Universe. The first paper, originally published in 1916, gives a complete account of the theory of general relativity and is to-day the classical one in this subject. The second paper deals with the most recent unified field theory of gravitation and electricity put forward by Einstein. With its purely formal results and its lack of contact with observation, it forms a striking contrast to the powerful theory of 1916. In the third contribution Einstein deals with the "cosmical constant," which he suggests should now be removed from the equations of gravitation. He adopts a theory of the Expanding Universe which differs from that of Lemaître and Eddington, in that the expansion must be supposed to start instantaneously at a certain instant of time. On the other hand, it is possible to deduce the average density of matter in the universe from the rate of expansion. The value found is 10^{-28} grs. per cub. cm., which is somewhat greater than that estimated by Hubble from observation.

[*The Editors do not hold themselves responsible for the views expressed by their correspondents.*]

Fig. 1.

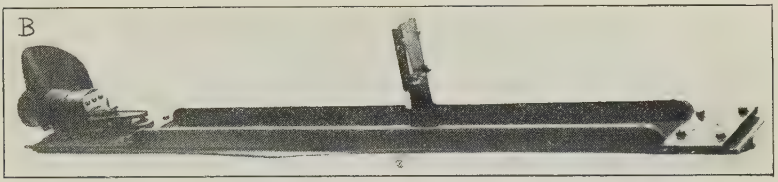

Fig. 3.

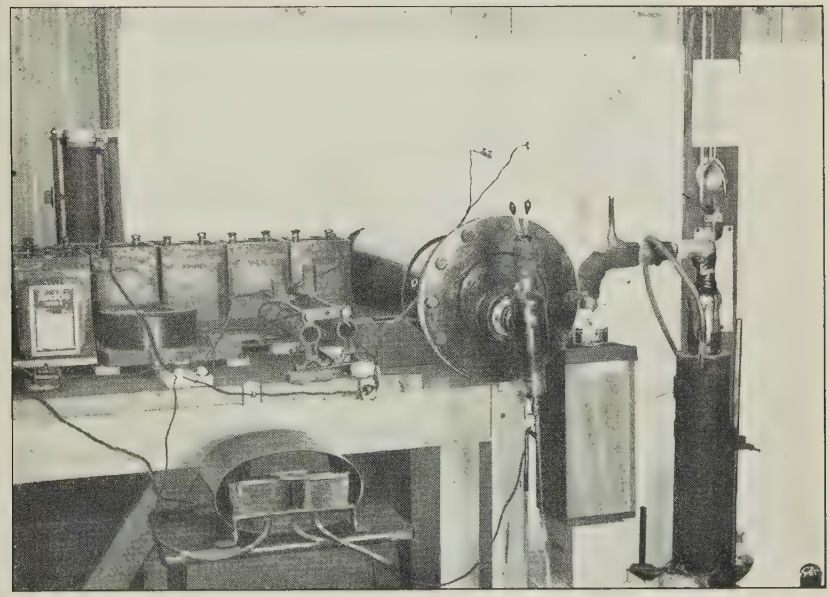

Fig. 5.

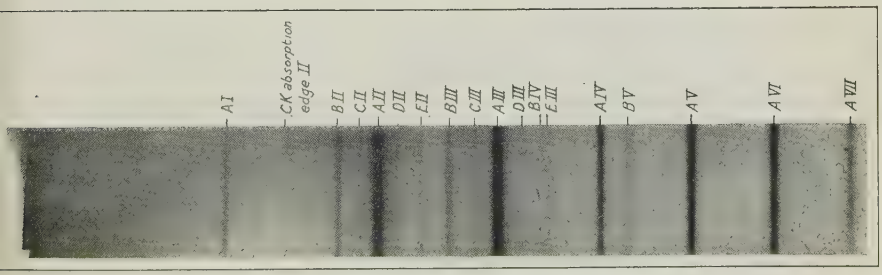

Molybdenum anti-cathode. Tungsten filament.

Fig. 4.

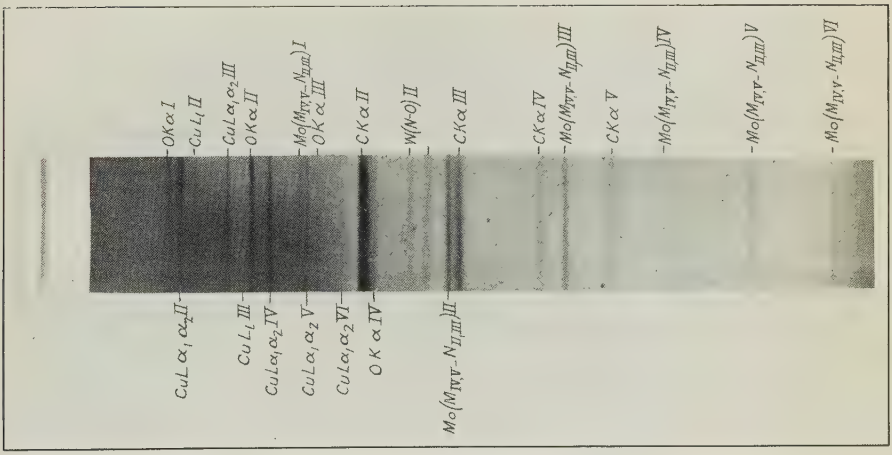

Copper anti-cathode. Tungsten and molybdenum filaments.

Fig. 6.

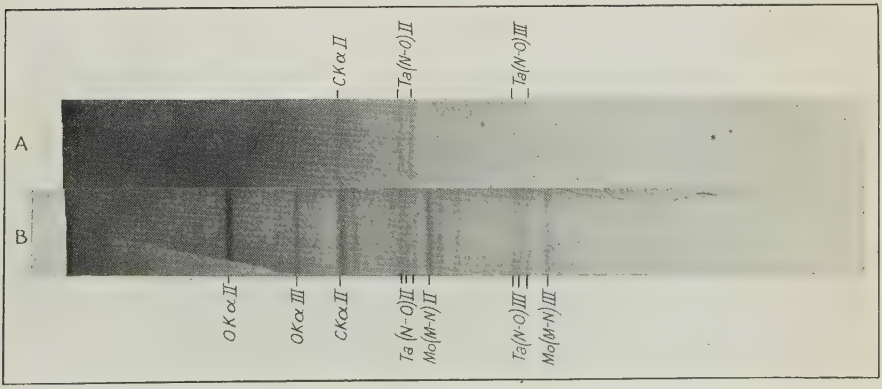

A. Tantalum anti-cathode. Tungsten filament.

B. Nickel silver anti-cathode. Tantalum and molybdenum filaments.

Fig. 2.

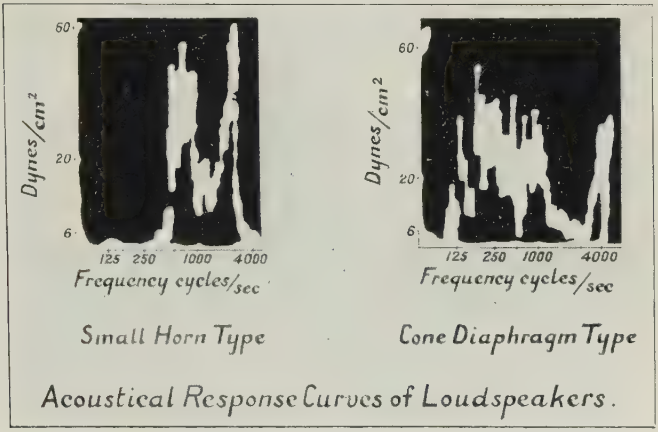

Acoustical Response Curves of Loudspeakers.

Fig. 3.

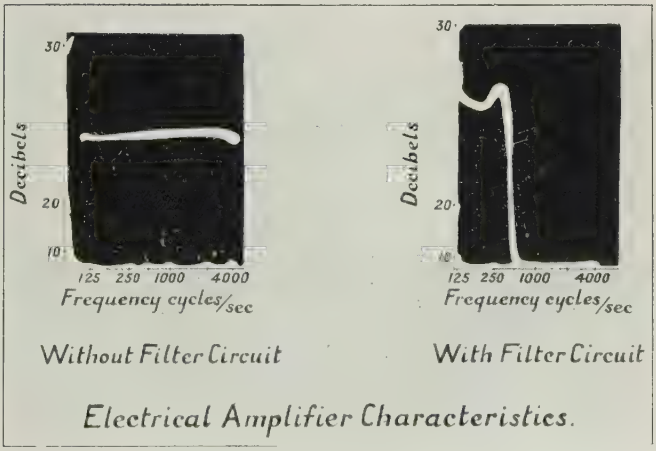

Electrical Amplifier Characteristics.

Fig. 2.

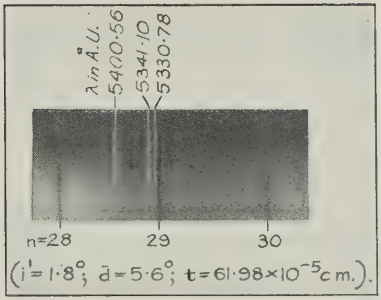

Above:—Spectrum of Neon.

Below:—Spectrum of plane-polarized white light reflected from a lamina of mica at a small grazing angle.

Intensity distribution in the spectrum of beryllium oxide.

Mercury jets in air. Cylindrical nozzle.

Fig. 1.

d=·30 mm.

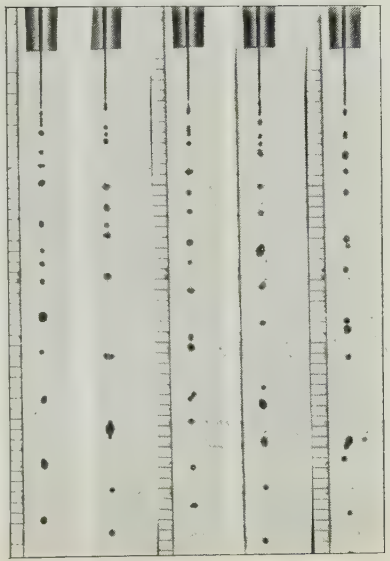

V=84 cm./sec.
L=·55 cm. (average).

Fig. 2.

d=·30 mm.

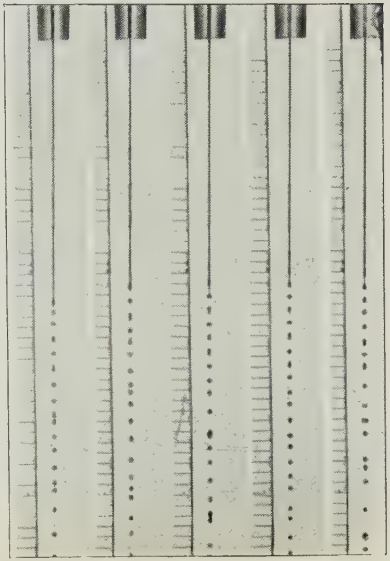

V=118 cm./sec.
L=2·32 cm. (average).

Fig. 3.

d=·30 mm.

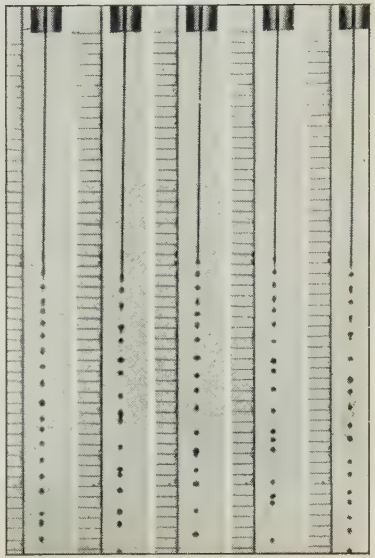

V=122 cm./sec.
L=2·40 cm. (average).

Water jets in air. Cylindrical nozzle.

Fig. 4.
$d = \cdot 450$ mm.

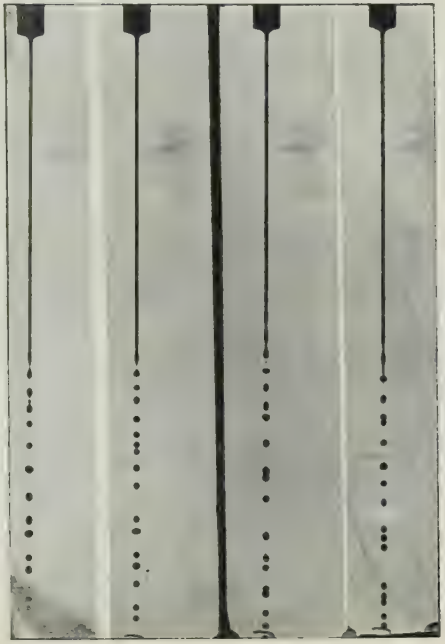

V = 187 cm./sec.
Magnification = 1·29.

Fig. 5.
$d = \cdot 450$ mm

V = 210 cm./sec.
Magnification = 1·25.

Aniline jets in air. Cylindrical nozzle.

Fig. 6.
$d = \cdot 450$ mm.

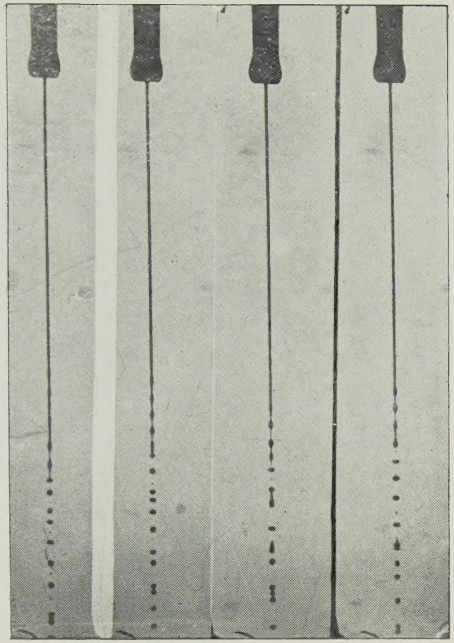

V = 251 cm./sec.
Magnification = 1·25.

Fig. 7.
$d = \cdot 650$ mm.

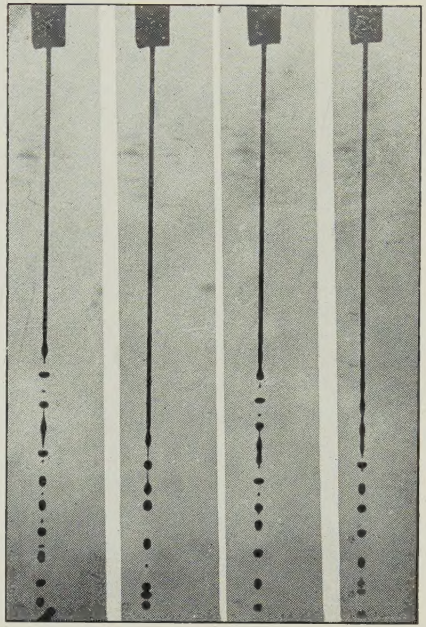

V = 156 cm./sec.
Magnification = 1·22.

Fig. 1.